ENERGY

OZONE

PNL-2981

OZONE FIELD STUDIES ADJACENT TO A HVDC TRANSMISSION TEST LINE

By
J. G. Droppo
O. B. Abbey
D. W. Glover

March 1979

Work Performed Under Contract No. EY-76-C-06-1830

Battelle
Pacific Northwest Laboratory
Richland, Washington

U. S. DEPARTMENT OF ENERGY

Division of Electric Energy Systems
Resource Applications

NOTICE

PNL-2981
Distribution Category UC-97a

OZONE FIELD STUDIES ADJACENT TO A HVDC TRANSMISSION TEST LINE

J. G. Droppo
O. B. Abbey
D. W. Glover

March 1979

Prepared for U.S. Department of Energy
Division of Electric Energy Systems
under Contract EY-76-C-06-1830

PACIFIC NORTHWEST LABORATORY
Richland, Washington 99352

PREFACE

Because the environment near high voltage direct current (HVdc) transmission test lines is affected by the high voltage and corona losses of conductors, concerns over the potential environmental effects have been raised. Among these effects are: complex electric fields, space charges, noise, radio/television (RTV) interference and oxidants. In response to these concerns, the Bonneville Power Administration (BPA) in cooperation with the Pacific Northwest Laboratory (PNL) is developing a generic characterization of effects of operating HVdc transmission lines. This report, as PNL's part of the effort, concerns the *in situ* definition of oxidant production rates by definition of maximum levels of environmental changes. The research was conducted at BPA's HVdc Test Facility in The Dalles, Oregon.

The authors wish to acknowledge BPA for their aid and cooperation during this study, Dan Bracken and Vern Chartier for their scientific input, and L. Gray and W. Lewis for their aid in the field-study logistics.

SUMMARY

Field studies of atmospheric ozone concentrations adjacent to high voltage direct current (HVdc) transmission test lines were conducted at the Bonneville Power Administration's (BPA) HVdc Test Facility at The Dalles, Oregon. The transmission lines were operating at voltages from ±400 to ±600 kV during the field studies.

The downwind ozone plumes were studied using a roving vertical profiling system. This approach allowed definition of very small relative changes in the vertical profile of ozone. Ambient meteorological and test line parameters were also recorded to allow comparison of predicted and observed ozone plumes.

For fair weather conditions no ozone plumes were evident. This is not surprising since the predicted ozone concentrations are smaller during fair weather conditions, and the background ozone concentrations are in the range of 20 to 60 ppb. Predicted ozone concentrations of up to 0.5 and 3.0 ppb would not be discernible in the natural variability of ±5 ppb. The absence of identifiable changes in ozone concentrations by the energized lines demonstrates the trivial nature of the ozone concentrations from the energized lines for fair weather conditions.

Precipitation conditions are the most likely conditions for detection of any effects from the energized HVdc test line as a result of the combination of the increased ozone production rates on the conductors and the depressed background atmospheric ozone concentrations. Since corona loss is largest during precipitation, the ozone production is also largest. The natural background atmospheric ozone concentrations are depressed by the scavenging effect of the precipitation.

With the exception of precipitation cases, the vertical profiles of ozone concentration demonstrated no discernible evidence of ozone plumes from the energized conductors. Ozone plumes, if any, were masked in the natural background ozone variability, which is expected considering the very low ozone concentrations predicted for conditions without precipitation.

During precipitation conditions, ozone plumes from the energized conductors were identified for two cases: one with low wind speeds and the other with moderate-to-high wind speeds. The magnitudes of the peak ozone concentrations observed 26 m downwind for these two sets of data during precipitation are relatively small. The low wind speed case has the maximum elevated peaks of ozone on the order of 5 to 10 ppb. The moderate-to-high wind speed case has maximum peaks of the order of 2 ppb. These peak concentrations were consistent with predicted values based on the test line and ambient meteorological parameters.

CONTENTS

PREFACE. iii
SUMMARY. v
1.0 INTRODUCTION 1-1
2.0 EXPERIMENT DESIGN CONSTRAINTS. 2-1
2.1 BACKGROUND OZONE CONCENTRATIONS 2-1
2.2 OZONE PRODUCTION RATES 2-3
2.3 LINE-SOURCE DISPERSION 2-4
2.4 OZONE CONCENTRATION ESTIMATES 2-5
2.5 MEASUREMENT METHOD. 2-7
3.0 MEASUREMENT PROGRAM 3-1
3.1 SITE 3-1
3.2 FIELD STUDIES SUMMARY. 3-6
3.2.1 Tracer Tests 3-6
3.2.2 Roving Profile Studies 3-8
3.2.3 Fixed-Height Monitoring Studies 3-8
3.2.4 Aerosol Measurements. 3-8
3.2.5 Windfield Definition. 3-8
4.0 DISCUSSION OF RESULTS 4-1
4.1 TRACER TESTS. 4-1
4.2 ROVING PROFILE STUDY 4-5
4.2.1 Profile Case Study #1: Low Wind Speeds and Precipitation. 4-14
4.2.2 Profile Case Study #2: Moderate-to-High Wind Speeds and Precipitation. 4-17
4.3 TRACER TESTS IMPLICATIONS 4-18
4.4 OZONE PROFILE DATA. 4-20
4.4.1 Profile Case Study #1 4-20
4.4.2 Profile Case Study #2 4-23
5.0 CONCLUSIONS. 5-1
6.0 REFERENCES 6-1
7.0 GLOSSARY. 7-1

APPENDIX A - Computing Corona Loss. A-1
APPENDIX B - Windfield Definition for Case Study #2 . . . . . B-1
APPENDIX C - Windfield Definition C-1
APPENDIX D - Aerosol Data Summary D-1
APPENDIX E - Fixed-Height Ozone Studies E-1
APPENDIX F - Individual Profiles for Case Study #1 . . . . . F-1
APPENDIX G - Profiles for Case Study #2 . . . . . G-1

LIST OF TABLES

2.1	Summary of Maximal Oxidant Concentrations in Selected Cities, 1964-1967	2-2
2.2	Cumulative Frequency Distribution of Hourly Average Oxidant Concentrations in Selected Cities, 1964-1965	2-2
2.3	Estimates of Fair-Weather Elevated Ozone Concentrations for a Range of Atmospheric Conditions	2-6
2.4	Estimates of Precipitation-Condition Ozone Concentrations for a Range of Atmospheric Conditions	2-7
4.1	Corona Loss for Profile Case Study #1, November 28, 1977	4-15
4.2	Voltages and Corona Loss Data for Profile Case Study #2, December 2, 1977	4-18
4.3	Comparisons of Observed and Predicted Ozone Source Terms for Case Study #2, December 1977	4-25
4.4	Summary of Profile and Conductor Variables for Case Study #2	4-26
B-1	Wind and Temperature Conditions for Individual Profiles, Case Study #2	B-2
B-2	Meteorological Profile of Ozone, Temperature and Moisture.	B-10
B-3	Meteorological Profile of Ozone, Temperature and Moisture.	B-10
B-4	Meteorological Profile of Ozone, Temperature and Moisture.	B-10
D-1	Size Range #1	D-3
D-2	Size Range #2	D-3

LIST OF FIGURES

1.1	Typical Range of Corona Loss Variation Because of Rain, Fog and Snow.	1-3
2.1	Diagram of Effects on Ozone Profiles Upwind and Downwind of an Energized HVdc Transmission Line	2-10
3.1	Schematic of The Dalles Site	3-2
3.2	Relative Heights of Instrumentation at The Dalles, Oregon.	3-3
3.3	Schematic of Ozone Monitoring Intake System	3-4
3.4	Aerosol Generator	3-7
4.1	Tracer Tests, September 22, 1977	4-2
4.2	Tracer Tests, September 22, 1977	4-3
4.3	Tracer Tests, September 22, 1977	4-4
4.4	Tracer Tests, September 28, 1977	4-6
4.5	Tracer Tests, September 28, 1977	4-7
4.6	Tracer Tests, September 28, 1977	4-8
4.7	Tracer Tests, September 28, 1977	4-9
4.8	Tracer Tests, September 28, 1977	4-10
4.9	Vertical Profiles for December 2, 1977	4-12
4.10	Vertical Profiles for December 2, 1977	4-12
4.11	Vertical Profiles for December 2, 1977	4-13
4.12	Vertical Profiles for December 2, 1977	4-13
4.13	Average Ozone (O_3), Temperature (T), and Humidity (r) Profiles.	4-19
B-1	Windfield Summaries for Three Measurement Heights: Case Study #2	B-11
B-2	Windfield Summaries for Three Measurement Heights: Case Study #2	B-14
B-3	Windfield Summaries for Three Measurement Heights: Case Study #2	B-17
C-1	Computed Height Change Between Near Surface and Conductor Height Trajectories at 26 m Downwind: Low Wind Speed Example	C-2
C-2	Computed Trajectory Heights 26 m Downwind for the Three Heights of Wind Data: Low Wind Speed Example. . .	C-3

C-3	Computed Height Change Between Near Surface and Conductor Height at 26 m Downwind: Moderate Wind Speed Example.	C-4
C-4	Computed Trajectory Heights 26 m Downwind for the Three Heights of Wind Data: Moderate Wind Speed	C-5
D-1	Particle Number Densities at The Dalles, Size Ranges #1 and #2	D-2
E-1	Ozone Concentration Values as a Function of Wind Speed at Upwind and Downwind Locations	E-2
E-2	Fixed-Height Monitoring Study of Background Conditions at The Dalles Site	E-3
F-1 to F-44	Profiles for Case Study #1	F-2 to F-23
G-1 to G-10	Profiles for Case Study #2	G-2 to G-6

1.0 INTRODUCTION

Transmission of electrical energy by high voltage direct current (HVdc) transmission lines over long distances has proven to be an attractive alternative to high voltage alternating current (HVac) transmission lines, primarily because of the greater efficiency of HVdc transmissions. The ±400 Celilo-Sylmar HVdc Intertie between Oregon and California has demonstrated the feasibility of the long-range HVdc systems in the United States, and other HVdc transmission lines are in the planning and construction stages. However, implementing this relatively new technology raises concerns about potential environmental effects.

Considerable data were obtained in the design studies for the Celilo-Sylmar Intertie; however, these data were largely aimed at performance and specific-effects definition rather than at a generic definition of environmental effects. As a result, this study, which is part of a larger effort being conducted by the Bonneville Power Administration (BPA), is to help provide a data base for a generic definition of the magnitudes of potential environmental effects.

The environment near HVdc transmission lines is affected by the operation of the lines, which are designed to operate at high voltages with the conductors near or in corona. The environmental effects include: complex electric fields, space charges, noise, radio and television interference (RI and TVI) and oxidants. One environmental concern--ozone production rates under actual field conditions from the operation of HVdc transmission line--is the topic of this report.

Although laboratory tests of corona discharge (Scherer, Jr. et al. 1973), provided the basis for models (Roach et al. 1974) that predicted low concentrations of ozone, questions have been raised concerning the validity of extrapolating laboratory tests to actual lines and conditions. For example, the greatest corona losses on either HVdc or HVac lines occur during precipitation, a condition difficult to model in laboratory tests.

During wind-tunnel studies on DC corona (Scherer, Jr. et al. 1973), the ozone production rates per unit of corona current were much greater for a negative pole than for a positive pole, and ozone production rates increased as the square of the magnitude of the surface gradient factor increased.

Corona loss has been shown to vary with transmission line configuration and changes in ambient atmospheric conditions (BPA 1977). The corona loss on HVdc transmission lines is a function of wind speed, rain, snow and fog with a slight dependence on relative humidity. Figure 1.1 shows the typical corona-loss dependence on snow, rain and fog as a function of the conductor maximum surface gradient. The corona loss on an operational HVdc line typically increased between a factor of 2 and 5 during the onset of precipitation conditions, with the greatest change being an order of magnitude increase. This increase was less than for HVac where the greatest change was on the order of 50 times. With regard to wind speed, the empirical relationship for variation of corona loss was:

$$CL = 1.6 + 0.44\ V \qquad (1)$$

where CL is corona current per kw per conductor (km) and V is the wind velocity (m/sec) between 0 and 10 m/sec. For detailed data on the variation of the corona losses in relation to transmission-line design parameters, see Transmission Line Reference Book HVdc ±600 kV (BPA 1977).

This PNL study is to define the ozone concentrations attributed to corona losses under actual field conditions. To accomplish this, specially formulated field studies were conducted at a HVdc transmission test line over a range of natural conditions. The test line was identical in design to the operating Celilo-Sylmar HVdc Intertie; however, the voltage could be varied above the ±400 kV operating voltage of the Intertie. The higher voltages on the test line resulted in more corona activity than on the operating Intertie.

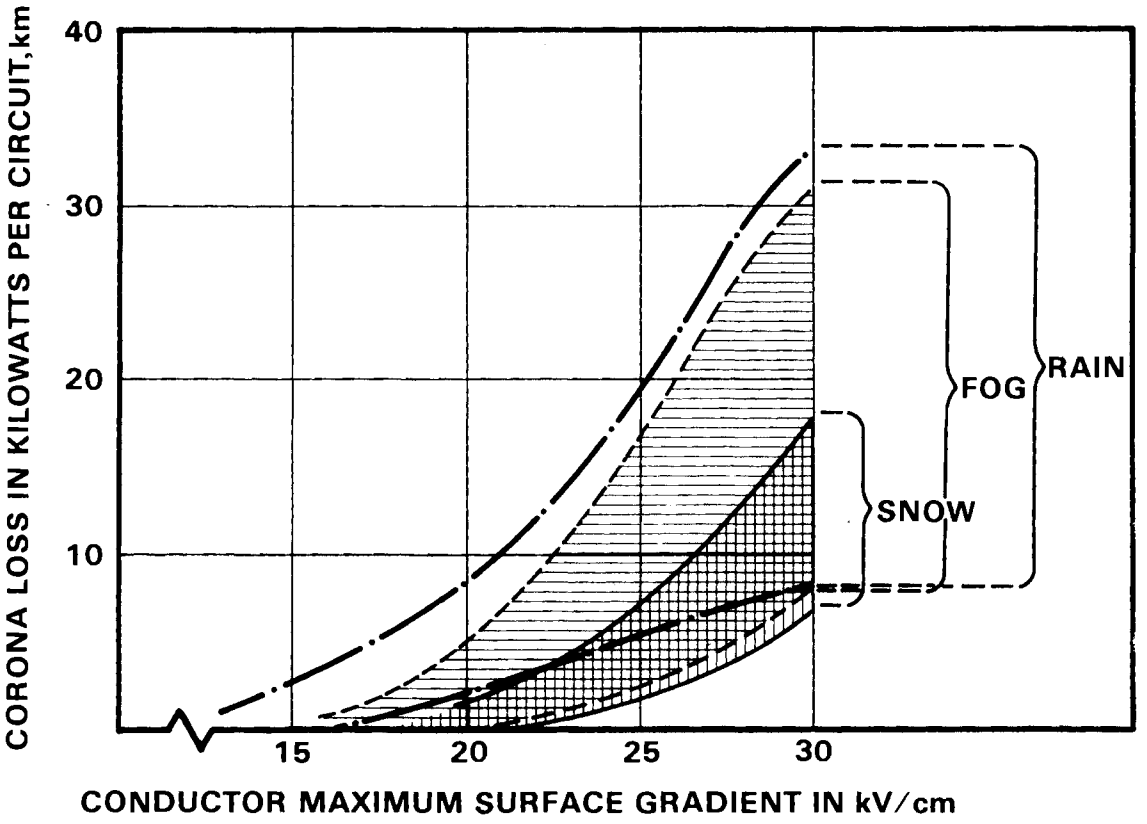

FIGURE 1.1. Typical Range of Corona Loss Variation Because of Rain, Fog and Snow

For each experiment at the HVdc test facility, the corona losses were measured in terms of the total current losses on the test conductors. Measurements of ambient meteorological conditions, transmission-line variables, and ozone concentrations were used to define the magnitude of the ozone line-source on the HVdc test lines.

The ozone source terms were studied using sensitive, micrometeorological profile techniques, which incorporate a roving input system and provide better vertical resolution than fixed-height monitoring systems. Definition of the ozone plumes is possible through analysis of profile characteristics.

2.0 EXPERIMENT DESIGN CONSTRAINTS

The field experiments are to define any significant ozone production by the HVdc conductors. Ideally, the experimental design and associated instrumentation should be capable of measuring and distinguishing background ozone and conductor-generated ozone concentrations. In practice, the ozone from the conductors will be distinguishable when it is significant compared to background concentration variability. Consideration of the constraints on the experimental design will depend on the background ozone concentrations and the conductor ozone production with atmospheric dispersion.

2.1 BACKGROUND OZONE CONCENTRATIONS

Ozone concentrations that represent conditions void of man's influence are difficult to define because of the potential long-range effects of manmade sources of air pollutants on ozone concentrations. In addition, the influence of natural emissions is not completely understood. Natural hydrocarbon emissions from vegetation may be important in defining influences on ambient ozone concentrations (Sandberg et al. 1978). In addition, the vertical mixing in the entire troposphere is important in the control of surface-layer concentrations of ozone (Coffey and Stasiuk, Jr. 1975). Tables 2.1 and 2.2 are summaries of maximal oxidant concentrations and cumulative frequency distributions of hourly average oxidant concentrations. These tables indicate ambient ranges of oxidant concentrations whose primary component is ozone at a number of urban locations, where data are available.

Although the federal ambient-air-quality standard is defined at 80 ppb, some researchers contend that natural background conditions exceed this standard. Others contend that natural background concentrations will rarely be greater than 50 to 60 ppb near the surface and that higher concentrations are the result of manmade emissions (Committee on Medical and Biological Effects of Environmental Pollutants 1977).

Table 2.1. Summary of Maximal Oxidant Concentrations in Selected Cities, 1964-1967

Station	Total Data Days	Days with Maximal Hourly Average ≥ Percent of Data Concentration Specified: 150 ppb	100 ppb	50 ppb	Maximal Hourly Average, ppb	Peak Concentration, ppb
Pasadena, California	728	41.1	55.1	75.0	460	670
Los Angeles, California	730	30.1	48.5	74.0	580	650
San Diego, California	623	5.6	20.9	70.6	380	460
Denver, Colorado	285	4.9	17.9	79.3	250	310
St. Louis, Missouri	582	2.4	10.1	62.2	350	850
Philadelphia, Pennsylvania	556	2.3	10.9	41.9	210	250
Sacramento, California	711	2.3	14.6	62.3	260	450
Cincinnati, Ohio	613	1.6	9.0	52.0	260	320
Santa Barbara, California	723	1.5	10.5	70.5	250	280
Washington, D.C.	577	1.2	11.3	54.2	210	240
San Francisco, California	647	0.9	4.5	28.6	180	220
Chicago, Illinois	530	0	4.5	50.8	130	190

TABLE 2.2. Cumulative Frequency Distribution of Hourly Average Oxidant Concentrations in Selected Cities, 1964-1965 (Committee on Medical and Biomedical Effects of Environmental Pollutants 1977)

City	Percent of Hours with Concentrations ≥ Stated Concentrations, ppb: 90	70	50	30	10	5	2	1	1964-1965 Yearly Average, ppb
Pasadena, California	10	10	20	40	120	180	230	260	42
Los Angeles, California	10	10	20	40	100	140	180	220	36
San Diego, California	10	20	30	40	80	100	120	140	36
Denver, Colorado	10	20	30	40	60	80	100	120	36
St. Louis, Missouri	10	20	30	40	60	70	90	110	31
Philadelphia, Pennsylvania	10	20	20	30	60	80	110	140	26
Sacramento, California	10	10	20	40	60	80	100	120	30
Cincinnati, Ohio	10	20	20	40	60	70	80	100	30
Santa Barbara, California	20	20	30	40	60	80	90	100	30
Washington, D.C.	10	10	20	30	60	70	90	100	29
San Francisco, California	10	10	20	30	40	50	60	70	19
Chicago, Illinois	10	10	20	30	50	60	80	80	28

Concentration patterns for ozone are discussed in an international air quality criteria document for photochemical oxidants and hydrocarbons (Committee on Medical and Biomedical Effects of Environmental Pollutants 1977). Urban ozone concentrations for an urban site (Delff, Netherlands) showed monthly average values of ozone ranging from a peak in August of 31 ppb to a low of 1 ppb in January. Mean daily maximum values ranged from 71 to 2 ppb for the same months.

In addition to an annual variation, ozone concentrations, in some reported data, demonstrate a diurnal trend with a peak during the daylight hours. This peak results from the photochemical production of ozone and from the greater downward vertical-mixing of higher ozone concentrations during the day.

Although the causes of and the influences on ambient surface-layer ozone concentrations may be debated, the magnitudes of typical ozone concentrations may be defined for comparative purposes in this study as:

- Values ranging up to 50 to 60 ppb are typical ambient values at remote sites.
- Values exceeding the 80 ppb federal ambient air quality standard often occur in urban areas.

2.2 OZONE PRODUCTION RATES

The rate of ozone production is assumed to be directly related to the rate of corona loss. Production rates $P_{\pm}$ for ozone from dc-corona based on wind-tunnel tests are (Scherer, Jr. 1973):

$$P - = 1.2 \times 10^{-9} \text{ kg/W/sec} \quad (2)$$

$$P + = 0.4 \times 10^{-9} \text{ kg/W/sec} \quad (3)$$

Applications of these production rates to The Dalles HVdc test line (see Appendix A) result in the following source strength ($S_{\pm}$) for the dc-test line at the site for each 1 mA of corona current ($I_{C\pm}$) and for each 100 kV of voltage ($V_{\pm}$).

$$S_- = 1.9 \times 10^{-2} I_{c-} V_- \text{ ppb m}^2 \text{ s}^{-1} \quad (4)$$

$$S_+ = 0.6 \times 10^{-2} I_{c+} V_+ \text{ ppb m}^2 \text{ s}^{-1} \quad (5)$$

For an average source term from both poles that is based on total corona current (I_c) and average bipolar voltage (V), the expression is:

$$\bar{S} = 1.2 \times 10^{-2} I_c V \text{ ppb m}^2 \text{ s}^{-1} \quad (6)$$

2.3 LINE-SOURCE DISPERSION

The ozone produced on the conductors consists of two elevated parallel line sources of ozone, one on each pole. Using a Gaussian plume model for flow perpendicular to the conductors, the centerline ozone concentration (χ) from a conductor is given by:

$$\chi(x) = \frac{1.60\ Q_L}{\sigma_z\ \bar{u}} \left[1 + \text{EXP}\left(-\frac{2h^2}{(\sigma_z)^2}\right)\right] \quad (7)$$

where

- χ is air concentration, mass per volume
- Q is the source term, mass per time per length (equal to $S_{\pm}$ or $\bar{S}$)
- h is the release height, length
- σ_z is the vertical standard deviation of plume spread, length (The downwind distance appears only implicitly in the value of σ_z.)
- $\bar{u}$ is the average wind speed, length per time.

Equation (7) includes a ground-level reflection factor and refers to the average plume centerline concentration from a uniform line source. Observations of the visible corona on HVdc test lines to 600 kV support the use of uniform line-source assumption, particularly for rain conditions (Morris and Rakoshadas 1964). Roach (1973) uses a similar formulation for

nonzero winds in his evaluation of potential ozone concentrations from HVac transmission lines.

For zero winds Roach (1973) derives a relationship for ozone concentrations based on eddy dispersion alone. This provides a useful upper-limit estimate of ozone concentrations. In practice the actual wind speed is seldom zero for any extended time period.

2.4 OZONE CONCENTRATION ESTIMATES

The source term and dispersion relationships can be used to predict potential downwind ozone concentrations for The Dalles experiment site. The downwind distance for measurements is 26 m from the centerline between the HVdc conductors. The line voltages are ±600 kV. Typical high values of total corona loss are 10 mA for fair weather conditions and 150 mA for precipitation conditions, based on operational experience of the test line.

At the distances used in this study, the standard deviation σ_z is highly dependent on local roughness, ambient heat flux, and the averaging period. Extrapolating the σ_z values (for averages on the order of one hour) gives a range of 0.1 to 6 m at 26 m downwind (Pasquill 1974). These values bracket extreme natural conditions for direct flow from the conductors. The low value is for a surface roughness length of 10^{-5} m and a heat flux of -2 m W/cm^2, and the high value is for a roughness length of 1 m and a heat flux of 26 m W/cm^2. The former roughness length is for very smooth surfaces such as mud flats or ice. The latter roughness length is greater than for a woodland forest and less than for urban areas. A similar range of extrapolated σ_z values (0.6 to 8 m) were obtained from a summary of the results of a number of dispersion experiments (Strom 1976).

The experimental site, which will be described later, does not correspond to the ideal site (i.e., good fetch, uniform surfaces upwind, no slope, etc.) where the above σ_z numbers apply. The roughness length at the site is estimated to be about 0.03 m with greater values at distances as close as 100 or 200 m. The projected values of σ_z for an ideal site with a roughness length of 0.03 m are 0.7 m, 2 m and 3 m for stable, neutral and

unstable conditions, respectively. For the current nonuniform site, the actual σ_z values are expected to be larger than for the ideal site, because complex flows generally increase the dispersion rate at the site. A range of 0.5 m to 12 m for σ_z values 26 m downwind is selected to represent the largest reasonable range anticipated for the current site.

The wind speed and corona loss terms in Equation 7 cannot be considered independently for prediction of realistic ozone concentrations, because the corona loss rate depends directly on wind speed (Equation 1). The typically higher values of corona loss quoted above will correspond to higher values of wind speed; however, high corona loss values and very low winds are considered an unrealistic combination of conditions.

Tables 2.3 and 2.4 give predicted ozone concentrations using a range of wind speeds and dispersion rates for fair weather and precipitation conditions, respectively. For fair weather conditions with limited vertical dispersion (σ_z = 0.5 m), the predicted ozone concentrations range from about one ppb to several tenths of a ppb, assuming the winds are between 3 and 15 m/sec. Values corresponding to the higher winds are considered more realistic estimates of actual fair weather conditions. For the precipitation condition, a range of 24 to 3 ppb are predicted during limited vertical dispersion and winds between 3 and 15 m/sec. Ratios of ground to elevated concentrations are given for each standard deviation value.

TABLE 2.3. Estimates of Fair-Weather Elevated Ozone Concentrations for a Range of Atmospheric Conditions

Plume Vertical Standard Deviation, m	Wind Speed, m/sec					Ground Concentration Ratio
	1	3	5	10	15	
0.5	2.8 ppb	0.94 ppb	0.56 ppb	0.28 ppb	0.18 ppb	$<10^{-10}$
1	1.4	0.47	0.28	0.14	0.93	$<10^{-10}$
3	0.47	0.16	0.093	0.047	0.031	3×10^{-4}
5	0.28	0.093	0.056	0.028	0.019	0.056
10	0.15	0.049	0.029	0.105	0.10	0.49
12	0.011	0.044	0.026	0.010	0.009	0.93

TABLE 2.4. Estimates of Precipitation-Condition Ozone Concentrations for a Range of Atmospheric Conditions

Plume Vertical Standard Deviation, m	Wind Speed, m/sec					Ground Concentration Ratio
	1	3	5	10	15	
0.5	42 ppb	14 ppb	8.4 ppb	2.2 ppb	2.8 ppb	$<10^{-10}$
1	21	7.1	4.2	2.10	1.4	$<10^{-10}$
3	7.1	2.4	1.4	0.71	0.47	3×10^{-4}
5	4.2	1.4	0.84	0.84	0.29	0.056
10	2.3	0.74	0.44	0.23	0.15	0.49
12	0.17	0.66	0.39	0.20	0.14	0.93

The above estimates define ranges of sensitivity required for field verification of ozone production rates on the energized test lines. Typical predicted values of ozone concentrations range between 0.1 ppb and 15 ppb for precipitation conditions. Fair weather predicted ozone concentrations are much lower, ranging between 1 ppb and 0.01 ppb.

2.5 MEASUREMENT METHOD

Field measurements are to define the effects of ozone generated by energized HVdc transmission lines under actual field conditions. This objective can be accomplished by: 1) directly determining plume concentrations if the ozone plumes are discernible over background concentrations, or 2) by demonstrating that the ozone plumes are less than those that can be discerned in background concentrations. The latter method demonstrates the trivial nature of ozone source terms; the former method allows direct assessment of source terms.

The estimates given in Section 2.4 provide a basis for defining the sensitivity, based on maximum predicted values for ozone concentrations. An alternative basis for sensitivity is the magnitude and variability of

the natural ozone concentrations, which limit the definition of the ozone source terms under actual field conditions. (Section 2.1 considered the natural ozone concentrations.)

Natural ambient ozone concentrations range from a few ppb up to summertime, fair weather values in the range of 40 to 60 ppb. Polluted atmospheres may have values over 100 ppb. Although the anticipated ozone concentrations from transmission lines will normally be small fractions of ambient concentrations, the potential for detecting ozone concentrations, as given in Section 2.4, does exist during times of very low ambient atmospheric ozone concentrations. Hence, the sensitivity requirements for the field installation should be such that the concentrations plumes discussed in Section 2.4 can be detected.

An ideal approach for detecting plumes is to accurately monitor the ozone concentrations at a rapid rate at many heights, both upwind and downwind of the energized lines. This allows detailed definitions of any changes in ozone concentrations over background values. In practice this is logistically impossible, so approximate methods are used.

The placement of upwind and downwind monitors fixed at line height and ground level can be used to define major effects of ozone concentrations. This method's accuracy is limited by the accuracy of the relative calibration of the ozone monitors. Under the best conditions, the drift and noise in state-of-the-art ozone monitors are typically ±2 ppb, making field resolution of a typical concentration unlikely for most conditions. Nevertheless, this monitoring approach does have the advantage of being able to demonstrate the absence of large changes in ozone concentrations with a relatively simple field installation.

In this study, a novel alternative approach to monitoring has been adopted, based on determining a detailed downwind profile to allow definition of ozone plumes from the energized HVdc lines. This approach has

its origin in studies of the structure of the natural ozone profiles in the atmospheric surface layer from the viewpoint of estimating natural dry-removal rates of ozone.[a] In the current application, a roving ozone monitoring intake line is used to accurately define the shape of the downwind ozone profile. Upwind ozone concentrations are monitored at line height to define the ambient ozone concentrations. Using a single intake line and monitoring system results in better profile accuracies than those received using multiple fixed-height systems. The relative calibration errors between monitors are eliminated, resulting in the profile accuracy depending on the sensitivity of the ozone monitor alone (±0.34 ppb). Thus, the possibility of detecting the typical predicted ozone concentrations is greatly improved. Detailed profiles of ozone are examined for identifiable ozone plumes. The energized lines are considered as an elevated line source of ozone. The downwind profile of ozone not only detects ozone plumes with almost an order of magnitude of better sensitivity than that of the fixed-level monitors but also provides detailed information on the vertical extent of the plumes (see Figure 2.1).

Another important feature of Figure 2.1 is that the earth's surface is a sink for ozone. The natural vertical ozone upwind profile reflects the ozone-removal processes at the earth's surface. Changes of 0.5% to 10% in the ozone concentrations between typical conductor heights and the near surface values (1 m) are the normal order of magnitude for this variation, which depends on the ambient atmospheric conditions.

This natural profile of ozone increases the difficulty in interpreting fixed-height profile measurements. Even if sufficient accuracy is obtained among the fixed systems, the natural variation of ozone concentrations with

---

(a) See Droppo and Doran 1978; Regener and Aldaz 1969; Aldaz 1969; Galbally 1971; Galbally 1968; Droppo et al. 1976.

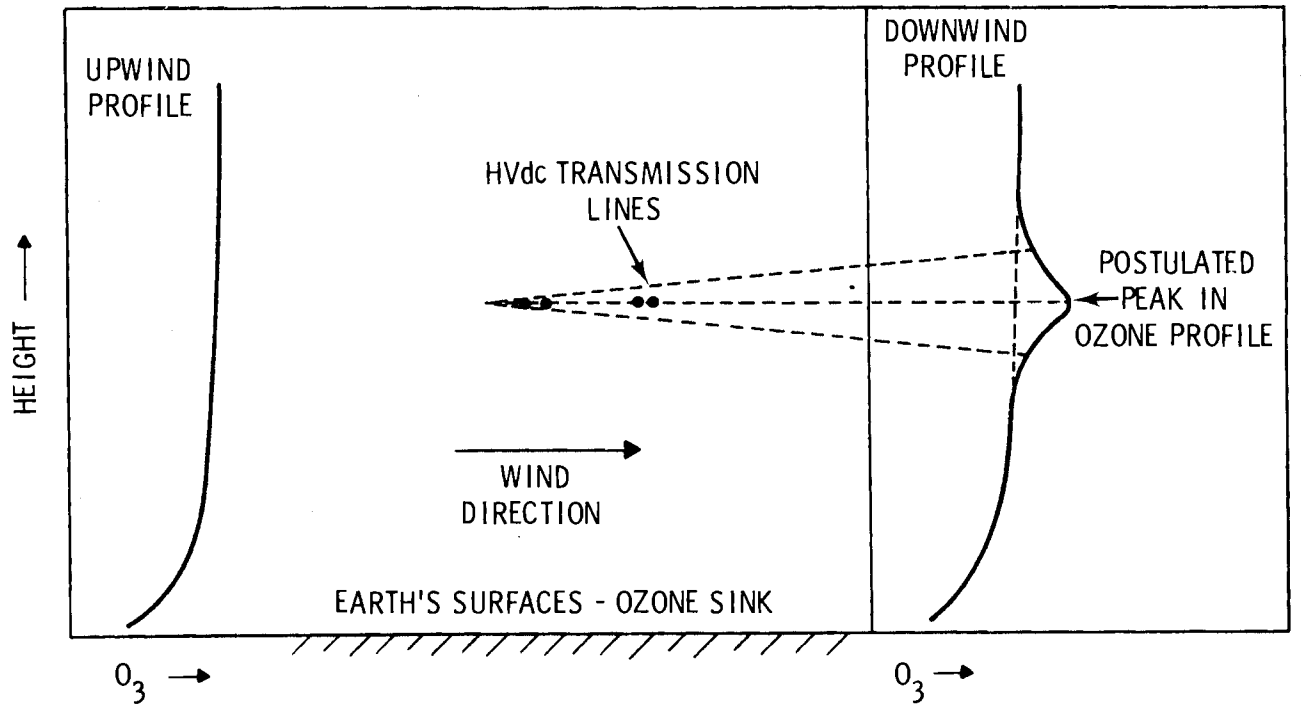

FIGURE 2.1. Diagram of Effects on Ozone Profiles Upwind and Downwind of an Energized HVdc Transmission Line

height is often greater than the magnitude of typical ozone concentrations given in Section 2.4. The use of fixed-height monitors is thus limited to comparing ozone concentrations at the same height both upwind and downwind.

The roving profile method provides detailed vertical profiles, which allow definition of upwind sources of ozone. In addition, the roving profile method allows the peak values and widths of the plumes to be estimated.

Individual, instantaneous natural profiles will show more variability than that illustrated in Figure 2.1. Smooth profiles are defined as averages over periods of thirty minutes or greater. The analysis of detailed profiles is in two modes: individual profiles and average profiles. The individual profiles can show the effects of ozone plumes, which are significant compared to background ozone variability. Because the average profiles can reduce random natural variation, any consistent increases in average

ozone concentrations associated with the line height, such as those shown in a postulated manner in Figure 2.1, would be evident.

The profiles in Figure 2.1 apply to an ideal site with a good uniform fetch for development of vertical profiles. The complex flow and generally poor fetch at the present site indicates that complex profiles can be anticipated. Nevertheless, the profile technique is still a powerful tool under nonuniform conditions, although additional steps are required to assure that the actual origins of ozone concentration changes can be identified. Tracer tests are necessary to assure that the airflow from the conductors will pass by the measurement points. Definition of both horizontal and vertical components of wind will be required during tracer and profile measurements. In the profile studies, ozone changes originating from local flow patterns will have to be separated from ozone changes associated with HVdc conductors.

To separate the sources of ozone changes, concurrent detailed profiles of ozone, temperature, and moisture must be made. These profiles will have corresponding structure reflecting the local flow patterns. Local flow patterns driven by density differences will be reflected in the temperature and moisture profiles. The ozone, temperature, and moisture of the air can be considered a tracer of the recent origin of the air. The source/sink properties of the earth's surface and complimentary sink/source nature of the free atmosphere are reflected in the temperature, moisture, and ozone profiles. For example, if a definite change in ozone occurs with corresponding changes in temperature and/or moisture, then the ozone profile changes are probably the result of local circulations and not the energized conductors.

Combining detailed profiles with the upwind ozone monitor record allows identification of ozone plumes from energized conductors. Ozone from the conductors will appear as a measurable change in the downwind ozone profile without corresponding changes in the downwind temperature and moisture profiles or in the upwind ozone monitor. The roving profile method is the primary method used in this study; however, the fixed-height method was used as a secondary method for monitoring studies.

3.0 MEASUREMENT PROGRAM

This section provides a description of the site, experimental installations, instrumentation, and field tests.

3.1 SITE

The field studies were conducted at BPA's HVdc Test Facility at The Dalles, Oregon. The field data were taken on a sloping site adjacent to studies being conducted by BPA. This field site was located on line section 1, which had 40-mm conductors for each pole supported by truncated, double-circuit, steel towers. The poles were spaced 12.2 m apart with 457 mm subspacing of conductors. The average conductor height on this section of line was 18.3 m; for the site, the height was about 12 m.

Figure 3.1 is a schematic of the site, including the experiment installation and instrumentation. This figure shows the instrumentation in an ideal configuration on a flat site with horizontal distances collapsed. The actual site was on sloping terrain, with the heights relative to a central point between the conductors (see Figure 3.2). The heights are in parenthesis and refer to ground levels except for the conductors, which refer to the conductor heights.

The field installation (see Figure 3.1) has ozone monitors at both sides of the conductors. Based on the prevailing wind direction at the site, the left side of this site (see Figure 3.1) was instrumented with the "upwind" monitor for ozone concentrations at the conductor height. The right side was intensively instrumented as the "downwind" monitor. The right side included roving-profile capabilities for ozone, air temperature and humidity. Fast-response wind and temperature sensors were at three fixed heights on the "profile tower". The site was also instrumented for precipitation. A fixed-height wind speed and direction system was used for real-time monitoring. Except for the latter system, the outputs of all systems were recorded on magnetic tape in data blocks at the rate of 1.5 Hz per data block.

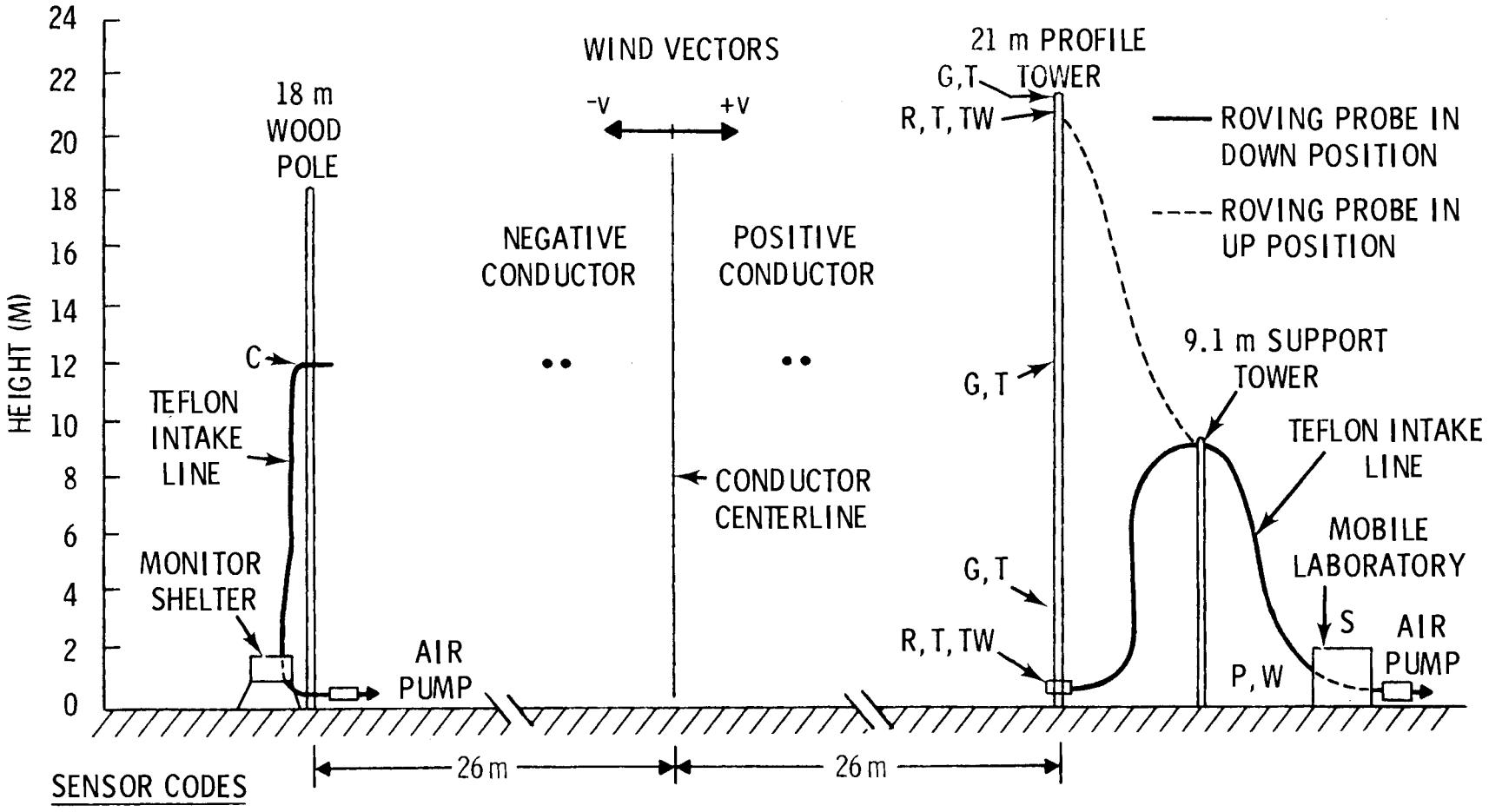

SENSOR CODES

R → ROVING PROBE INTAKE FOR OZONE CONCENTRATION

C → FIXED HEIGHT CONTROL INTAKE FOR OZONE CONCENTRATIONS

G THREE WIND COMPONENTS

T DRY BULB TEMPERATURE

TW WET BULB TEMPERATURE

S SOLAR RADIATION

P PRECIPITATION

W WIND SPEED AND DIRECTION CHART RECORD

FIGURE 3.1. Schematic of The Dalles Site

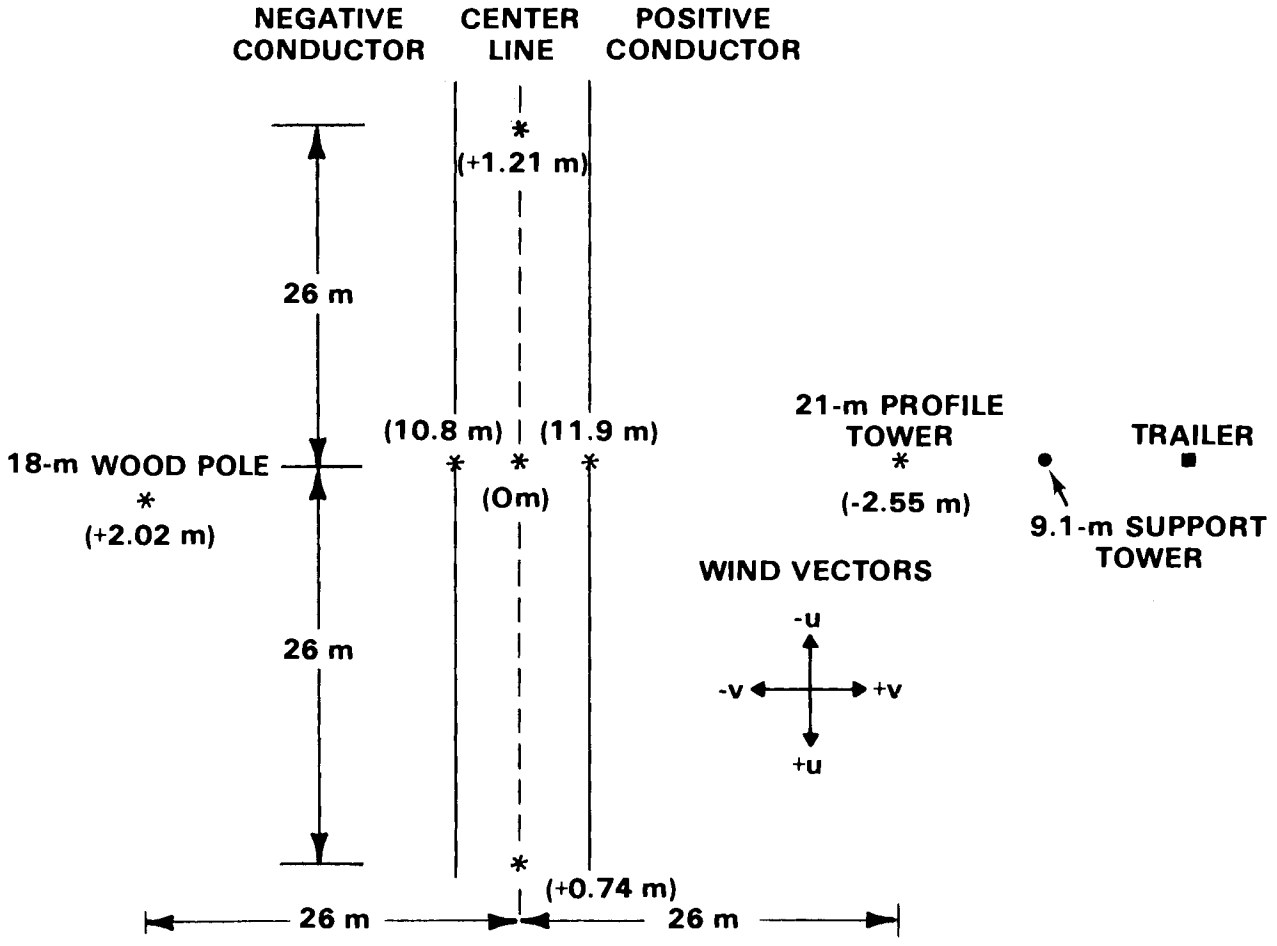

FIGURE 3.2. Relative Heights of Instrumentation at The Dalles, Oregon

The profiles were measured with an Ozone Analyzer Model 10516 manufactured by Monitor Labs. The response time of this instrument is about 60% in 1 sec. The fixed-height monitor was a Beckman Model 950 Ozone Analyzer with response time of about 7 or 8 sec. Tests were conducted to assure that the monitors gave comparable readings of ozone concentrations.

The best demonstration of the matched response of the monitors was the close correspondence of the trends in the two monitors under actual field tests. Results of these tests will be presented in the following section.

The intake systems for monitoring the ozone concentrations are an adaptation of a system developed on field studies of the rate of atmospheric ozone destruction of the earth's surface (Droppo and Doran 1978). This monitoring system is shown in Figure 3.3. Fast-response (within several seconds), accurate, ozone measurements were required from the tops of 20-m towers. Ozone is highly reactive on all surfaces, including the clean, medical-grade, teflon tubes used to pull the sample to the monitors.

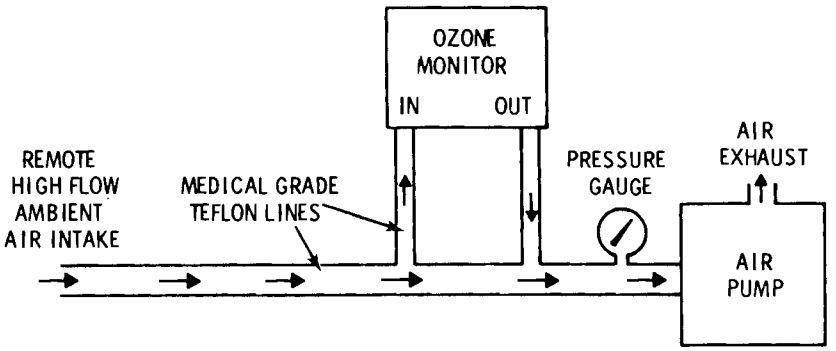

Note: Low-flow line, OD = 6.30 mm, ID = 4.70 mm
High-flow line, OD = 12.7 mm ID = 11.1 mm
Pressure drop ∿150 mm Hg
High-flow rate = 1.3 x 10^{-3} m^3/sec
Time Delay ∿2.5 sec

FIGURE 3.3. Schematic of Ozone Monitoring Intake System

This roving, single-intake, line system was developed as a result of the following observations (Droppo et al. 1976). First, the residence time in the intake lines could not be greater than a few seconds if the line losses were to be kept acceptably small. This short residence time was also dictated by the potential for photochemically controlled reactions changing the ozone concentration within the intake line. The latter can quickly increase or decrease measured ozone concentrations depending on ambient light and oxidant concentrations. Second, the use of any stainless steel valves or stainless steel fittings were found unacceptable as a result of small but measurable losses (5%) in ozone concentrations when they were incorporated in the intake lines. Saturation of the stainless steel by passing ozone through the line for extended periods was attempted; however, this was only able to eliminate temporarily the losses that reappeared on the subsequent day. Third, tests demonstrated that the variability between clean and apparently identical intake lines in terms of the line loss values was larger than the need for detecting ±1% changes in the profiles.

In the monitoring system that was developed, ambient air flows at a high rate through the larger teflon tube. The smaller diameter teflon inlet and exhaust lines of the ozone monitor are connected to the high-flow intake line as shown in Figure 3.3. The ozone monitor is operated at about 2/3 of atmospheric pressure. At higher flow rates, the greater reduction in pressure will cause significant changes in the absolute calibration of the ozone monitors. The ozone monitor draws a relatively small sample from the high-flow intake line. In this manner the residence time of the ozone in the monitoring system is kept sufficiently small so that significant line losses do not occur. The delay time to ozone monitor intake is about two seconds.

The ozone monitors are calibrated at ambient atmospheric pressures with an Analytical Instrument Device (AID) ozone generator. A conservative, absolute accuracy of ozone calibrations is 10% of a full scale. The consistency of the AID ozone generator when compared to standards suggests that at least 10% accuracy was attained.

The ±10% is a worst case value for the absolute concentrations. The relative calibration between the two ozone monitors calibrated side-by-side will be considerably better and is estimated to be on the order of ±3% of full scale.

Since calibrations are made at ambient pressure and measurements made at reduced pressure, the question of calibrations at reduced pressures was studied. Alternating measurements were made of ambient ozone concentrations through the low-pressure, long, intake lines and the ambient-pressure, short, intake lines. No discernible differences in measurement ambient ozone concentrations were noted. The operation of the ozone monitors at two-thirds atmosphere pressure did not significantly change the absolute calibrations.

In addition to routine calibrations during field studies, several special studies were made to assure that the two ozone monitors were responding to ambient ozone concentrations in an identical manner. These studies involved parallel operation of the two ozone monitors on the same intake line.

3.2 FIELD STUDIES SUMMARY

The field studies at The Dalles HVdc test site were divided into five categories: tracer test, roving profile studies, fixed-height monitoring studies, aerosol measurement, and windfield definition.

3.2.1 Tracer Tests

Two groups of tracer tests were conducted to define the wind trajectories across the conductors. The tracer was a neutrally buoyant, aerosol cloud of kerosene drops. This tracer was generated by the instrument operating on the positive conductor as shown in Figure 3.4. In the first group, the tracer was released from each of the de-energized conductors to define the path of any noncharged emissions. In the second group the tracer was released from the upwind pole (see Figure 3.1) at line height, with the line both energized and de-energized, to study effects on the aerosol plume trajectory. These tracer tests were documented by notes, slides and 16-mm movie film. The wind recording system was used to define the ambient conditions.

FIGURE 3.4. Aerosol Generator

3.2.2 Roving Profile Studies

The roving profile studies are aimed at defining the ozone effects of the operation of HVdc transmission lines. These experiments were conducted under a variety of ambient conditions with the conductors both energized and de-energized. The normal rate of profile data acquisition was about one profile every 2.8 min.

3.2.3 Fixed-Height Monitoring Studies

The roving probe intake system was fixed at 12.1 m for a series of fixed-height monitoring studies. Tests were taken without the line energized to define the ambient site influences on the ozone concentrations on both sides of the conductors. Tests were also taken to define the ambient ozone concentrations over extended time periods. Fixed-height monitoring studies results are presented in Appendix E.

3.2.4 Aerosol Measurements

A lazer system was used to define the ambient aerosols at the site. Tests were conducted at various locations on the field site to define both the number of particles and their size distribution. The results of the aerosol monitoring tests are given in Appendix D.

3.2.5 Windfield Definition

In each of the above tests, detailed windfield data was recorded as described in Section 3.1.

The use of three heights of wind sensors provides definition of three layers of the flow at the downwind tower. The complex number of potential influences on the winds at the site resulted in the need to define clearly the site flow characteristics at several heights in order to interpret both the ozone studies and BPA concurrent studies of other HVdc effects. The wind data from the studies have been analyzed and a summary of these results are given in Appendix B and C.

4.0 DISCUSSION OF RESULTS

This section contains the results of tracer tests and roving profile studies. Implications of the tracer tests are explained, and the ozone profile results are analyzed in terms of observed and predicted ozone emissions by the energized conductors.

4.1 TRACER TESTS

Two tracer tests from the conductors were performed: one during unstable conditions and the other during neutral conditions. The conductors were not energized during these tests.

Figures 4.1 to 4.3 are three photographs, taken on September 22, 1977, of the tracer plumes originating at the positive conductor and traveling towards the downwind profile tower. The width of the visible plume at the tower varied between 3 and 9 m during unstable atmospheric conditions with wind speeds on the order of 1 to 3 m/sec. For reference, the middle wind speed sensors are mounted at conductor height on the tower.

As illustrated by these photographs, considerable variability in the plume height existed at the profile tower during unstable conditions. A definite tendency appeared for the plume to rise upwards away from the general downslope of the site as part of a complex flow at the site. A shallow upslope wind, under and about perpendicular to the winds at conductor height, contributed to the general upward tendency of the wind at conductor height. The variability of the plume was such that the plume from the conductors intersected the profile tower at all heights from ground level to over the top of the tower. As a result of these tracer tests, the 9.1- to 18.3-m original profile design shown in the photographs was expanded to a 1- to 23.1-m profile system.

The tracer plume from the conductors followed the slope of the site more closely during the neutral stability tests on September 28, 1977, than during tests of unstable conditions. Less variation occurred in the height of intersection within the profile tower during neutral stability tests than

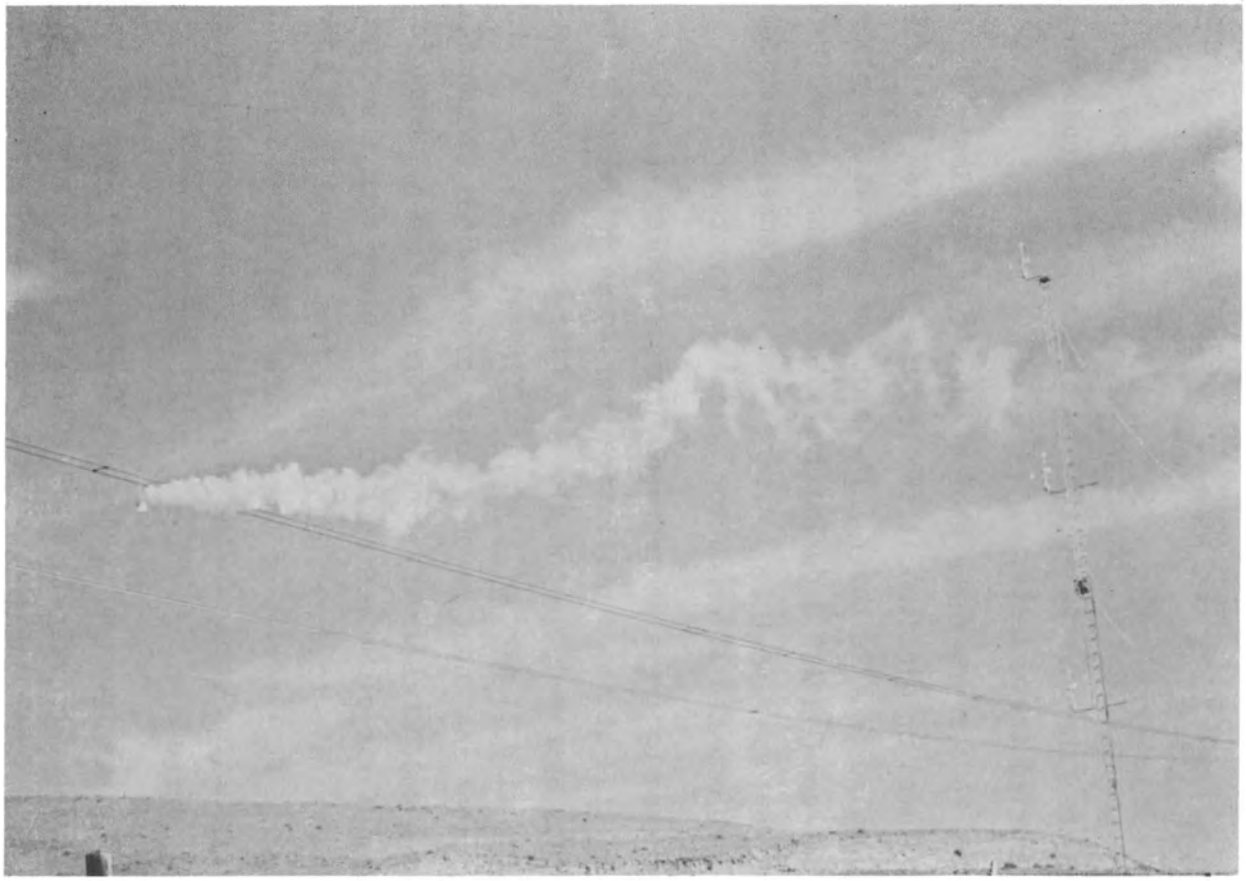

FIGURE 4.1. Tracer Tests, September 22, 1977

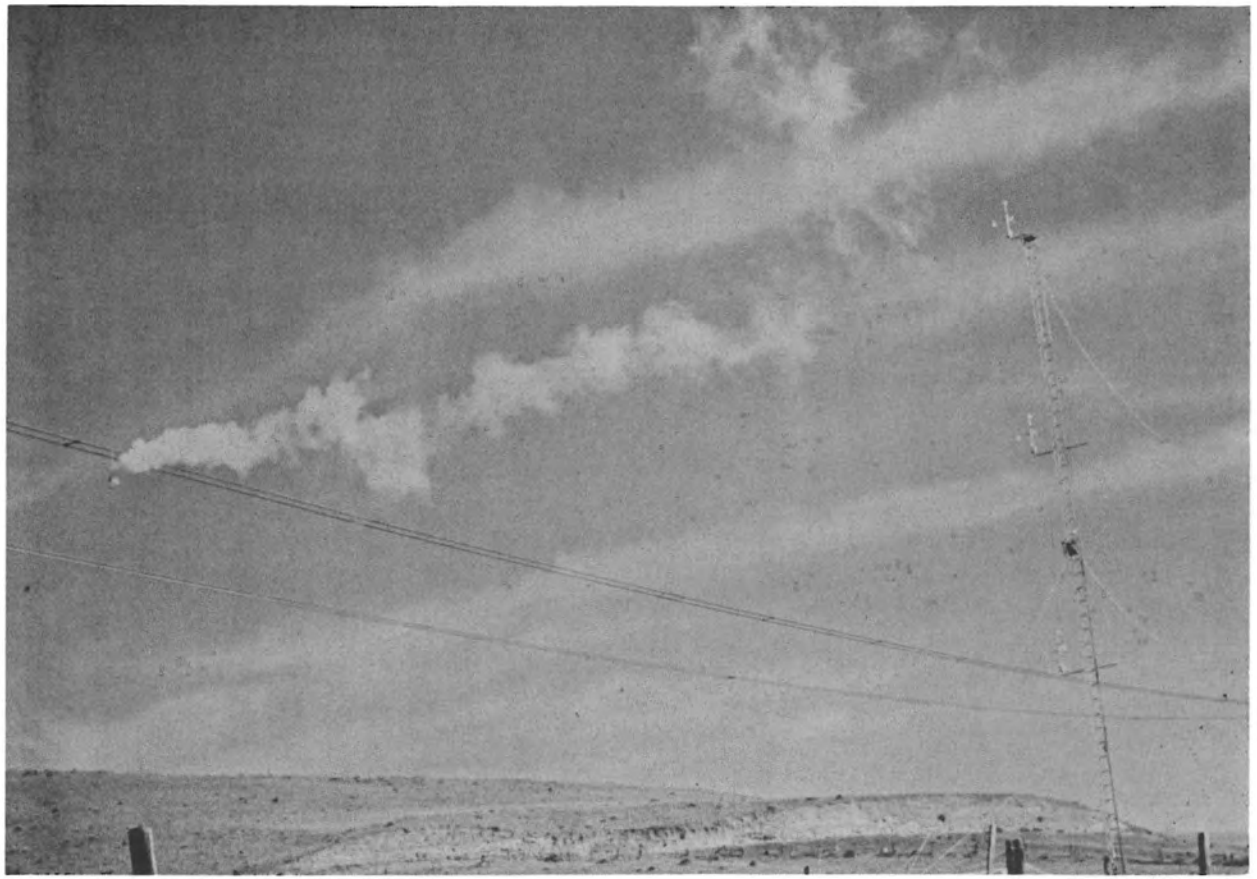

FIGURE 4.2. Tracer Tests, September 22, 1977

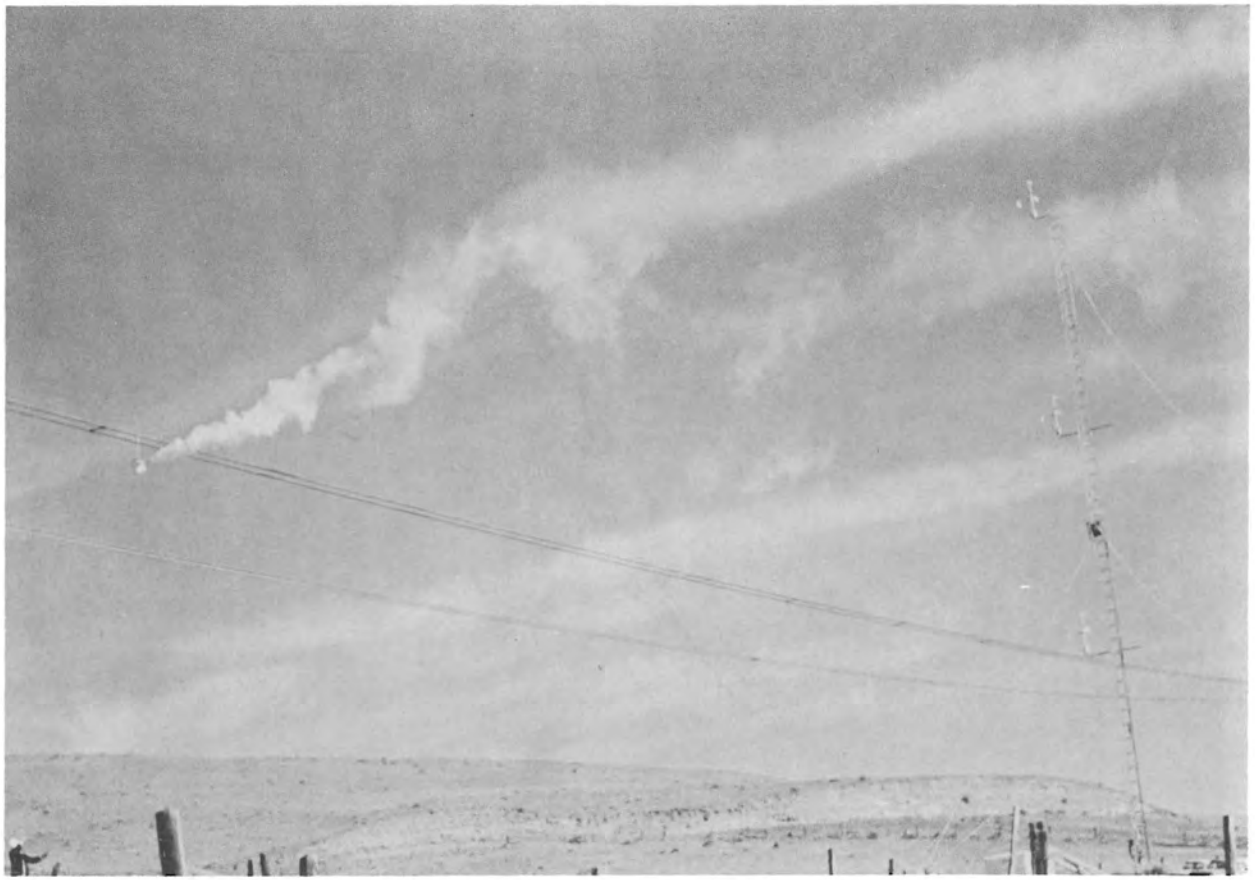

FIGURE 4.3. Tracer Tests, September 22, 1977

in the height of intersection under unstable tests. Figures 4.4 to 4.8 are examples of the plumes under neutral-to-slightly-unstable conditions taken at 10-sec intervals. Although the "average" plume intersected the profile tower near 12 m, these photographs show that the variation was still great enough for the plume positions to vary from ground level to the top of the tower (18.3 m).

No effects of the energized lines were noted for the tracer tests across the conductors with the source on the wooden pole upwind of the conductors. The conductors were alternately energized up to ±600 kV and de-energized to test for effects of energized conductors on tracer movement past the lines. There were no noticeable local effects of the tracer plumes passing immediately by the conductors or on the height of the tracer plume downwind of the lines.

4.2 ROVING PROFILE STUDY

With the exception of two cases during precipitation, the vertical profiles of ozone concentration demonstrated no discernible evidence of ozone plumes from the energized conductors. Ozone plumes, if any, were masked in the natural, background ozone variability, which is expected considering the very low ozone concentrations predicted for conditions without precipitation.

The results of the two data sets during precipitation with evidence of ozone from the energized conductors will be presented in this section. These data sets are the only two cases in the field studies in which ozone concentrations were discernible over background ozone concentrations. From these data sets, comparisons to predicted concentrations can be made.

These data sets represent conditions for maximum ozone production and as such are not typical tests, but rather worst-case conditions. As discussed earlier, precipitation maximizes corona loss and hence ozone production. Wind speed has two opposing effects on potential atmospheric ozone concentrations; that is, both the corona loss and the dispersion rate increase with wind speed. The relative magnitude of these opposing effects

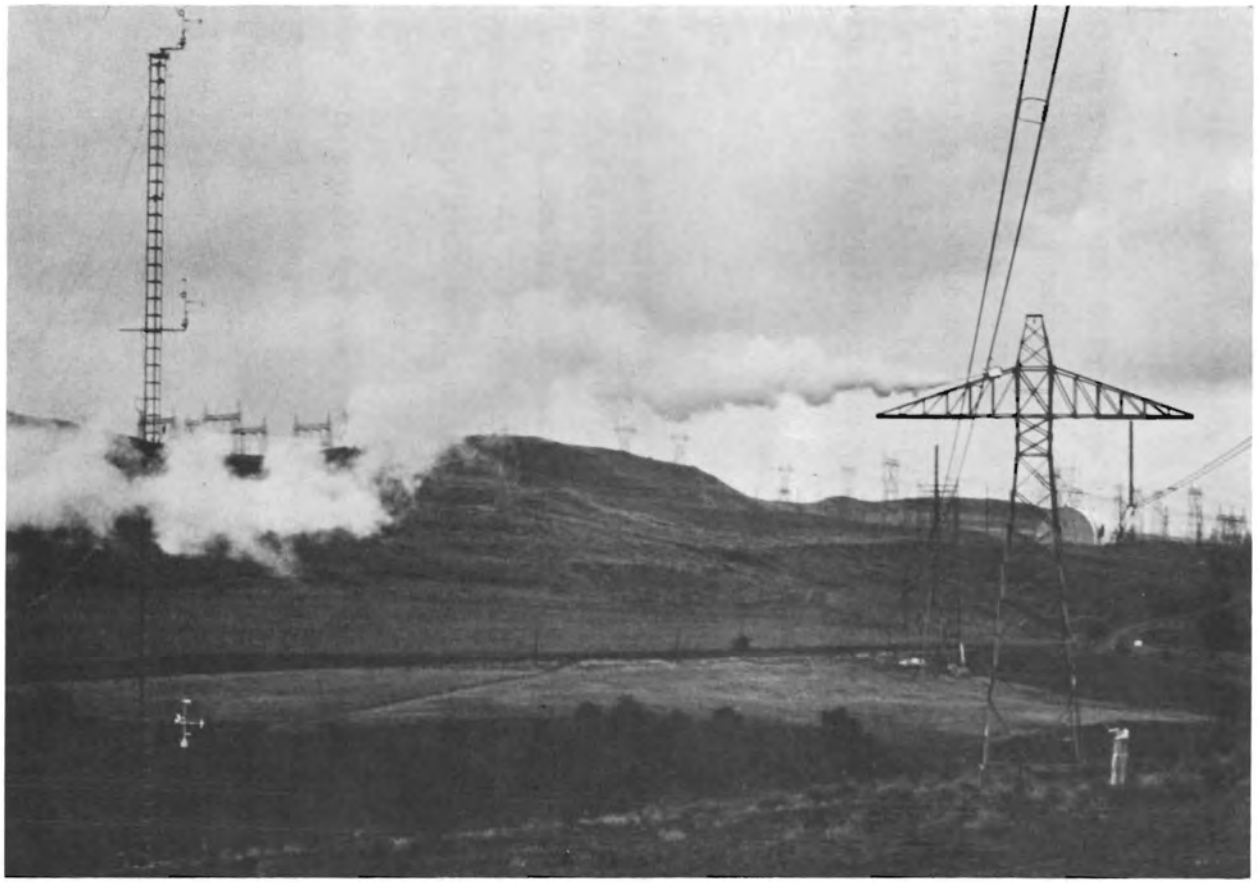

FIGURE 4.4. Tracer Tests, September 28, 1977

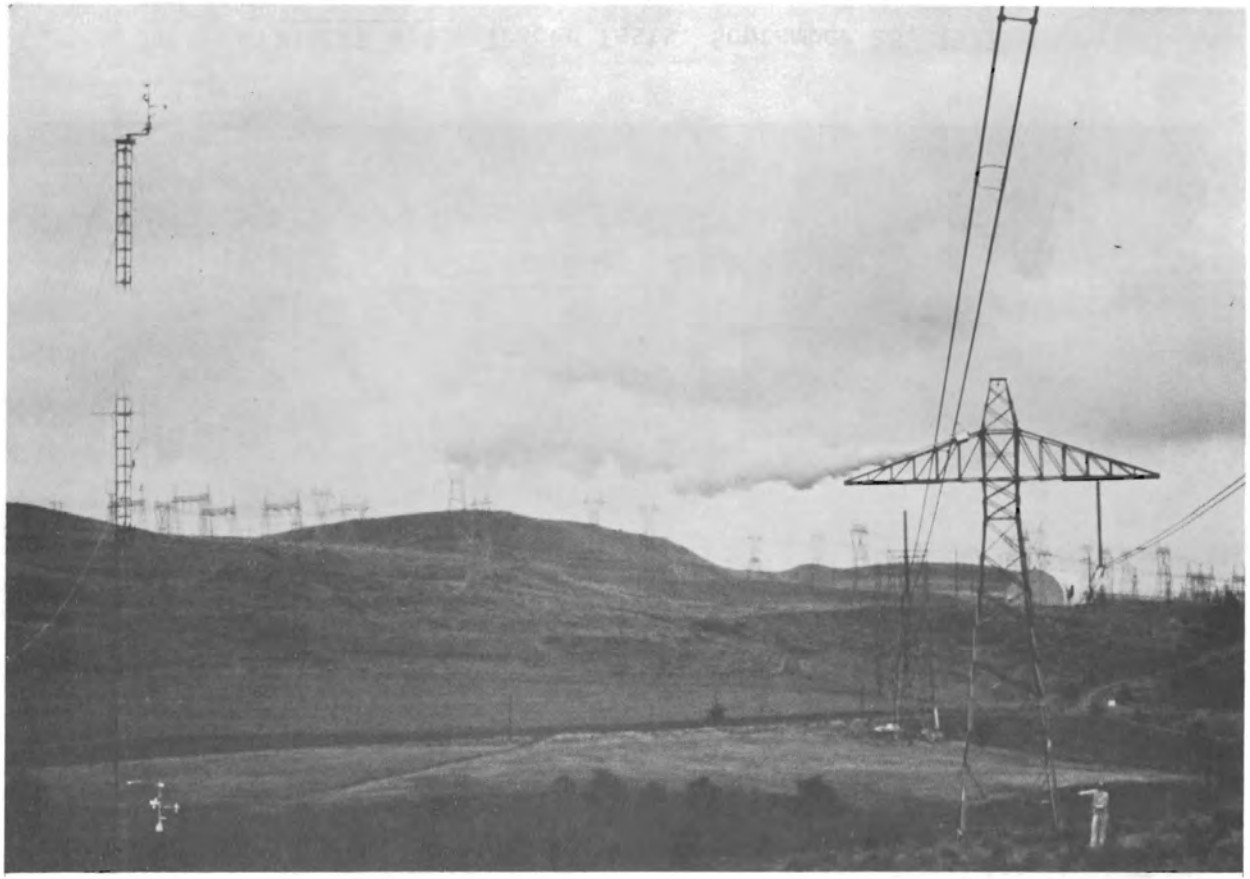

FIGURE 4.5. Tracer Tests, September 28, 1977

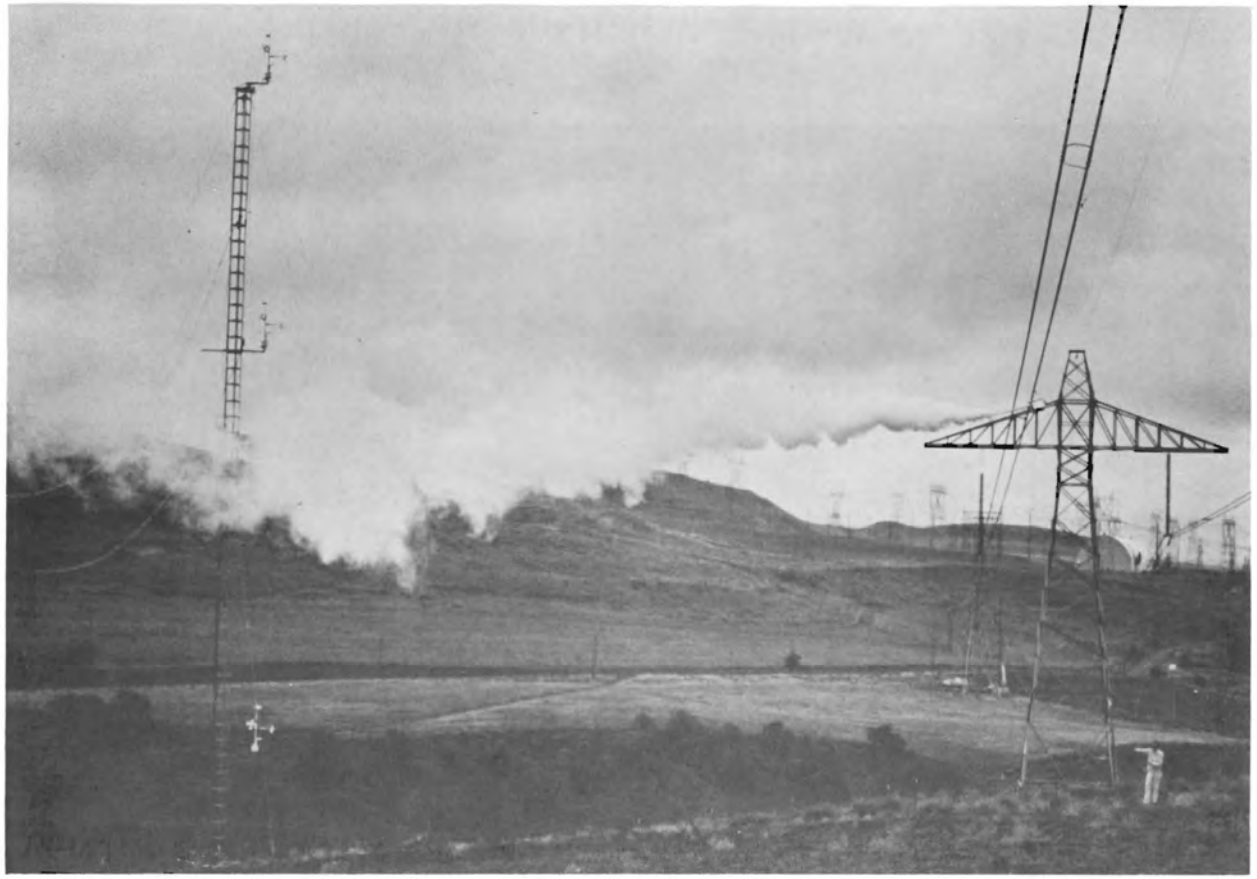

FIGURE 4.6. Tracer Tests, September 28, 1977

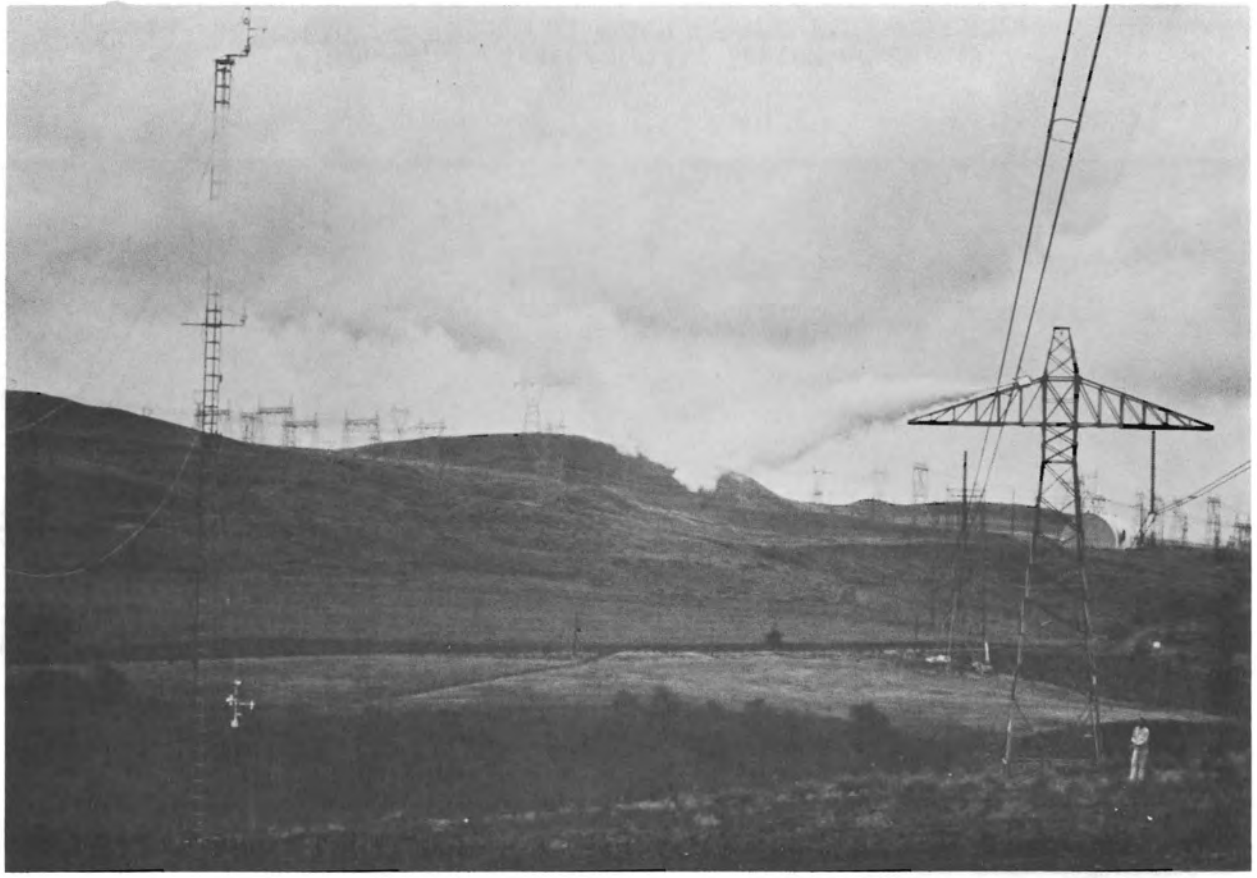

FIGURE 4.7. Tracer Tests, September 28, 1977

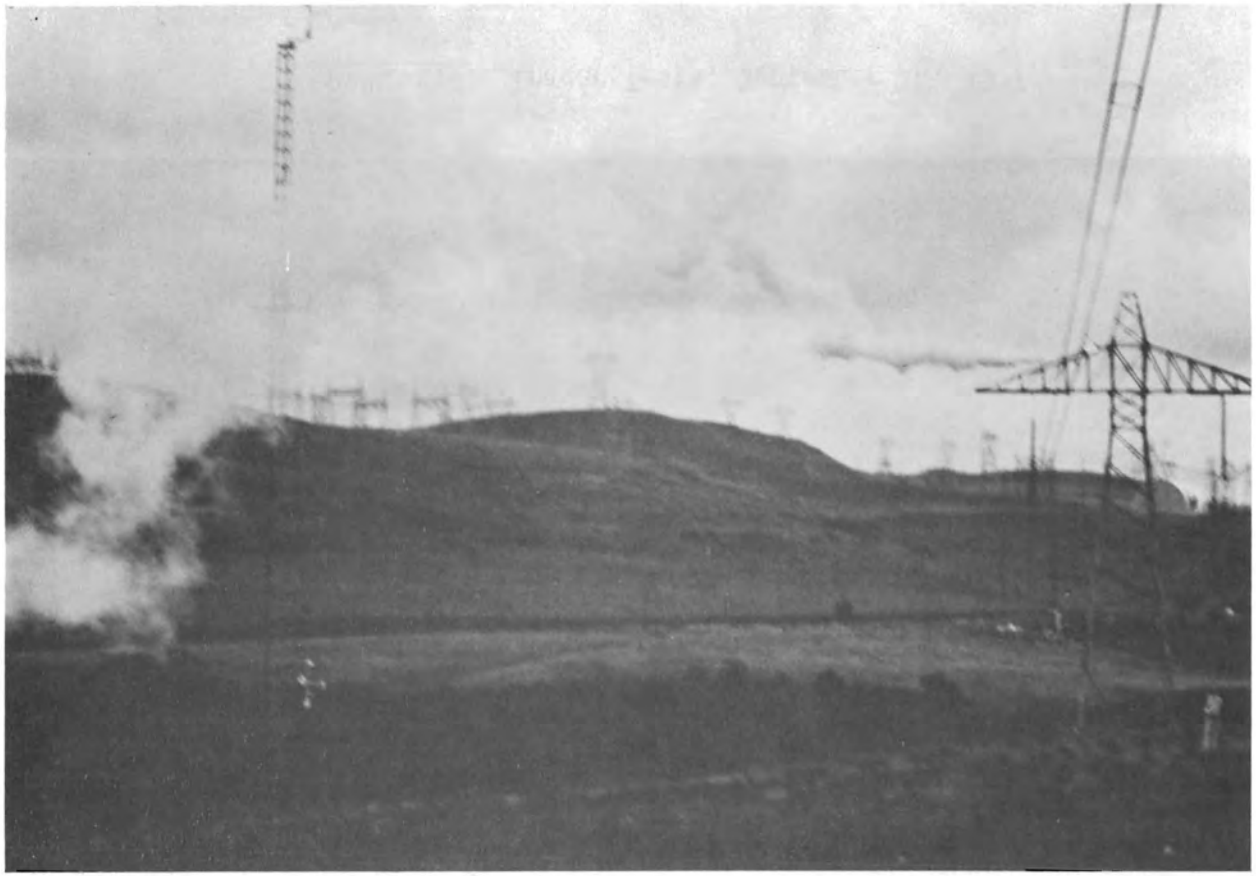

FIGURE 4.8. Tracer Tests, September 28, 1977

is of the same order of magnitude. The two tests reported below provide a basis for checking environmental effects during precipitation at both low and moderate wind speeds.

The results are plotted profiles of ozone concentrations, air temperature mixing ratio and relative humidity (see, for example, Figure 4.9). The fixed-height, (~12 m) ozone-monitor data on the "upwind" side of the conductors are also plotted on the same scale to allow point-by-point comparison with the roving profile ozone values; this is a time series of data at a fixed height, plotted as a profile.

An ozone plume from the energized conductors in the profile studies requires the following for definition:

- An identifiable ozone change over background ozone concentrations occurring in the downwind profile.
- No evidence of ozone change existing in the fixed-height time series on the upwind side.
- The downwind profiles of temperature and moisture not having changes that correspond to the identifiable ozone change.
- The horizontal and vertical wind fields being consistent with the location of the identifiable ozone change.

To illustrate the method of analysis, profiles with effects not attributable to the energized lines will be presented. This example clearly demonstrates that the roving ozone monitor and the fixed-height ozone monitor on opposite sides of the HVdc conductors respond in an identical fashion to ambient ozone concentrations.

Figures 4.9 to 4.12 contain a record of an event in the ozone concentration traces. This event occurred during precipitation and the ozone concentrations were relatively low (~13 ppb) at both monitors. The profiles of roving ozone, fixed ozone, temperature and moisture variables are identified in the key. These figures are in pairs: first the upsweep profile and then the downsweep profile for the time period given on the x-axis.

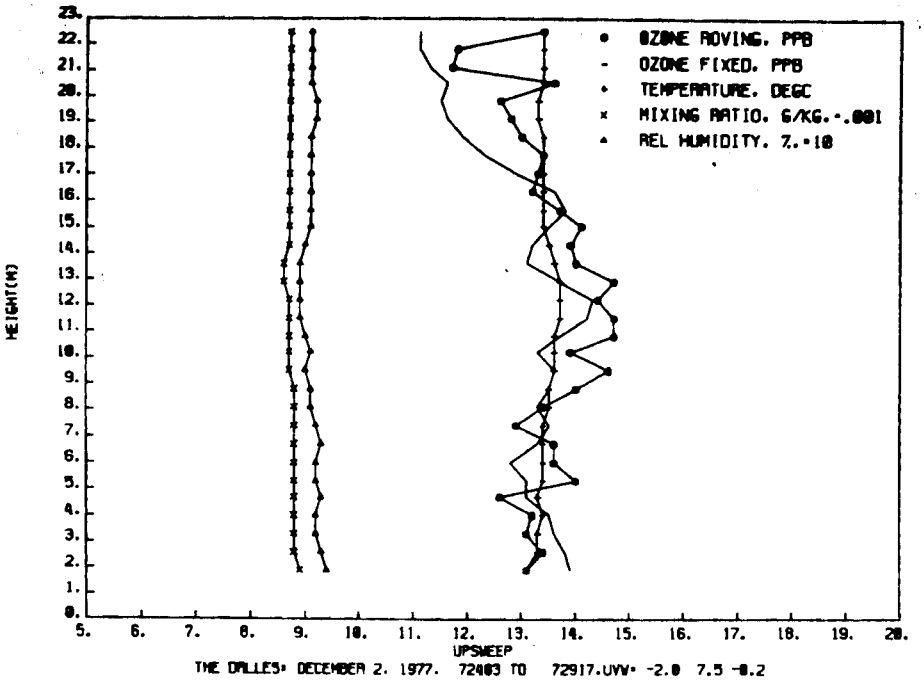

FIGURE 4.9. Vertical Profiles for December 2, 1977 (±500 kV)

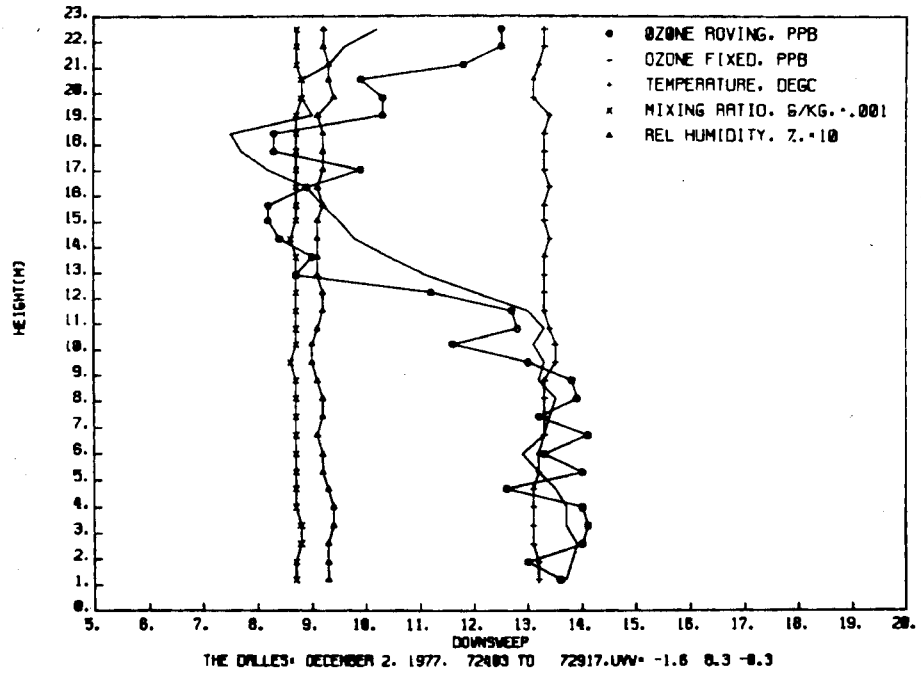

FIGURE 4.10. Vertical Profiles for December 2, 1977 (±500 kV)

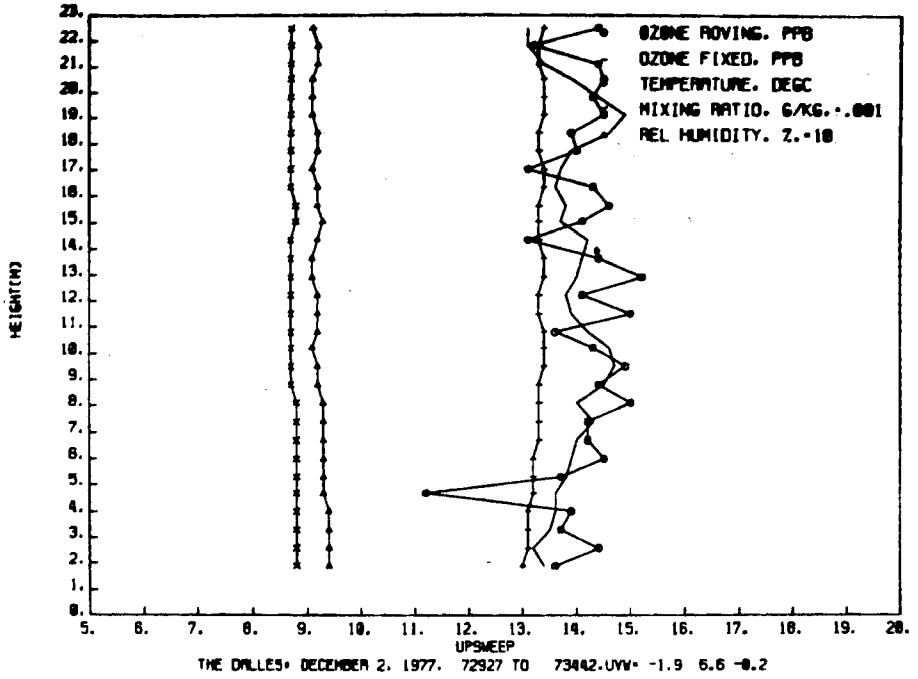

FIGURE 4.11. Vertical Profiles for December 2, 1977 (±500 kV)

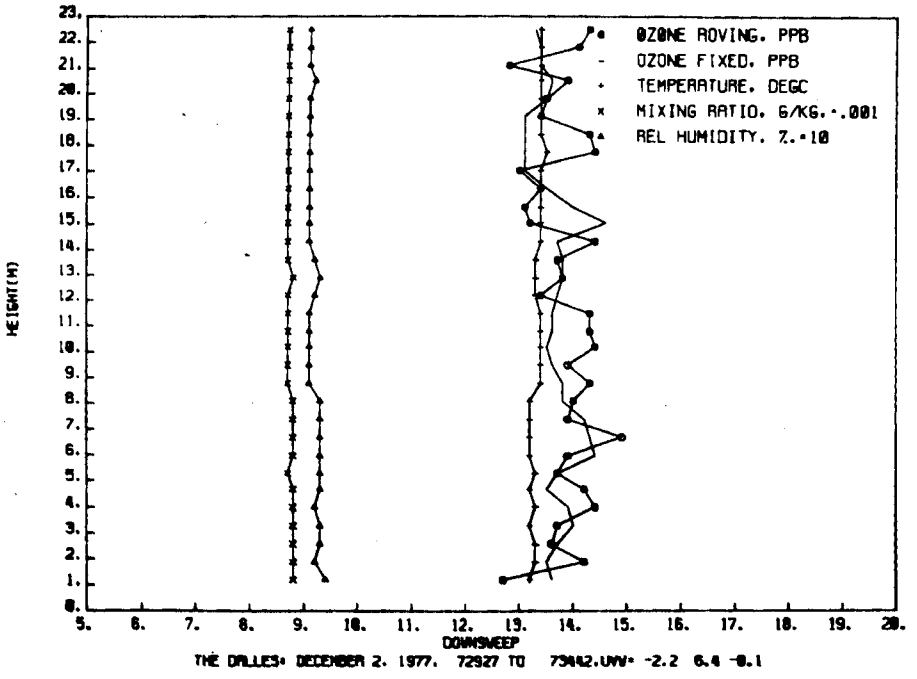

FIGURE 4.12. Vertical Profiles for December 2, 1977 (±500 kV)

The terms upsweep and downsweep refer to the physical direction of movement of the profiling sensors. The u, v, and w average wind speed components at conductor height are given in m/sec after the time period. These components show that the winds were nearly directly across the conductors towards the profiling tower.

In Figure 4.9, the ozone of the fixed monitor and the roving, intake monitor are in reasonably close agreement on the lower portion of the first upsweep. The ozone levels decrease for both monitors as the roving intake reaches the top of its sweep. Figure 4.10 shows the fixed-height-monitor ozone concentrations dropping to almost 7 ppb on the subsequent downsweep profile. A corresponding drop in ozone concentration is measured by the roving, intake line at about a 17-m height. Then as the roving intake reaches the same height as the fixed monitor, the measured concentration from both monitors returns to the ∿13 ppb level. Changes in the temperature profiles indicate an association of the decrease in the roving ozone concentrations with atmospheric circulations. Figures 4.11 and 4.12 are the next upsweep and downsweep profiles. The decrease in ozone concentration appears to have passed. Subsequent profiles did not repeat this event, which clearly cannot be attributed to the energized conductors.

The "large depression" of ozone concentrations that clearly registered on both the upwind and downwind monitors is only about a 6 ppb change in concentration. The absolute concentrations of the monitors for the concurrent measurements at a 12-m height agree with ±0.5 ppb These results demonstrate that profiles with structure features of several ppb can be detected and comparably identified with the data from both monitors.

4.2.1 Profile Case Study #1: Low Wind Speeds and Precipitation

Profile data were obtained from 14:53 to 18:00 on November 28, 1977. During this late afternoon test, the winds were near calm and shifting. Steady precipitation amounting to 2.19 mm occurred during the 3-hr measurement period.

The individual plots of ozone, temperature, and moisture for 15:32 to 17:56 on November 28, 1977 are given in Appendix F. These are similar in format to previous plots, but the coding is slightly different. These are plots of roving system profiles and time series data from the fixed-height ozone monitor. The times given on the x-axis label are for pairs of plots, one upsweep and one downsweep. This series includes all profiles with major ozone changes. Of these, only certain typical and worst-case profiles have been selected for discussion in the text. The corona loss values for this case summarized from the records at the BPA HVdc control room are given in Table 4.1.

TABLE 4.1. Corona Loss for Profile Case Study #1, November 28, 1977

Time	Positive Corona Current, mA	Negative Corona Current, mA	Bipolar Potential, kV
14:30	30	28	500
15:00	57	52	550
15:30	59	60	550
16:00	65	57	550
16:30	36	38	550
17:00	55	36	550
17:15	70	67	550
17:30	38	45	550
18:00	34	39	500

The above corona loss values are typical of the larger values associated with precipitation at the test facility. The highest observed values in earlier tests at this facility were on the order of 100 mA for the negative pole (BPA, 1977). This case study represents conditions of up to 70% of the worst-case corona loss values based on these earlier studies.

Ambient ozone concentrations were on the order of 2 to 4 ppb. Although near the detection limit of the monitors, the dual ozone traces were consistent within ±0.5 ppb during periods without ozone plumes.

The winds were defined by the auxiliary wind speed and direction system located near the mobile laboratory, since the three-level wind data system was not functional during this test. The near-calm conditions made the exact definition of trajectories very difficult, because the wind direction has little meaning when major shifts and sensor stalls occur during the plume travel time from the conductors to the monitor. For the shortest distance and a steady 1 m/sec wind, the travel time is about 0.5 minutes. Typically, at least several minutes of travel time are anticipated for these conditions of constantly shifting wind direction with calm periods. Definition of the trajectories between the energized conductors and the monitoring points cannot be expected to be reliable under these conditions.

The method of analysis for these conditions is to inspect the dual ozone concentration traces for unexplained perturbations between the profile and fixed-height monitors. If these cannot be clearly attributed to natural variability when they are presented and analyzed as possible effects of the HVdc test lines. The shape and height of the ozone profile peaks are used as sensitive indicators to check the consistency of considering the source on the energized conductors.

During low, shifting, wind conditions, the temperature and moisture profiles underwent constant changes as the wind direction shifted. These changes indicate that when the wind shifts to a direction from the conductors to the monitors, concurrent, direction-dependent changes may occur in other profiles. Small changes in temperature and moisture profiles indicate the complexity of flows under near-calm conditions.

Major profile-structure changes such as those shown by Regener and Aldaz (1969) will normally be associated with local inversion or shear layers. The profile shapes will be highly correlated for such conditions. There is no evidence that such conditions existed during these tests.

The very low, background ozone concentrations on the order of 2 to 4 ppb make these profile data ideal for the detection and definition of any ozone plumes from the energized conductors. The shifting winds preclude the definition of the exact origin of profile structure on the basis of trajectories. However, the occurrence of a change in ozone on one side of the conductor and not on the other is strong evidence for a conductor source. Such analysis will envelope the possible environmental effects by including all observed changes across the conductors during the worst-case conditions.

4.2.2 Profile Case Study #2: Moderate-to-High Wind Speeds and Precipitation

Profile data were obtained from 7:13:32 to 10:27:55 on December 2, 1977, with the line operating at ±500 kV. Fifty-two vertical profiles were recorded during this period. Appendix G contains ten selected sets of ozone, temperature, and moisture profiles and fixed-height ozone plots for this case study. These profiles are from the same series as the plots in Figures 4.1 to 4.4 and have an identical format. The plots in Appendix G were selected to illustrate both typical and extreme profiles.

The corona loss and voltage levels for this period are shown in Table 4.2. These values are from the records at the BPA HVdc control room. The corona loss values are about 50% of the worst-case historical values for the test facility. There was 0.95 mm of precipitation during the 3.25-hr study period.

Winds from the three-level, wind-data system were reduced and used in the analysis. The components at conductor height are used in the discussion below. A complete summary of the wind fields for this case are included in Appendix B as part of the general characterization of winds at this site.

The average, vertical-velocity component is downward in each profile set. The magnitude approximately matches the value for flow parallel to the sloping site. The average, intersection point on the profile tower is near the 12-m conductor height.

TABLE 4.2. Voltages and Corona Loss Data for Profile Case Study #2, December 2, 1977

	Positive Pole		Negative Pole	
Time	Voltage, kV	Corona Loss, mA	Voltage, kV	Corona Loss, mA
07:00	501	24	496	34
07:30	506	37	495	57
08:00	506	65	495	38
08:30	503	46	497	39
09:00	503	49	495	51
09:30	503	63	497	47
10:00	506	59	496	41
10:30	503	48	496	52

The wind direction was relatively steady with a downwind component across the conductors towards the profile tower. The speeds were between 6 and 10 m/sec. The average speed was 7.5 m/sec compared to the average speed component of 7.3 m/sec perpendicular to the conductors. In contrast to the first case study, the winds during the second case study allow a clear and consistent definition of trajectories.

Ozone, temperature and humidity profiles based on 52 sweeps are plotted in Figure 4.13. In addition the average upsweep and downsweep ozone profiles are given.

4.3 TRACER TESTS IMPLICATIONS

Tracer tests demonstrated the variability in the plume portion at the downwind profile tower. The plume can intersect at the tower at any height for neutral and unstable conditions. This vertical variability is largely a function of nonuniform aspects at the site. This confirms that the vertical standard deviation for dispersion is larger than given in the literature for uniform sites.

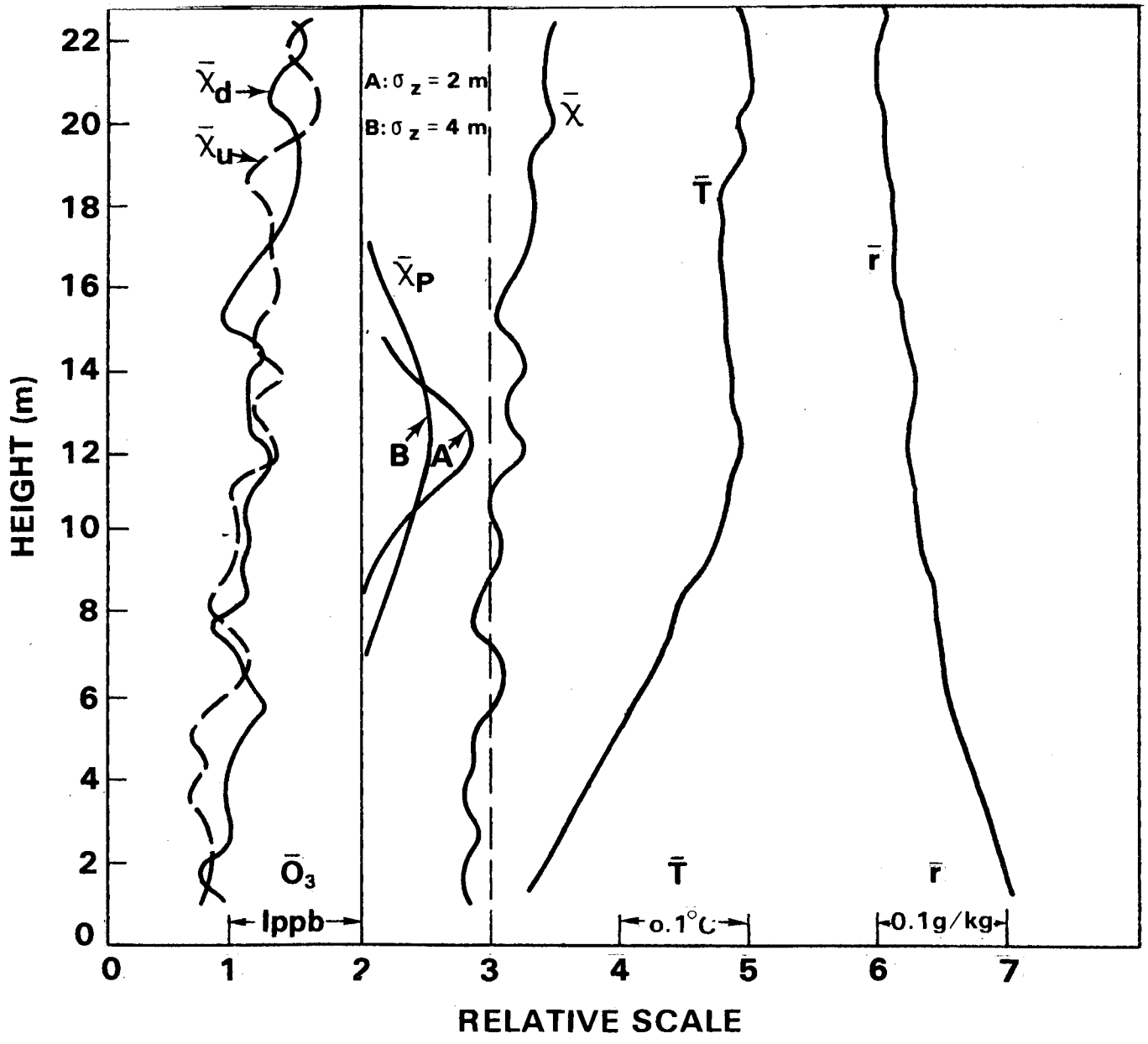

FIGURE 4.13. Average Ozone (O_3), Temperature (T) and Humidity (r) Profiles

Vertical variability has important implications in profile studies. Actual plumes from conductors will be detected in individual profiles under relatively steady flow conditions; these conditions appear to be the exception for the flows observed in the tracer tests. Thus, the tracer test results indicate that a plume, such as the one illustrated in Figure 2.1, will only occasionally be identifiable. The effect of the rapidly varying position of significant ozone plume will generally be to increase the ozone variability at the downwind profile tower.

An additional effect of this greater dispersion will be lowering the height of the predicted peak value, as a result of the contribution of the plume's reflection at the earth's surface. For sufficiently large dispersion rates, the plume will appear as a peak at the earth's surface.

Although the plume from the conductors may intersect at any height on the profile tower, there will generally be a distribution around a central intersection height. For winds perpendicular to the lines, the plume during the unstable condition has a tendency to intersect at heights greater than 12 m on the profile tower. Winds with components parallel to the conductors will have trajectories from areas where the conductor heights are greater than 12 m. Hence, the potential appears best for average plume intersections equal to or greater than the 12-m conductor height, with individual intersection at any height.

4.4 OZONE PROFILE DATA

The results of these two precipitation case studies are discussed below in terms of the consistency of observed ozone peaks, ambient meteorological conditions, and predicted ozone source terms on the energized conductors.

4.4.1 Profile Case Study #1

The series of profiles shown in Appendix F have complex characteristics that reflect the low and shifting winds during the test period. (The line was operating at ±500 kV during the test period.) The first peaks of

interest in this series occur in Figures F-3 and F-4. A major peak of 5 ppb occurs at about 20 m in both the upsweep and downsweep. A second "near noise" peak of 1 to 2 ppb occurs close to the 12-m height. These two peaks, which were repeated in two subsequent profile sweeps, are suggestive of the positive and negative poles. The next sequential profile (F-5) shows a slight upper-level peak and no discernible peak at 12 m. The subsequent few profiles demonstrate no discernible peaks.

A predicted ratio of the peaks for Figures F-3 and F-4 may be computed from experiment parameters independent of the profiles. Accounting for the different distances to the conductors, corona currents (59 mA for the positive pole and 60 mA for the negative pole), and the unequal production rates for each pole, and the ±550 kV voltage on the conductors results in a predicted ratio of 0.38 (5 to 2) for the negative-to-positive pole ozone contributions. This is close to the ratio of the observed major and minor peaks.

The major peak in Figures F-3 and F-4 has a centerline value of about 5 ppb and a vertical standard deviation of about 4 m. Note that for σ_z = 4 m and h = 12, the exponential term in Equation 7 has a value of 1.5×10^{-8} which is insignificant when added to 1.0. As a result the approximation may be dropped from Equation 7 for this case study.

In this situation with very low wind speeds, implied wind speeds will be used to test the consistency of computed ozone production rates. Ozone production rates may be computed two ways: as a function of line voltage and corona current (Equations 4, 5 and 6) and as a function of profile characteristics and wind speed perpendicular to the conductors (Equation 7). Combining these two methods assumes identical source terms and results in the following expression for an implied wind speed, $\bar{u}_{i\pm}$:

$$\bar{u}_{i\pm} = \frac{1.6}{\chi\ \sigma_z} S_{\pm} \times I_{c\pm} \times V_{\pm} \qquad (8)$$

where

- $\pm$ refers to values for either the positively or negatively energized conductors
- χ is the centerline profile peak value
- σ_z is the vertical standard deviation of plume spread.

S is the normalized ozone source term, I_c the corona current, and V the potential of the conductors.

When Equation (8) is applied to the major profile peaks in Figures F-3 and F-4 an implied wind speed of 0.5 m/sec results. This wind speed is within the observations of 0 to 1 m/sec winds during the testing period. Hence, the ozone peaks in Figures 4.9 and 4.10 are consistent with the ozone source terms predicted from laboratory tests for the negative conductor poles.

The minor peak at 12 m is not as well defined as the peaks at 20 m. If a positive conductor source for the peak is assumed and σ_z = 3 m is used (derived by adjusting the negative σ_z value for a shorter distance), the peak of 1 to 2 mb produces implied wind speeds of 0.3 to 0.5 m/sec. Again the wind speed estimates are consistent with the observed values, thus implying a consistency between observed profile and computed conductor production rates.

The maximum of corona loss occurred at 17:15 during this case study (see Table 4.1). This maximum loss was associated with several ozone profiles with larger changes in ozone concentrations than those discussed for Figures F-3 and F-4. The peaks in profiles, such as F-30, range up to 10 ppb with standard deviations on the order of 10 m. A value of $\bar{u}$ of 0.25 m/sec is predicted using Equation (8) with a value of 137 mA for total corona loss. As in the first case, the observed profiles are consistent with the production rates and ambient conditions. For these profiles, the difference between large ozone peaks and the background values was interpreted as being the effect of the energized conductors. Observations indicated that the smaller profile changes corresponded closely to

temperature profile changes, while the larger ozone did not demonstrate the same correspondence.

The change in the σ_z values is an important difference between the above two examples. The first example has a σ_z value of about 4 m, which is the approximate magnitude expected for neutral conditions, and a 26-m fetch. The second example has a much larger σ_z value, estimated to be 10 m. The larger σ_z values are indicative of either greater dispersion or a longer fetch. The ambient atmospheric conditions have changed little between these two cases and a fetch change appears to be the most likely cause of the change in σ_z values. Winds at an angle to the conductor will have a longer fetch and the change in σ_z values may be explained by a change in wind direction: the first peaks are for winds nearly perpendicular to the conductors as realized by the small σ_z values, and the second peaks are for winds with a significant component parallel to the conductors allowing the additional fetch for generation of the larger values of σ_z.

4.4.2 Profile Case Study #2

The profile peaks attributable to the energized conductors are not as clearly defined in the second case study as those in the first case study. (The line was operating at ±500 kV.) There are distinctive ozone profile peaks, which are clearly not from the conductors. The latter are presented and discussed in Section 4.2.

Variation of the ozone concentrations is large for certain profiles. Some of these, such as the variations indicated in Figure G-4 (downsweep), demonstrate similar variations in the upwind (ozone-fixed) and downwind (ozone-roving) profiles. These variations are coupled with variations in the temperature and moisture profiles and are clearly the result of natural variability not associated with the energized conductors.

The upsweep profile for 07:34:52 to 07:40:11 is an interesting example, having both natural and apparent conductor-derived ozone variations (see Figure G-3). Up to 10 m, the dual ozone traces show similar variations

indicating natural variations. At 13- and 19-m height ozone peak features occur, both with concentration peaks of about 1.5 mb and a vertical standard deviation of about 1.5 m. Lack of similar structure in either the upwind or concurrent micrometeorological profiles indicates that a local source caused these peak ozone variations.

This dual peak has two alternative interpretations: the ozone plumes from the conductors may have been intersected twice by the roving sensor, or the two peaks may be separate plumes from the two energized conductor lines. The ratios of the predicted atmospheric ozone concentrations from the negative and positive conductors are 0.25 at 07:30 to 0.65 at 08:30 based on the data given in Table 4.2. Without real-time, corona-loss data, the variability in such values makes equal peaks for the negative and positive conductors a possibility.

Although almost masked by the background variability, discernible peak ozone features such as these are attributed to ozone from the energized conductors. No corresponding peak structure exists in the upwind monitor record. These ozone peaks are identifiable because their peak values and vertical extents are larger than those exhibited by the background variability. These peaks are not coupled with variations in temperature or moisture profiles. These ozone peaks occur during periods when the variability in wind speed is smaller than the variability during periods when no peaks are discernible. These observations indicate that these peaks are likely the result of energized conductors.

Table 4.3 contains a comparison of observed and predicted ozone source terms for this example and several other profiles with similar ozone peaks. Table 4.4 has the values used in each computation. Predicted values are computed both for an average source term from both conductors pole (see Equation 6) and based on single poles (see Equations 4 and 5) as noted in the table. Input data is derived from Table 4.2. The observed source term values are computed from Equation (7) when solved for Q_L:

TABLE 4.3. Comparisons of Observed and Predicted Ozone Source Terms for Case Study #2, December 2, 1977

Profile Figures in Appendix G	Profile Source Terms, ppb m^2 sec^{-1}	Predicted Source Terms, ppb m^2 sec^{-1}	
		Both Poles	Single Poles[a]
G-1	18	4.8	4.4
G-2	6.4	5.8	5.5
G-3	8.0	6.2	4.5
			1.5 (p)
G-3	8.0	6.2	4.5
G-5	15.1	5.7	4.3
G-7	9.5	6.9	4.5
G-10	8.0	6.9	4.5
Averages	10.4 ± 4.4	6.1 ± 0.7	4.6 ± 0.4

[a] Computed based on emission from the negative conductor; Positive values indicated by (P).

TABLE 4.4. Summary of Profile and Conductor Variables for Case Study #2

Profile Figures in Appendix G	Observed Variables				Conductor Variables		
	Observed Profile Peak, ppb	Profile Vertical Standard Deviation, m	Height of peak, m	Wind Speed, m/sec	Bipolar Potential, kV	Corona Loss, mA Both Poles	Corona Loss, mA Single Poles[a]
G-1	1.5	2.0	15	9.6	500	77	46
G-2	1.0	1.6	10	6.4	500	94	57
G-3	1.5	1.2	11.5	7.1	500	99	48 51 (P)
G-3	1.5	1.2	19	7.1	500	99	48
G-5	1.2	2.4	17	6.9	500	93	45
G-7	0.9	2.0	13	8.4	500	110	47
G-10	1.0	1.6	12	8.0	500	97	48
Averages	1.2	1.7	13.9	7.6	500	97	48

[a] Computed based on emission from negative conductor except for values marked with (P), which are based on the positive conductor.

$$Q_L = \frac{\chi(x)\sigma_z\bar{u}}{1.60\left[1 + EXP\left(\frac{-2h^2}{(\sigma_z)^2}\right)\right]} \qquad (9)$$

Values of χ and σ_z are directly from the ozone profiles; $\bar{u}$ is the wind component perpendicular to the conductors as measured by the 12-m Gill anemometer.

There is a bias in the computation of the values in Table 4.3 that will tend to produce slightly larger observed estimates than predicted estimates for a given set of conditions. This bias results from using observations for maximum conditions (ozone peaks) and predictions based on half-hour average values (corona currents).

The results in Table 4.3 show that conductor source term interpretations of the peaks in Figure G-3 are consistent with the predicted ozone production rates. The agreement in Table 4.3 is quite good considering the variability in the profiles and uncertainty in the corona loss estimates. The observed values are slightly higher than the predicted values, but are still within the scatter of the data. The maximum observed changes in ozone concentrations 26 m downwind under worst-case precipitation conditions with moderate-to-high winds are consistent with predicted ozone production rates.

The average profiles for case study #2 are given in Figure 4.13. The average of ozone upsweep profiles, of ozone downsweep profiles and of ozone temperature and moisture for all sweeps are plotted. The shapes of the average ozone upsweep and ozone downsweep are consistent in their general slope and have similar detailed structure.

Average profiles of temperature and moisture are reasonable. The temperature profile shows a clear decrease near the earth's surface, and the moisture profile shows an increase at the earth's surface. These temperature and moisture profiles are consistent with evaporation from the wet earth's surface. Both of these profiles demonstrate an approximate exponential behavior at the earth's surface.

The average ozone profile does not have the expected exponential decay at the earth's surface; a linear fit with height is possible with a decrease of ozone towards the earth's surface. Little evidence of a major peak at about 12 m exists, possibly because of the great variability in plume position. The explanation of the absence of an exponential profile might be the result of the vertical variability, causing an apparent ground source term of ozone. However, the ozone concentrations required for even a slight filling of the ozone profile exceed the concentration plumes predicted or observed for these conditions. The predicted peak of ozone based on two values of σ_z has been plotted in Figure 4.13.

Another explanation for the absence of the exponential decay in the lower portion of the ozone profile is that there are other surfaces in addition to the energized conductors in corona. Kasemir (1978) notes that the maximum natural electric field is limited to ±10 kV/m by natural corona discharge at the earth's surface. Over very smooth surfaces, such as lakes, the corona discharge will not be limiting and maximum fields may occur of ±50 to ±100 kV/m (Toland and Vonnegut 1977). The 10 kV/m is much below the induced gradient values at ground level under these conductors; hence, corona may be expected at the ground surface. The possibility that the ozone produced by the high voltages may be from ground surfaces has, as far as the authors are aware, not been considered previously. The apparent increases in ozone concentration of 1 to 2 ppb in the lower portion of the profile are very small compared to ambient background concentrations, ranging up to 50 ppb during test periods. Such an increase is consistent with a small source of ozone near the earth's surface affecting the lower portion of the natural ozone profiles.

Whether the result of large dispersion values or corona at the earth's surface (more likely a combination of these effects), the average profiles in Figure 4.13 do demonstrate that large changes in ozone concentrations are not occurring as a result of energized conductors. Any increase in near-surface ozone concentrations under these worst-case conditions was less than the natural decrease near the earth's surface.

5.0 CONCLUSIONS

The test results indicate that environmental ozone from HVdc transmission lines, even for worst-case conditions, is reasonably predicted by extrapolating ozone production rates from wind-tunnel tests. This confirmation of the production rates is based on agreement between observed and predicted ozone plume parameters during precipitation conditions.

The magnitudes of changes in ozone concentrations attributable to the energized conductors are small for all conditions. For fair weather conditions, the effects, if any, are not detectable in the natural variability of ambient ozone. The worst-case plume for an elevated plume is a 10 ppb increase for low wind precipitation conditions 26 m from the conductor centerline with ±500 kV and a total of 137 mA corona current for both poles. The surface level increase in ozone is less but of the same order of magnitude. This high value and extended vertical distribution is attributed to the long fetch created by winds nearly parallel to the conductors.

The roving-profile technique has proven to be an effective method for defining the low concentrations of ozone emission from HVdc transmission lines. The origins of ozone plumes are identified in a reliable and consistent fashion as a result of the sensitivity of the approach for determining small changes in ozone concentrations.

6.0 REFERENCES

Aldaz, L. 1969. "Flux Measurements of Atmospheric Ozone Near Land and Water." Journal of Geophysical Research 74:6939-6946.

Bonneville Power Administration 1977. Transmission Line Reference Book HVDC to ±600kV. Published by Electric Power Research Institute, Palo Alto, California.

Coffey, P. E. and W. M. Stasiuk, Jr. 1975. "Evidence of Atmospheric Transport of Ozone into Urban Areas." Environmental Science Technology 9:59-62.

Committee on Medical and Biological Effects of Environmental Pollutants 1977. Ozone and Other Photochemical Oxidants. National Academy of Sciences, Washington, DC.

Droppo, J. G. and J. C. Doran 1978. "Dry Deposition of Gaseous Pollutants from Coal-Fired Power Plants." In Part 3 of Pacific Northwest Laboratory Annual Report for 1977 to the DOE Assistant Secretary for Environment. PNL-2500 PT3, p.1.27, Pacific Northwest Laboratory, Richland, Washington.

Droppo, J. G., et al. 1976. Measurement of Dry Deposition of Fossil Fuel Pollutants. Prepared for the EPA under Contract 62-02-1747, Battelle, Pacific Northwest Laboratories, Richland, Washington.

Galbally, I. 1971. "Ozone Profiles and Ozone Fluxes in the Atmospheric Surface Layer." Quarterly Journal of the Royal Meteorological Society 97:18-29.

Galbally, I. 1968. "Ozone Variation and Destruction in the Atmospheric Surface Layer." Nature 218:456-457.

Kasemir, H. W. 1978. "Corona Discharge and Thunderstorm Fields." Preprint of Conference on Cloud Physics and Atmospheric Electricity, Seattle, Washington.

Morris, R. M. and B. Rakoshadas 1964. "An Investigation of Corona Loss and Radio Interference from Transmission Line Conductors at High Direct Voltages." In Proceedings of Power Apparatus and Systems, IEEE, New York, New York.

Pasquill, F. 1974. Atmospheric Diffusion. 2nd ed. John Wiley and Sons, New York, New York.

Regener, V. H. and L. Aldaz 1969. "Turbulent Transport Near the Ground as Determined from Measurements of the Ozone Flux and the Ozone Gradient." Journal of Geophysical Research 74:6935-6942.

Roach, J. F., V. L. Chartier and F. M. Dietrich 1974. "Experimental Oxidant Production Rates for EHV Transmission Lines and Theoretical Estimates of Ozone Concentrations Near Operating Lines." Scientific Paper 73-1L3-COCEM-P1, Westinghouse Electric Corporation, Pittsburg, Pennsylvania.

Roach, J. F. 1973. Ozone Concentrations Near EHV and UHV Transmission Lines. Research Report 73-1L3-COCEM-R1, Westinghouse Electric Laboratories, Pittsburg, Pennsylvania.

Sandberg, J. S., M. J. Basso and B. A. Okin 1978. "Winter Rain and Summer Ozone: A Predictive Relationship." Science 200:1051-54.

Scherer, H. N. Jr., B. J. Ware and C. H. Shih 1973. "Gaseous Effluents Due to EHV Transmission Line Corona." IEEE Trans. Power, Apparatus and Systems 92:1043-1049.

Strom, G. H. 1976. "Transport and Diffusion of Stack Effluents." Air Pollution. 3rd edition. Ed. Arthur C. Stern. Academic Press, New York, New York.

Toland, R. B. and B. Vonnegut 1977. "Measurement of Maximum Electric Field Intensities over Water During Thunderstorm." Journal of Geophysical Research 82(3):438-440.

7.0 GLOSSARY

Corona (discharge):	A luminous, and often audible, electric discharge that is intermediate in nature between spark discharges and point discharges. It is associated with the high voltages in both HVac and HVdc transmission lines. Corona also occurs when the natural electric field strength near surfaces exceeds ±10 kV/m.
Gaussian Model:	A mathematical model that expresses downwind transport and dispersion of an atmospheric release in terms of a normal distribution. The statistical estimates of the dispersion rates are standard deviations of plume spread in downwind (σ_x), lateral (σ_y) and vertical direction (σ_z).
Line Source, Q_L:	The magnitude of a release to the atmosphere occurring from an extended horizontal line. The release rate is normalized to mass per length per time.
Ozone:	A nearly colorless gaseous triatomic form of oxygen with an odor similar to weak chlorine. The molecular weight is 48 and formula is O_3. Ozone is a product of corona discharge.
Profile:	The graph of the magnitude of a variable as a function of height.
Release Height, h:	The elevation over the surface at which a release to the atmosphere occurs.
Roughness Length, z_o:	A measure of the roughness of the natural surfaces over which the air flows. The value is defined as a fraction of the average height of surface irregularities.
Tracer:	A visible cloud released to study air motions.

APPENDIX A

Computing Corona Loss

Corona loss and ozone production were computed as follows for tests conducted at the BPA HVdc Test Facility.[a]

The two sections of the test line are: L = 2.02 km for line section 1, and 0.75 km for the wood pole section. The ratio of the corona current for these two sections as determined by simultaneous measurements of total current to line section 1 is 0.6. For every 1 mA of total corona current, I_c, at the control house as reported in the test, about 0.6 mA is for line section 1 on which the tests were conducted.

The corona current density (I) at the test site is:

$$I = \frac{0.6\ I_c}{L} = 3 \times 10^{-4}\ I_c, \text{ amperes per meter}$$

This current loss converted to corona loss (CL), for each pole of the test line is

$$CL = 30\ I_c V, \text{ watts per meter}$$

where I_c is in amperes and V is the voltage on the pole in hundreds of kV.

Production rates, P_+, P_-, for ozone on DC conductors are (Scherer, et al. 1973):

$$P_- = 1.2 \times 10^{-9} \text{ kg/W/sec}$$

$$P_+ = 0.4 \times 10^{-9} \text{ kg/W/sec}$$

These are relatively independent of a gradient factor. The resulting predicted ozone source strengths (S_+,S_-) of the dc test line are:

---

[a] BPA supplied this procedure.

$$S_- = 1.9 \times 10^{-2} I_{c-} V_- \quad \text{ppb m}^2 \text{ s}^{-1}$$

$$S_+ = 0.6 \times 10^{-2} I_{c+} V_+ \quad \text{ppb m}^2 \text{ s}^{-1}$$

The mean ozone source strength (S) for both conductors is:

$$\overline{S} = 1.2 \times 10^{-2} I_c \overline{V} \quad \text{ppb m}^2 \text{ s}^{-1}$$

REFERENCE

H. N. Scherer, Jr., B. J. Ware and C. H. Shih, "Gaseous Effluents Due to EHV Transmission Line Corona", IEEE Trans. Power Apparatus and Systems, Vol. PAS-92, pp. 1043-1049, May/June 1973.

APPENDIX B

Windfield Definition for Case Study #2

Case Study #2

For case study #2, a detailed summary of winds and temperatures during precipitation conditions at three heights is given in Tables B-1, B-2 and B-3.

Tables B-1 is a summary of conditions for each profile sweep. UP refers to an upsweep and DN to a downsweep. The three numbers under DN or UP are the date, time of the last data point in the sweep, and cumulative number of values. These may be matched with profiles in Appendix C using the indicated times. The three values from top to bottom are for the 21.3-m, 12.2-m and 3.1-m heights and are in m/sec unless otherwise specified. Starting from the right of the tables, WS is the average wind speeds, WV the ratios of the vector wind speeds to the average wind speeds, T the air temperatures in °C, and UM and SD are average wind speeds and their standard deviation parallel to the conductors. Continuing across the table, VM and SD are average wind speeds and their standard deviations perpendicular to the conductors, WM the average vertical velocities, CO the average concentrations from the Monitor Labs Ozone, Beckman Ozone, and REM NO_x monitors. TIME indicates the times computed at each height for the winds to travel from the midline between the conductors and the measurement tower. HEIGHT refers to the computed changes in height for the winds between the conductors and the measurement tower. The negative value of the intersection height corresponds to the slope of the site for this data set with a tendency for winds to be closer to horizontal and less parallel to the slope at higher heights.

Tables B-2, B-3 and B-4 contain average values for longer time periods from the same data period. WS, UM, VM, WM and T have the same definition as in B-1.

Figures B-1, B-2 and B-3 are frequency plots of the occurrence of wind speed groups for the three heights in m/sec (across the page) and wind direction in tens of degrees (down the page).

TABLE B-1. Wind and Temperature Conditions for Individual Profiles, Case Study #2

2.3 MIN

DN	WS	WV	T	UM	SD	VM	SD	WM	CO	TIME	HEIGHT
120277.	8.68	0.995	13.0	-0.932	0.902	8.58	0.870	-0.761	12.9	5.84	-2.93
71318.	8.03	0.996	13.1	-0.811	0.782	7.95	0.936	-0.575	12.3	4.15	-2.59
31.	7.03	0.993	13.0	-0.515	0.863	6.96	1.13	-0.847	124.	4.74	-4.02

2.6 MIN

UP	WS	WV	T	UM	SD	VM	SD	WM	CO	TIME	HEIGHT
120277.	9.12	0.997	12.7	-1.52	0.844	8.96	1.66	-0.903	12.7	5.68	-3.32
71553.	8.17	0.997	12.7	-1.32	0.728	8.04	1.33	-0.674	12.6	4.11	-2.77
62.	6.81	0.990	12.7	-1.03	0.994	6.66	1.54	-0.659	124.	4.96	-3.27

2.7 MIN

DN	WS	WV	T	UM	SD	VM	SD	WM	CO	TIME	HEIGHT
120277.	11.0	0.997	12.6	-2.65	0.906	10.7	0.881	-0.691	14.2	3.09	-2.14
71833.	9.89	0.996	12.6	-2.31	0.787	9.57	1.23	-0.550	15.6	3.45	-1.89
94.	8.41	0.993	12.8	-1.96	0.878	8.12	1.38	-0.886	119.	4.07	-3.60

2.7 MIN

UP	WS	WV	T	UM	SD	VM	SD	WM	CO	TIME	HEIGHT
120277.	9.62	0.998	12.5	-2.32	0.662	9.32	0.885	-0.461	15.7	5.54	-1.63
72112.	8.76	0.998	12.7	-2.00	0.570	8.51	0.870	-0.546	13.6	5.88	-2.12
126.	7.21	0.995	12.8	-2.04	0.637	6.86	1.17	-0.757	122.	4.79	-3.63

2.6 MIN

DN	WS	WV	T	UM	SD	VM	SD	WM	CO	TIME	HEIGHT
120277.	10.1	0.997	12.5	-2.33	0.922	9.77	0.765	-0.661	14.1	5.58	-2.23
72348.	9.34	0.997	12.5	-2.03	0.777	9.09	0.898	-0.617	13.9	5.63	-2.24
157.	7.42	0.996	12.7	-1.55	0.566	7.23	1.20	-0.784	135.	4.57	-3.58

2.7 MIN

UP	WS	WV	T	UM	SD	VM	SD	WM	CO	TIME	HEIGHT
120277.	9.63	0.997	12.5	-2.32	0.818	9.31	1.03	-0.606	11.7	5.54	-2.15
72633.	8.71	0.998	12.5	-2.01	0.694	8.45	1.11	-0.606	11.5	3.90	-2.37
190.	7.14	0.997	12.6	-1.88	0.632	6.87	1.18	-0.735	124.	4.80	-3.53

2.7 MIN

DN	WS	WV	T	UM	SD	VM	SD	WM	CO	TIME	HEIGHT
120277.	9.28	0.996	12.5	-2.93	0.857	8.76	1.10	-0.524	13.5	3.77	-1.97
72913.	8.01	0.995	12.6	-2.55	0.750	7.56	1.09	-0.426	12.9	4.37	-1.86
222.	6.91	0.992	12.7	-2.30	0.880	6.46	1.23	-0.735	126.	5.11	-3.74

TABLE B-1. continued

2.7 MIN

UP	WS	WV	T	UM	SD	VM	SD	WM	CO	TIME	HEIGHT
120277.	8.55	0.995	12.5	-3.35	0.907	7.81	0.998	-0.524	13.8	4.22	-2.21
73157.	7.23	0.993	12.7	-2.91	0.779	6.56	1.11	-0.220	13.7	5.03	-1.11
255.	6.33	0.991	12.7	-2.78	0.909	5.63	1.15	-0.402	125.	5.87	-2.56

2.7 MIN

DN	WS	WV	T	UM	SD	VM	SD	WM	CO	TIME	HEIGHT
120277.	8.44	0.996	12.5	-2.84	0.682	7.91	0.816	-0.307	14.1	4.17	-1.28
73437.	7.15	0.996	12.8	-2.47	0.590	6.67	1.03	-0.215	13.9	4.94	-1.06
287.	5.66	0.991	12.8	-2.30	0.823	5.12	0.979	-0.266	122.	6.44	-1.71

2.7 MIN

UP	WS	WV	T	UM	SD	VM	SD	WM	CO	TIME	HEIGHT
120277.	9.16	0.995	12.5	-3.69	1.00	8.34	1.21	-0.524	14.0	3.96	-1.28
73722.	8.15	0.994	12.8	-3.19	0.871	7.44	1.48	-0.184	14.0	4.44	-0.815
320.	6.55	0.993	12.7	-2.55	1.01	5.98	1.28	-0.541	118.	5.52	-1.88

2.8 MIN

DN	WS	WV	T	UM	SD	VM	SD	WM	CO	TIME	HEIGHT
120277.	8.94	0.996	12.6	-3.34	0.836	8.25	0.970	-0.194	13.7	4.00	-0.777
74007.	7.83	0.996	12.8	-2.89	0.722	7.24	1.02	-0.134	13.5	4.56	-0.609
353.	6.98	0.995	12.8	-3.09	1.10	6.21	1.15	-0.445	134.	5.31	-2.56

2.7 MIN

UP	WS	WV	T	UM	SD	VM	SD	WM	CO	TIME	HEIGHT
120277.	9.35	0.995	12.5	-3.37	1.04	8.68	0.891	-0.171	13.4	3.80	-0.652
74251.	8.24	0.995	12.8	-2.92	0.693	7.66	1.10	-0.340	13.5	4.31	-1.46
386.	6.92	0.989	12.8	-2.66	1.05	6.30	1.17	-0.617	117.	5.24	-3.23

2.7 MIN

DN	WS	WV	T	UM	SD	VM	SD	WM	CO	TIME	HEIGHT
120277.	8.68	0.996	12.5	-4.00	0.942	7.67	1.19	-0.112	13.6	4.30	-0.480
74536.	7.54	0.996	12.8	-3.47	0.818	6.66	0.958	-0.278	13.5	4.95	-1.38
419.	5.96	0.996	12.7	-2.81	0.767	5.23	0.988	-0.443	124.	6.31	-2.79

2.8 MIN

UP	WS	WV	T	UM	SD	VM	SD	WM	CO	TIME	HEIGHT
120277.	9.16	0.994	12.5	-4.10	0.954	8.13	0.891	-0.263	13.7	4.06	-1.07
74821.	7.93	0.994	12.8	-3.56	0.829	7.03	0.968	-0.330	13.3	4.69	-1.55
452.	7.00	0.995	12.7	-3.45	0.901	6.04	0.924	-0.623	109.	5.46	-3.40

2.7 MIN

DN	WS	WV	T	UM	SD	VM	SD	WM	CO	TIME	HEIGHT
120277.	7.29	0.994	12.6	-3.60	0.804	6.29	0.867	-0.903E-01	12.8	5.24	-0.474
75106.	6.36	0.995	12.8	-3.13	0.712	5.49	0.853	-0.231	13.2	6.01	-1.39
485.	6.09	0.996	12.8	-3.29	0.756	5.09	0.887	-0.418	126.	6.49	-2.71

TABLE B-1. continued

2.8 MIN

DN	WS	WV	T	UM	SD	VM	SD	AM	CU	TIME	HEIGHT
120277.	11.3	0.998	12.7	-2.54	0.452	11.0	1.32	-0.571	9.61	3.00	-1.71
84051.	10.7	0.998	12.7	-2.20	0.724	10.5	1.06	-0.684	9.68	3.16	-2.16
47.	8.48	0.995	13.0	-2.20	0.724	8.15	1.23	-0.908	109.	4.05	-3.68

2.8 MIN

UP	WS	WV	T	UM	SD	VM	SD	AM	CU	TIME	HEIGHT
120277.	11.0	0.996	12.7	-2.44	0.912	10.7	1.32	-0.923	11.9	3.07	-2.84
84341.	10.2	0.998	12.8	-2.13	0.748	10.0	1.29	-1.08	11.5	3.30	-3.55
81.	8.67	0.995	13.0	-1.87	0.864	8.45	1.37	-0.951	95.9	5.92	-3.73

2.8 MIN

DN	WS	WV	T	UM	SD	VM	SD	AM	CU	TIME	HEIGHT
120277.	10.5	0.999	12.6	-1.70	0.605	10.3	1.19	-0.510	11.8	3.20	-1.65
84631.	9.49	0.999	12.8	-1.48	0.529	9.36	1.24	-0.934	11.7	3.53	-3.30
115.	7.83	0.994	12.8	-1.24	0.912	7.68	1.41	-0.765	102.	4.30	-3.37

2.7 MIN

UP	WS	WV	T	UM	SD	VM	SD	AM	CU	TIME	HEIGHT
120277.	10.3	0.996	12.6	-2.51	0.978	9.94	0.703	-0.701	12.3	3.32	-2.33
84915.	9.36	0.996	12.7	-2.00	0.829	9.11	0.828	-0.690	11.9	3.62	-2.50
148.	7.99	0.996	12.7	-1.72	0.730	7.77	1.23	-0.857	89.2	4.25	-3.55

2.8 MIN

DN	WS	WV	T	UM	SD	VM	SD	AM	CU	TIME	HEIGHT
120277.	9.48	0.997	12.6	-2.23	0.722	9.18	0.993	-0.549	12.1	3.59	-1.98
85205.	8.58	0.997	12.7	-1.94	0.613	8.33	0.895	-0.431	11.9	3.96	-1.71
182.	7.40	0.996	12.7	-1.65	0.762	7.19	1.18	-0.765	113.	4.59	-3.50

2.8 MIN

UP	WS	WV	T	UM	SD	VM	SD	AM	CU	TIME	HEIGHT
120277.	9.20	0.998	12.6	-1.53	0.582	9.05	0.977	-0.547	12.0	3.64	-1.99
85455.	8.52	0.999	12.7	-1.33	0.485	8.40	0.968	-0.551	12.2	3.93	-2.16
216.	7.02	0.994	12.7	-1.22	0.797	6.87	1.24	-0.673	100.	4.80	-3.23

2.8 MIN

DN	WS	WV	T	UM	SD	VM	SD	AM	CU	TIME	HEIGHT
120277.	10.4	0.999	12.6	-2.34	0.696	10.1	1.03	-0.951	12.5	3.26	-3.03
85745.	9.46	0.998	12.7	-2.03	0.596	9.22	1.21	-0.917	12.2	3.58	-3.28
250.	7.88	0.994	12.7	-1.95	0.697	7.59	1.14	-0.862	103.	4.35	-3.75

TABLE B-1. continued

2.7 MIN

UP	WS	WV	T	UM	SD	VM	SD	WM	CO	TIME	HEIGHT
120277.	10.3	0.997	12.6	-2.49	0.752	9.99	1.16	-0.662	13.1	3.30	-2.19
90029.	9.40	0.997	12.7	-2.15	0.646	9.13	0.989	-0.692	13.1	3.62	-2.50
283.	7.54	0.994	12.7	-1.69	0.942	7.51	1.56	-0.723	102.	4.52	-3.27

2.8 MIN

DN	WS	WV	T	UM	SD	VM	SD	WM	CO	TIME	HEIGHT
120277.	10.1	0.997	12.6	-2.71	0.816	9.72	0.937	-0.524	13.7	3.39	-1.78
90319.	9.49	0.996	12.8	-2.35	0.709	9.16	1.00	-0.607	13.6	3.60	-2.19
317.	7.65	0.996	12.8	-1.83	0.786	7.39	1.14	-0.657	107.	4.46	-2.93

2.8 MIN

UP	WS	WV	T	UM	SD	VM	SD	WM	CO	TIME	HEIGHT
120277.	9.51	0.996	12.7	-2.52	0.952	9.19	1.10	-0.543	13.5	3.59	-1.95
90609.	8.80	0.996	12.9	-2.02	0.818	8.53	1.02	-0.547	13.1	3.87	-2.12
351.	7.18	0.996	12.8	-1.65	0.635	6.96	1.22	-0.789	102.	4.74	-3.74

2.8 MIN

DN	WS	WV	T	UM	SD	VM	SD	WM	CO	TIME	HEIGHT
120277.	10.3	0.996	12.7	-2.99	1.02	9.83	1.00	-0.700	13.8	3.36	-2.35
90854.	9.44	0.995	13.0	-2.58	0.890	9.02	1.11	-0.731	13.4	3.66	-2.68
384.	7.59	0.996	12.9	-1.73	0.647	7.35	1.41	-0.847	101.	4.49	-3.80

2.8 MIN

UP	WS	WV	T	UM	SD	VM	SD	WM	CO	TIME	HEIGHT
120277.	10.9	0.997	12.8	-3.19	0.931	10.4	1.47	-0.546	14.1	3.16	-1.73
91143.	9.88	0.997	13.1	-2.76	0.804	9.46	1.48	-0.499	13.6	3.49	-1.74
418.	7.84	0.996	13.0	-2.28	0.659	7.47	1.66	-0.721	99.8	4.42	-3.19

2.8 MIN

DN	WS	WV	T	UM	SD	VM	SD	WM	CO	TIME	HEIGHT
120277.	10.8	0.998	12.9	-3.00	0.749	10.3	0.997	-0.717	14.2	3.19	-2.29
91433.	10.0	0.998	13.2	-2.59	0.648	9.67	1.02	-0.647	14.1	3.41	-2.21
452.	8.12	0.995	13.3	-2.26	0.812	7.76	1.46	-0.902	98.6	4.25	-3.84

2.8 MIN

UP	WS	WV	T	UM	SD	VM	SD	WM	CO	TIME	HEIGHT
120277.	8.72	0.994	13.0	-3.07	0.897	8.11	1.70	-0.302	13.9	4.07	-1.23
91723.	7.87	0.996	13.3	-2.66	0.776	7.37	1.51	-0.409	13.9	4.47	-1.83
486.	6.50	0.993	13.3	-2.02	0.653	6.14	1.42	-0.488	100.	5.38	-2.62

TABLE B-1. continued

2.8 MIN

DN	WS	WV	T	UM	SD	VM	SD	WM	CO	TIME	HEIGHT
120277.	7.91	0.994	13.0	-3.27	0.919	7.15	0.977	0.259E-01	14.1	4.62	0.120
92012.	7.11	0.992	13.2	-2.85	0.795	6.46	1.17	-0.377	13.9	5.11	-1.93
520.	5.88	0.989	13.1	-2.35	0.841	5.31	1.11	-0.472	107.	6.21	-2.93

2.8 MIN

UP	WS	WV	T	UM	SD	VM	SD	WM	CO	TIME	HEIGHT
120277.	9.18	0.995	13.0	-3.08	0.816	8.60	1.26	-0.199	14.1	3.84	-0.762
92302.	8.25	0.996	13.1	-2.66	0.702	7.78	1.34	-0.344	13.8	4.24	-1.46
554.	6.74	0.992	13.1	-2.24	0.833	6.30	1.14	-0.577	106.	5.24	-3.02

2.8 MIN

DN	WS	WV	T	UM	SD	VM	SD	WM	CO	TIME	HEIGHT
120277.	10.2	0.996	12.9	-2.97	0.864	9.70	1.20	-0.236	14.3	3.40	-0.802
92547.	9.03	0.996	13.2	-2.57	0.748	8.62	1.34	-0.519	13.9	3.83	-1.99
587.	7.05	0.993	13.1	-2.02	0.902	6.71	1.12	-0.653	112.	4.92	-3.21

2.8 MIN

UP	WS	WV	T	UM	SD	VM	SD	WM	CO	TIME	HEIGHT
120277.	9.62	0.996	13.0	-2.66	0.860	9.21	0.869	-0.465	14.2	3.58	-1.67
92837.	8.37	0.997	13.1	-2.30	0.744	8.01	1.04	-0.565	13.7	4.12	-2.33
621.	6.87	0.994	13.1	-1.90	0.672	6.56	1.13	-0.618	101.	5.03	-3.11

2.8 MIN

DN	WS	WV	T	UM	SD	VM	SD	WM	CO	TIME	HEIGHT
120277.	9.33	0.996	12.9	-2.56	0.993	8.94	0.957	-0.370	13.8	3.69	-1.37
93126.	8.44	0.996	13.0	-2.22	0.860	8.11	0.970	-0.622	13.2	4.07	-2.53
655.	6.59	0.994	13.0	-1.72	0.611	6.32	1.45	-0.501	111.	5.22	-2.62

2.8 MIN

UP	WS	WV	T	UM	SD	VM	SD	WM	CO	TIME	HEIGHT
120277.	9.49	0.997	12.8	-2.56	0.698	9.11	0.874	-0.307	13.5	3.62	-1.11
93416.	8.32	0.998	12.9	-2.22	0.601	8.00	1.12	-0.525	13.5	4.13	-2.16
689.	6.65	0.997	12.9	-1.67	0.665	6.41	1.26	-0.594	101.	5.14	-3.06

2.8 MIN

DN	WS	WV	T	UM	SD	VM	SD	WM	CO	TIME	HEIGHT
120277.	9.72	0.997	12.7	-2.57	0.819	9.34	0.878	-0.597	13.9	3.53	-2.11
93706.	8.66	0.997	12.8	-2.22	0.706	8.35	0.995	-0.486	13.2	3.95	-1.92
723.	7.26	0.996	12.9	-1.87	0.596	6.99	1.42	-0.760	110.	4.72	-3.59

TABLE B-1. continued

2.7 MIN

UP	WS	WV	T	UM	SD	VM	SD	AM	CU	TIME	HEIGHT
120277.	9.32	0.996	12.7	-2.22	0.924	9.02	1.07	-0.262	13.1	3.66	-1.05
93956.	8.24	0.997	12.8	-1.92	0.793	7.98	1.12	-0.450	12.7	4.14	-1.86
34.	6.69	0.995	12.9	-1.57	0.733	6.47	1.11	-0.545	97.5	5.10	-2.78

2.7 MIN

DN	WS	WV	T	UM	SD	VM	SD	AM	CU	TIME	HEIGHT
120277.	9.42	0.997	12.7	-3.22	0.620	8.83	0.846	-0.454	13.5	3.74	-1.70
94240.	8.23	0.997	12.9	-2.79	0.533	7.71	0.927	-0.405	13.4	4.28	-1.73
67.	6.19	0.995	12.9	-1.70	0.648	5.92	1.00	-0.592	108.	5.58	-3.30

2.8 MIN

UP	WS	WV	T	UM	SD	VM	SD	AM	CU	TIME	HEIGHT
120277.	8.64	0.996	12.7	-2.63	0.806	8.13	0.568	-0.501	13.7	4.06	-2.05
94530.	7.57	0.996	13.0	-2.45	0.689	7.15	0.995	-0.568	13.2	4.63	-2.63
101.	6.00	0.995	12.9	-1.76	0.637	5.71	0.909	-0.559	104.	5.78	-3.23

2.8 MIN

DN	WS	WV	T	UM	SD	VM	SD	AM	CU	TIME	HEIGHT
120277.	7.87	0.996	12.7	-2.41	0.709	7.45	0.795	-0.261	12.8	4.43	-1.16
94820.	7.09	0.997	13.0	-2.68	0.605	6.76	0.977	-0.238	12.8	4.88	-1.16
135.	5.44	0.994	12.9	-1.56	0.471	5.18	1.24	-0.441	105.	6.37	-2.81

2.8 MIN

UP	WS	WV	T	UM	SD	VM	SD	AM	CU	TIME	HEIGHT
120277.	6.72	0.995	12.7	-2.78	0.729	6.09	0.997	-0.653E-01	12.8	5.42	-0.554
95109.	5.94	0.995	13.0	-2.41	0.629	5.59	0.963	-0.155	12.9	6.12	-0.946
169.	4.80	0.995	12.9	-1.98	0.640	4.54	0.765	-0.405	103.	7.60	-3.08

2.8 MIN

DN	WS	WV	T	UM	SD	VM	SD	AM	CU	TIME	HEIGHT
120277.	5.78	0.990	12.7	-2.79	0.829	5.00	0.836	0.886E-01	12.9	6.60	0.585
95359.	5.55	0.993	13.0	-2.43	0.769	4.75	0.801	-0.230	12.8	6.98	-1.61
203.	4.38	0.991	13.0	-2.15	0.672	3.77	0.599	-0.314	116.	8.76	-2.75

2.8 MIN

UP	WS	WV	T	UM	SD	VM	SD	AM	CU	TIME	HEIGHT
120277.	6.98	0.995	12.7	-2.96	0.998	6.29	1.02	0.364E-01	13.6	5.25	0.191
95649.	6.13	0.996	13.0	-2.56	0.863	5.54	1.15	-0.265	13.3	5.96	-1.58
237.	4.86	0.994	13.0	-1.99	0.690	4.40	1.19	-0.559	115.	7.50	-2.69

TABLE B-1. continued

2.8 MIN

DN	WS	WV	T	UM	SD	VM	SD	WM	CO	TIME	HEIGHT
120277.	6.75	0.996	12.7	-2.89	0.575	6.07	0.865	-0.205	13.9	5.43	-1.12
95939.	5.83	0.995	13.1	-2.51	0.494	5.23	0.989	-0.324	13.9	6.31	-2.05
271.	4.63	0.989	13.1	-1.78	0.750	4.22	0.911	-0.345	123.	7.83	-2.68

2.8 MIN

UP	WS	WV	T	UM	SD	VM	SD	WM	CO	TIME	HEIGHT
120277.	6.16	0.994	12.7	-2.31	0.627	5.67	0.814	-0.251	13.2	5.82	-1.46
100228.	5.52	0.995	13.1	-2.00	0.538	5.11	0.805	-0.321	13.4	6.45	-2.07
305.	4.38	0.994	13.1	-1.43	0.560	4.11	0.730	-0.351	118.	8.03	-2.82

2.8 MIN

DN	WS	WV	T	UM	SD	VM	SD	WM	CO	TIME	HEIGHT
120277.	5.98	0.994	12.7	-2.55	0.716	5.38	0.859	-0.151	12.8	6.14	-0.929
100518.	5.30	0.995	13.0	-2.19	0.623	4.79	0.911	-0.202	12.9	6.89	-1.39
339.	4.41	0.992	13.0	-1.81	0.561	3.98	0.831	-0.354	122.	8.29	-2.93

2.8 MIN

UP	WS	WV	T	UM	SD	VM	SD	WM	CO	TIME	HEIGHT
120277.	6.37	0.997	12.6	-1.98	0.602	6.03	0.484	-0.499E-01	12.8	5.48	-0.273
100808.	5.58	0.996	13.0	-1.72	0.523	5.08	0.652	-0.257	12.8	6.50	-1.67
373.	4.39	0.995	13.0	-1.20	0.377	4.20	0.728	-0.532	125.	7.85	-2.60

2.8 MIN

DN	WS	WV	T	UM	SD	VM	SD	WM	CO	TIME	HEIGHT
120277.	6.30	0.994	12.6	-1.89	0.618	5.97	0.830	-0.358	12.3	5.53	-1.98
101058.	5.74	0.995	12.9	-1.63	0.533	5.47	0.788	-0.449	12.0	6.03	-2.71
407.	4.26	0.995	12.9	-1.29	0.466	4.03	0.696	-0.427	122.	8.18	-3.49

2.8 MIN

UP	WS	WV	T	UM	SD	VM	SD	WM	CO	TIME	HEIGHT
120277.	7.39	0.995	12.6	-1.78	0.791	7.13	0.730	-0.554	12.8	4.63	-2.56
101347.	6.50	0.994	12.8	-1.54	0.685	6.27	0.851	-0.505	12.6	5.26	-2.66
441.	4.97	0.992	12.9	-1.15	0.682	4.80	0.760	-0.458	132.	6.88	-3.15

2.7 MIN

DN	WS	WV	T	UM	SD	VM	SD	WM	CO	TIME	HEIGHT
120277.	7.19	0.998	12.5	-1.31	0.492	7.06	0.612	-0.362	12.8	4.68	-1.69
101632.	6.50	0.998	12.8	-1.15	0.412	6.39	0.800	-0.502	12.6	5.17	-2.59
474.	5.73	0.996	12.9	-1.01	0.518	5.62	0.750	-0.617	129.	5.88	-3.62

TABLE B-1. continued

2.9 MIN

	UP WS	WV	T	UM	SD	VM	SD	WM	CU	TIME	HEIGHT
120277.	7.58	0.996	12.5	-1.56	0.734	7.18	0.779	-0.321	12.9	4.60	-1.47
101927.	6.79	0.997	12.8	-1.37	0.615	6.63	0.874	-0.412	13.0	4.98	-2.05
509.	5.35	0.992	12.8	-1.27	0.656	5.16	0.692	-0.455	136.	6.40	-2.91

2.7 MIN

	DN WS	WV	T	UM	SD	VM	SD	WM	CU	TIME	HEIGHT
120277.	7.87	0.996	12.4	-1.19	0.655	7.75	0.921	-0.527	13.0	4.26	-2.24
102211.	6.94	0.997	12.7	-1.04	0.558	6.84	0.659	-0.443	12.9	4.82	-2.14
542.	5.61	0.994	12.8	-0.911	0.624	5.51	1.15	-0.479	125.	5.99	-2.87

2.8 MIN

	UP WS	WV	T	UM	SD	VM	SD	WM	CU	TIME	HEIGHT
120277.	7.04	0.994	12.4	-0.780	0.736	6.96	0.765	-0.381	12.4	4.74	-1.81
102501.	6.66	0.995	12.7	-0.673	0.641	6.60	0.749	-0.463	12.6	5.00	-2.32
576.	5.65	0.985	12.7	-0.418	0.987	5.55	0.766	-0.621	125.	5.95	-3.69

2.8 MIN

	DN WS	WV	T	UM	SD	VM	SD	WM	CU	TIME	HEIGHT
120277.	7.12	0.998	12.4	-1.38	0.467	6.97	0.749	-0.149	7.00	4.73	-0.705
102751.	6.42	0.998	12.6	-1.20	0.399	6.30	0.817	-0.253	8.10	5.24	-1.33
610.	5.39	0.994	12.6	-1.31	0.603	5.19	0.801	-0.562	138.	6.36	-3.57

2.8 MIN

	UP WS	WV	T	UM	SD	VM	SD	WM	CU	TIME	HEIGHT
120277.	7.58	0.997	12.3	-1.44	0.637	7.41	0.821	-0.577	11.0	4.45	-2.57
103041.	6.93	0.997	12.5	-1.24	0.543	6.80	0.731	-0.610	10.5	4.85	-2.96
644.	5.64	0.993	12.6	-1.02	0.758	5.51	0.936	-0.599	134.	5.99	-3.59

TABLE B-2. Meteorological Profiles of Ozone, Temperature and Moisture

DATE: 120277, TIME: 7:10:45 to 7:52:11, (86.3 min)

HT	WS(m/s)	SD	UM(m/s)	SD	VM(m/s)	SD	WM(m/s)	SD	T(°C)	SD
3	9.08	±1.37	-2.91	±1.23	8.50	±1.46	-0.437	±0.812	12.57	±0.13
2	8.03	±1.40	-2.53	±1.06	7.53	±1.53	-0.388	±0.682	12.74	±0.15
1	6.77	±1.42	-2.29	±1.17	6.25	±1.46	-0.587	±0.534	12.75	±0.09

TABLE B-3. Meteorological Profiles of Ozone, Temperature and Moisture

DATE: 120277, TIME: 8:37:07 to 9:37:06, (60.1 min)

HT	WS(m/s)	SD	UM(m/s)	SD	VM(m/s)	SD	WM(m/s)	SD	T(°C)	SD
3	9.92	±1.40	-2.59	±0.95	9.53	±1.42	-0.526	±0.782	12.75	±0.16
2	9.02	±1.42	-2.25	±0.81	8.70	±1.45	-0.615	±0.715	12.92	±0.20
1	7.39	±1.48	-1.86	±0.81	7.10	±1.50	-0.719	±0.540	12.93	±0.18

TABLE B-4. Meteorological Profiles of Ozone, Temperature and Moisture

DATE: 120277, TIME: 9:37:16 to 10:30:41, (53.5 min)

HT	WS(m/s)	SD	UM(m/s)	SD	VM(m/s)	SD	WM(m/s)	SD	T(°C)	SD
3	7.25	±1.32	-2.12	±0.99	6.86	±1.35	-0.280	±0.610	12.60	±0.13
2	6.47	±1.26	-1.84	±0.85	6.14	±1.29	-0.371	±0.533	12.86	±0.16
1	5.19	±1.15	-1.44	±0.77	4.93	±1.17	-0.463	±0.389	12.89	±0.15

LEVEL 1 (3.05M)

D/S	0	1	2	3	4	5	6	7	8	9	10	11	12	GT13	ALL
0=	0	0	0	0	0	0	0	0	0	0	0	0	0	0	0
1	0	0	0	0	0	0	0	0	0	0	0	0	0	0	0
2	0	0	0	0	0	0	0	0	0	0	0	0	0	0	0
3	0	0	0	0	0	0	0	0	0	0	0	0	0	0	0
4	0	0	0	0	0	0	0	0	0	0	0	0	0	0	0
5	0	0	0	0	0	0	0	0	0	0	0	0	0	0	0
6	0	0	0	0	0	0	0	0	0	0	0	0	0	0	0
7	0	0	0	0	0	0	0	0	0	0	0	0	0	0	0
8	0	0	0	0	0	0	0	0	0	0	0	0	0	0	0
9-	0	0	0	0	0	0	0	0	0	0	0	0	0	0	0
10	0	0	0	0	0	0	0	0	0	0	0	0	0	0	0
11	0	0	0	0	0	0	0	0	0	0	0	0	0	0	0
12	0	0	0	0	0	0	0	0	0	0	0	0	0	0	0
13	0	0	0	0	0	0	0	0	0	0	0	0	0	0	0
14	0	0	0	0	0	0	0	0	0	0	0	0	0	0	0
15	0	0	0	0	0	0	0	0	0	0	0	0	0	0	0
16	0	0	0	0	0	0	0	0	0	0	0	0	0	0	0
17	0	0	0	0	0	0	0	0	0	0	0	0	0	0	0
18=	0	0	0	0	0	0	0	0	0	0	0	0	0	0	0
19	0	0	0	0	0	0	0	0	0	0	0	0	0	0	0
20	0	0	0	0	0	0	0	0	0	0	0	0	0	0	0
21	0	0	0	0	0	0	0	0	0	0	0	0	0	0	0
22	0	0	0	0	0	0	0	0	0	0	0	0	0	0	0
23	0	0	0	0	0	0	0	0	0	0	0	0	0	0	0
24	0	0	0	0	0	0	0	0	0	0	0	0	0	0	0
25	0	0	0	0	0	0	0	0	1	0	0	0	0	0	1
26	0	0	0	0	1	0	1	0	0	1	1	0	0	0	4
27+	0	0	0	0	0	2	3	9	4	4	0	0	0	0	22
28	0	0	0	0	0	19	25	34	33	13	5	0	1	0	130
29	0	0	0	1	1	29	33	39	24	15	3	1	0	0	146
30	0	0	0	0	12	24	58	39	20	13	3	0	0	0	169
31	0	0	0	2	3	2	7	7	3	0	0	0	0	0	24
32	0	0	0	0	0	0	1	0	0	1	0	0	0	0	2
33	0	0	0	0	0	0	0	0	0	0	0	0	0	0	0
34	0	0	0	0	0	0	0	0	0	0	0	0	0	0	0
35	0	0	0	0	0	0	0	0	0	0	0	0	0	0	0
36T	0	0	0	3	17	76	128	128	85	47	12	1	1	0	0

FIGURE B-1. Wind Field Summaries for Three Measurement Heights: Case Study #2, 7:10:45 to 7:52:11

LEVEL 2 (12.19M)

D/S	0	1	2	3	4	5	6	7	8	9	10	11	12	GT13	ALL
0=	0	0	0	0	0	0	0	0	0	0	0	0	0	0	0
1	0	0	0	0	0	0	0	0	0	0	0	0	0	0	0
2	0	0	0	0	0	0	0	0	0	0	0	0	0	0	0
3	0	0	0	0	0	0	0	0	0	0	0	0	0	0	0
4	0	0	0	0	0	0	0	0	0	0	0	0	0	0	0
5	0	0	0	0	0	0	0	0	0	0	0	0	0	0	0
6	0	0	0	0	0	0	0	0	0	0	0	0	0	0	0
7	0	0	0	0	0	0	0	0	0	0	0	0	0	0	0
8	0	0	0	0	0	0	0	0	0	0	0	0	0	0	0
9-	0	0	0	0	0	0	0	0	0	0	0	0	0	0	0
10	0	0	0	0	0	0	0	0	0	0	0	0	0	0	0
11	0	0	0	0	0	0	0	0	0	0	0	0	0	0	0
12	0	0	0	0	0	0	0	0	0	0	0	0	0	0	0
13	0	0	0	0	0	0	0	0	0	0	0	0	0	0	0
14	0	0	0	0	0	0	0	0	0	0	0	0	0	0	0
15	0	0	0	0	0	0	0	0	0	0	0	0	0	0	0
16	0	0	0	0	0	0	0	0	0	0	0	0	0	0	0
17	0	0	0	0	0	0	0	0	0	0	0	0	0	0	0
18=	0	0	0	0	0	0	0	0	0	0	0	0	0	0	0
19	0	0	0	0	0	0	0	0	0	0	0	0	0	0	0
20	0	0	0	0	0	0	0	0	0	0	0	0	0	0	0
21	0	0	0	0	0	0	0	0	0	0	0	0	0	0	0
22	0	0	0	0	0	0	0	0	0	0	0	0	0	0	0
23	0	0	0	0	0	0	0	0	0	0	0	0	0	0	0
24	0	0	0	0	0	0	0	0	0	0	0	0	0	0	0
25	0	0	0	0	0	0	0	0	0	0	0	0	0	0	0
26	0	0	0	0	0	0	1	1	0	0	0	0	0	0	2
27+	0	0	0	0	0	0	1	4	8	0	2	0	0	0	15
28	0	0	0	0	0	0	5	28	37	45	30	10	3	0	158
29	0	0	0	0	0	2	15	41	55	41	19	7	1	0	181
30	0	0	0	0	0	13	27	32	33	17	4	0	0	0	126
31	0	0	0	0	0	2	4	5	4	0	0	0	0	0	15
32	0	0	0	0	0	0	0	0	1	0	0	0	0	0	1
33	0	0	0	0	0	0	0	0	0	0	0	0	0	0	0
34	0	0	0	0	0	0	0	0	0	0	0	0	0	0	0
35	0	0	0	0	0	0	0	0	0	0	0	0	0	0	0
36T	0	0	0	0	0	17	53	111	138	103	55	17	4	0	0

FIGURE B-1. continued

LEVEL 5 (21.34M)

D/S	0	1	2	3	4	5	6	7	8	9	10	11	12	GT13	ALL
0=	0	0	0	0	0	0	0	0	0	0	0	0	0	0	0
1	0	0	0	0	0	0	0	0	0	0	0	0	0	0	0
2	0	0	0	0	0	0	0	0	0	0	0	0	0	0	0
3	0	0	0	0	0	0	0	0	0	0	0	0	0	0	0
4	0	0	0	0	0	0	0	0	0	0	0	0	0	0	0
5	0	0	0	0	0	0	0	0	0	0	0	0	0	0	0
6	0	0	0	0	0	0	0	0	0	0	0	0	0	0	0
7	0	0	0	0	0	0	0	0	0	0	0	0	0	0	0
8	0	0	0	0	0	0	0	0	0	0	0	0	0	0	0
9-	0	0	0	0	0	0	0	0	0	0	0	0	0	0	0
10	0	0	0	0	0	0	0	0	0	0	0	0	0	0	0
11	0	0	0	0	0	0	0	0	0	0	0	0	0	0	0
12	0	0	0	0	0	0	0	0	0	0	0	0	0	0	0
13	0	0	0	0	0	0	0	0	0	0	0	0	0	0	0
14	0	0	0	0	0	0	0	0	0	0	0	0	0	0	0
15	0	0	0	0	0	0	0	0	0	0	0	0	0	0	0
16	0	0	0	0	0	0	0	0	0	0	0	0	0	0	0
17	0	0	0	0	0	0	0	0	0	0	0	0	0	0	0
18=	0	0	0	0	0	0	0	0	0	0	0	0	0	0	0
19	0	0	0	0	0	0	0	0	0	0	0	0	0	0	0
20	0	0	0	0	0	0	0	0	0	0	0	0	0	0	0
21	0	0	0	0	0	0	0	0	0	0	0	0	0	0	0
22	0	0	0	0	0	0	0	0	0	0	0	0	0	0	0
23	0	0	0	0	0	0	0	0	0	0	0	0	0	0	0
24	0	0	0	0	0	0	0	0	0	0	0	0	0	0	0
25	0	0	0	0	0	0	0	0	0	0	0	0	0	0	0
26	0	0	0	0	0	0	0	0	2	0	0	0	0	0	2
27+	0	0	0	0	0	0	0	2	6	3	4	0	0	0	15
28	0	0	0	0	0	0	0	13	20	43	42	23	7	2	150
29	0	0	0	0	0	0	1	17	33	66	50	18	7	2	194
30	0	0	0	0	0	0	13	22	23	32	29	6	0	0	125
31	0	0	0	0	0	1	0	3	3	3	1	0	0	0	11
32	0	0	0	0	0	0	0	0	0	1	0	0	0	0	1
33	0	0	0	0	0	0	0	0	0	0	0	0	0	0	0
34	0	0	0	0	0	0	0	0	0	0	0	0	0	0	0
35	0	0	0	0	0	0	0	0	0	0	0	0	0	0	0
36T	0	0	0	0	0	1	14	57	87	148	126	47	14	4	0

FIGURE B-1. continued

LEVEL 1 (3.05M)

D/S	0	1	2	3	4	5	6	7	8	9	10	11	12	GT13	ALL
0=	0	0	0	0	0	0	0	0	0	0	0	0	0	0	0
1	0	0	0	0	0	0	0	0	0	0	0	0	0	0	0
2	0	0	0	0	0	0	0	0	0	0	0	0	0	0	0
3	0	0	0	0	0	0	0	0	0	0	0	0	0	0	0
4	0	0	0	0	0	0	0	0	0	0	0	0	0	0	0
5	0	0	0	0	0	0	0	0	0	0	0	0	0	0	0
6	0	0	0	0	0	0	0	0	0	0	0	0	0	0	0
7	0	0	0	0	0	0	0	0	0	0	0	0	0	0	0
8	0	0	0	0	0	0	0	0	0	0	0	0	0	0	0
9=	0	0	0	0	0	0	0	0	0	0	0	0	0	0	0
10	0	0	0	0	0	0	0	0	0	0	0	0	0	0	0
11	0	0	0	0	0	0	0	0	0	0	0	0	0	0	0
12	0	0	0	0	0	0	0	0	0	0	0	0	0	0	0
13	0	0	0	0	0	0	0	0	0	0	0	0	0	0	0
14	0	0	0	0	0	0	0	0	0	0	0	0	0	0	0
15	0	0	0	0	0	0	0	0	0	0	0	0	0	0	0
16	0	0	0	0	0	0	0	0	0	0	0	0	0	0	0
17	0	0	0	0	0	0	0	0	0	0	0	0	0	0	0
18=	0	0	0	0	0	0	0	0	0	0	0	0	0	0	0
19	0	0	0	0	0	0	0	0	0	0	0	0	0	0	0
20	0	0	0	0	0	0	0	0	0	0	0	0	0	0	0
21	0	0	0	0	0	0	0	0	0	0	0	0	0	0	0
22	0	0	0	0	0	0	0	0	0	0	0	0	0	0	0
23	0	0	0	0	0	0	0	0	0	0	0	0	0	0	0
24	0	0	0	0	0	0	0	0	0	0	0	0	0	0	0
25	0	0	0	0	0	1	2	0	0	0	0	0	0	0	3
26	0	0	0	0	0	1	1	0	0	0	0	0	0	0	2
27+	0	0	0	2	4	15	8	2	2	0	0	0	0	0	33
28	0	0	0	4	50	74	62	35	6	2	0	0	0	0	253
29	0	0	0	18	67	75	45	23	10	1	0	0	0	0	239
30	0	0	0	5	38	35	17	3	2	0	0	0	0	0	100
31	0	0	0	3	5	3	3	0	0	0	0	0	0	0	14
32	0	0	0	0	0	0	0	0	0	0	0	0	0	0	0
33	0	0	0	0	0	0	0	0	0	0	0	0	0	0	0
34	0	0	0	0	0	0	0	0	0	0	0	0	0	0	0
35	0	0	0	0	0	0	0	0	0	0	0	0	0	0	0
36T	0	0	0	32	164	204	158	63	20	3	0	0	0	0	0

FIGURE B-2. Wind Field Summaries for Three Measurement Heights: Case Study #2, 8:37:07 to 9:37:06

LEVEL 2 (12.19M)

D/S	0	1	2	3	4	5	6	7	8	9	10	11	12	GT13	ALL
0=	0	0	0	0	0	0	0	0	0	0	0	0	0	0	0
1	0	0	0	0	0	0	0	0	0	0	0	0	0	0	0
2	0	0	0	0	0	0	0	0	0	0	0	0	0	0	0
3	0	0	0	0	0	0	0	0	0	0	0	0	0	0	0
4	0	0	0	0	0	0	0	0	0	0	0	0	0	0	0
5	0	0	0	0	0	0	0	0	0	0	0	0	0	0	0
6	0	0	0	0	0	0	0	0	0	0	0	0	0	0	0
7	0	0	0	0	0	0	0	0	0	0	0	0	0	0	0
8	0	0	0	0	0	0	0	0	0	0	0	0	0	0	0
9-	0	0	0	0	0	0	0	0	0	0	0	0	0	0	0
10	0	0	0	0	0	0	0	0	0	0	0	0	0	0	0
11	0	0	0	0	0	0	0	0	0	0	0	0	0	0	0
12	0	0	0	0	0	0	0	0	0	0	0	0	0	0	0
13	0	0	0	0	0	0	0	0	0	0	0	0	0	0	0
14	0	0	0	0	0	0	0	0	0	0	0	0	0	0	0
15	0	0	0	0	0	0	0	0	0	0	0	0	0	0	0
16	0	0	0	0	0	0	0	0	0	0	0	0	0	0	0
17	0	0	0	0	0	0	0	0	0	0	0	0	0	0	0
18=	0	0	0	0	0	0	0	0	0	0	0	0	0	0	0
19	0	0	0	0	0	0	0	0	0	0	0	0	0	0	0
20	0	0	0	0	0	0	0	0	0	0	0	0	0	0	0
21	0	0	0	0	0	0	0	0	0	0	0	0	0	0	0
22	0	0	0	0	0	0	0	0	0	0	0	0	0	0	0
23	0	0	0	0	0	0	0	0	0	0	0	0	0	0	0
24	0	0	0	0	0	0	0	0	0	0	0	0	0	0	0
25	0	0	0	0	0	0	0	0	0	0	0	0	0	0	0
26	0	0	0	0	0	1	0	0	0	0	0	0	0	0	1
27+	0	0	0	0	0	4	6	5	6	1	0	0	0	0	22
28	0	0	0	0	4	28	77	103	34	12	4	0	0	0	262
29	0	0	0	1	12	51	65	50	39	18	3	0	0	0	239
30	0	0	0	0	8	43	39	9	11	4	0	0	0	0	114
31	0	0	0	0	0	3	1	1	1	0	0	0	0	0	6
32	0	0	0	0	0	0	0	0	0	0	0	0	0	0	0
33	0	0	0	0	0	0	0	0	0	0	0	0	0	0	0
34	0	0	0	0	0	0	0	0	0	0	0	0	0	0	0
35	0	0	0	0	0	0	0	0	0	0	0	0	0	0	0
36T	0	0	0	1	24	130	188	168	91	35	7	0	0	0	0

FIGURE B-2. continued

LEVEL 3 (21.34M)

D/S	0	1	2	3	4	5	6	7	8	9	10	11	12	13	ALL
0=	0	0	0	0	0	0	0	0	0	0	0	0	0	0	0
1	0	0	0	0	0	0	0	0	0	0	0	0	0	0	0
2	0	0	0	0	0	0	0	0	0	0	0	0	0	0	0
3	0	0	0	0	0	0	0	0	0	0	0	0	0	0	0
4	0	0	0	0	0	0	0	0	0	0	0	0	0	0	0
5	0	0	0	0	0	0	0	0	0	0	0	0	0	0	0
6	0	0	0	0	0	0	0	0	0	0	0	0	0	0	0
7	0	0	0	0	0	0	0	0	0	0	0	0	0	0	0
8	0	0	0	0	0	0	0	0	0	0	0	0	0	0	0
9-	0	0	0	0	0	0	0	0	0	0	0	0	0	0	0
10	0	0	0	0	0	0	0	0	0	0	0	0	0	0	0
11	0	0	0	0	0	0	0	0	0	0	0	0	0	0	0
12	0	0	0	0	0	0	0	0	0	0	0	0	0	0	0
13	0	0	0	0	0	0	0	0	0	0	0	0	0	0	0
14	0	0	0	0	0	0	0	0	0	0	0	0	0	0	0
15	0	0	0	0	0	0	0	0	0	0	0	0	0	0	0
16	0	0	0	0	0	0	0	0	0	0	0	0	0	0	0
17	0	0	0	0	0	0	0	0	0	0	0	0	0	0	0
18=	0	0	0	0	0	0	0	0	0	0	0	0	0	0	0
19	0	0	0	0	0	0	0	0	0	0	0	0	0	0	0
20	0	0	0	0	0	0	0	0	0	0	0	0	0	0	0
21	0	0	0	0	0	0	0	0	0	0	0	0	0	0	0
22	0	0	0	0	0	0	0	0	0	0	0	0	0	0	0
23	0	0	0	0	0	0	0	0	0	0	0	0	0	0	0
24	0	0	0	0	0	0	0	0	0	0	0	0	0	0	0
25	0	0	0	0	0	0	0	0	0	0	0	0	0	0	0
26	0	0	0	0	0	0	0	1	0	0	0	0	0	0	1
27+	0	0	0	0	0	1	6	9	3	3	0	0	0	0	22
28	0	0	0	0	0	6	54	94	76	32	7	5	0	0	252
29	0	0	0	0	2	22	55	63	45	26	17	5	2	0	239
30	0	0	0	0	3	17	58	35	15	12	4	0	0	0	124
31	0	0	0	0	0	1	1	1	0	0	0	0	0	0	3
32	0	0	0	0	0	1	1	1	0	0	0	0	0	0	3
33	0	0	0	0	0	0	0	0	0	0	0	0	0	0	0
34	0	0	0	0	0	0	0	0	0	0	0	0	0	0	0
35	0	0	0	0	0	0	0	0	0	0	0	0	0	0	0
36T	0	0	0	0	5	48	155	204	139	75	28	8	2	0	0

FIGURE B-2. continued

LEVEL 1 (3.05M)

D/S	0	1	2	3	4	5	6	7	8	9	10	11	12	G113	ALL
0=	0	0	0	0	0	0	0	0	0	0	0	0	0	0	0
1	0	0	0	0	0	0	0	0	0	0	0	0	0	0	0
2	0	0	0	0	0	0	0	0	0	0	0	0	0	0	0
3	0	0	0	0	0	0	0	0	0	0	0	0	0	0	0
4	0	0	0	0	0	0	0	0	0	0	0	0	0	0	0
5	0	0	0	0	0	0	0	0	0	0	0	0	0	0	0
6	0	0	0	0	0	0	0	0	0	0	0	0	0	0	0
7	0	0	0	0	0	0	0	0	0	0	0	0	0	0	0
8	0	0	0	0	0	0	0	0	0	0	0	0	0	0	0
9-	0	0	0	0	0	0	0	0	0	0	0	0	0	0	0
10	0	0	0	0	0	0	0	0	0	0	0	0	0	0	0
11	0	0	0	0	0	0	0	0	0	0	0	0	0	0	0
12	0	0	0	0	0	0	0	0	0	0	0	0	0	0	0
13	0	0	0	0	0	0	0	0	0	0	0	0	0	0	0
14	0	0	0	0	0	0	0	0	0	0	0	0	0	0	0
15	0	0	0	0	0	0	0	0	0	0	0	0	0	0	0
16	0	0	0	0	0	0	0	0	0	0	0	0	0	0	0
17	0	0	0	0	0	0	0	0	0	0	0	0	0	0	0
18=	0	0	0	0	0	0	0	0	0	0	0	0	0	0	0
19	0	0	0	0	0	0	0	0	0	0	0	0	0	0	0
20	0	0	0	0	0	0	0	0	0	0	0	0	0	0	0
21	0	0	0	0	0	0	0	0	0	0	0	0	0	0	0
22	0	0	0	0	0	0	0	0	0	0	0	0	0	0	0
23	0	0	0	0	0	0	0	0	0	0	0	0	0	0	0
24	0	0	0	0	0	0	0	0	0	0	0	0	0	0	0
25	0	0	0	0	0	0	0	0	0	0	0	0	0	0	0
26	0	0	0	0	0	0	1	0	0	0	0	0	0	0	1
27+	0	0	0	0	0	2	3	6	7	4	0	0	1	0	23
28	0	0	0	0	0	28	59	90	101	66	29	7	1	0	361
29	0	0	0	0	5	31	40	62	57	42	12	6	0	0	255
30	0	0	0	0	0	12	21	15	6	2	1	0	0	0	57
31	0	0	0	0	1	3	2	0	0	0	0	0	0	0	6
32	0	0	0	0	0	0	0	0	0	0	0	0	0	0	0
33	0	0	0	0	0	0	0	0	0	0	0	0	0	0	0
34	0	0	0	0	0	0	0	0	0	0	0	0	0	0	0
35	0	0	0	0	0	0	0	0	0	0	0	0	0	0	0
36T	0	0	0	0	6	76	126	173	171	114	42	13	2	0	0

FIGURE B-3. Wind Field Summaries for Three Measurement Heights: Case Study #2, 9:37:16 to 10:30:41

LEVEL 2 (12.19M)

D/S	0	1	2	3	4	5	6	7	8	9	10	11	12	GT13	ALL
0=	0	0	0	0	0	0	0	0	0	0	0	0	0	0	0
1	0	0	0	0	0	0	0	0	0	0	0	0	0	0	0
2	0	0	0	0	0	0	0	0	0	0	0	0	0	0	0
3	0	0	0	0	0	0	0	0	0	0	0	0	0	0	0
4	0	0	0	0	0	0	0	0	0	0	0	0	0	0	0
5	0	0	0	0	0	0	0	0	0	0	0	0	0	0	0
6	0	0	0	0	0	0	0	0	0	0	0	0	0	0	0
7	0	0	0	0	0	0	0	0	0	0	0	0	0	0	0
8	0	0	0	0	0	0	0	0	0	0	0	0	0	0	0
9=	0	0	0	0	0	0	0	0	0	0	0	0	0	0	0
10	0	0	0	0	0	0	0	0	0	0	0	0	0	0	0
11	0	0	0	0	0	0	0	0	0	0	0	0	0	0	0
12	0	0	0	0	0	0	0	0	0	0	0	0	0	0	0
13	0	0	0	0	0	0	0	0	0	0	0	0	0	0	0
14	0	0	0	0	0	0	0	0	0	0	0	0	0	0	0
15	0	0	0	0	0	0	0	0	0	0	0	0	0	0	0
16	0	0	0	0	0	0	0	0	0	0	0	0	0	0	0
17	0	0	0	0	0	0	0	0	0	0	0	0	0	0	0
18=	0	0	0	0	0	0	0	0	0	0	0	0	0	0	0
19	0	0	0	0	0	0	0	0	0	0	0	0	0	0	0
20	0	0	0	0	0	0	0	0	0	0	0	0	0	0	0
21	0	0	0	0	0	0	0	0	0	0	0	0	0	0	0
22	0	0	0	0	0	0	0	0	0	0	0	0	0	0	0
23	0	0	0	0	0	0	0	0	0	0	0	0	0	0	0
24	0	0	0	0	0	0	0	0	0	0	0	0	0	0	0
25	0	0	0	0	0	0	0	0	0	0	0	0	0	0	0
26	0	0	0	0	0	0	0	0	0	0	0	0	0	0	0
27+	0	0	0	0	0	0	0	0	2	1	0	0	0	0	3
28	0	0	0	0	0	2	5	26	100	103	114	52	16	6	424
29	0	0	0	0	0	4	8	25	65	68	50	32	4	2	258
30	0	0	0	0	0	2	7	9	11	6	2	0	0	0	37
31	0	0	0	0	0	0	1	0	0	0	0	0	0	0	1
32	0	0	0	0	0	0	0	0	0	0	0	0	0	0	0
33	0	0	0	0	0	0	0	0	0	0	0	0	0	0	0
34	0	0	0	0	0	0	0	0	0	0	0	0	0	0	0
35	0	0	0	0	0	0	0	0	0	0	0	0	0	0	0
36T	0	0	0	0	0	8	21	60	178	178	166	84	20	8	0

FIGURE B-3. continued

LEVEL 3 (21.34M)

D/S	0	1	2	3	4	5	6	7	8	9	10	11	12	GT13	ALL
0=	0	0	0	0	0	0	0	0	0	0	0	0	0	0	0
1	0	0	0	0	0	0	0	0	0	0	0	0	0	0	0
2	0	0	0	0	0	0	0	0	0	0	0	0	0	0	0
3	0	0	0	0	0	0	0	0	0	0	0	0	0	0	0
4	0	0	0	0	0	0	0	0	0	0	0	0	0	0	0
5	0	0	0	0	0	0	0	0	0	0	0	0	0	0	0
6	0	0	0	0	0	0	0	0	0	0	0	0	0	0	0
7	0	0	0	0	0	0	0	0	0	0	0	0	0	0	0
8	0	0	0	0	0	0	0	0	0	0	0	0	0	0	0
9-	0	0	0	0	0	0	0	0	0	0	0	0	0	0	0
10	0	0	0	0	0	0	0	0	0	0	0	0	0	0	0
11	0	0	0	0	0	0	0	0	0	0	0	0	0	0	0
12	0	0	0	0	0	0	0	0	0	0	0	0	0	0	0
13	0	0	0	0	0	0	0	0	0	0	0	0	0	0	0
14	0	0	0	0	0	0	0	0	0	0	0	0	0	0	0
15	0	0	0	0	0	0	0	0	0	0	0	0	0	0	0
16	0	0	0	0	0	0	0	0	0	0	0	0	0	0	0
17	0	0	0	0	0	0	0	0	0	0	0	0	0	0	0
18=	0	0	0	0	0	0	0	0	0	0	0	0	0	0	0
19	0	0	0	0	0	0	0	0	0	0	0	0	0	0	0
20	0	0	0	0	0	0	0	0	0	0	0	0	0	0	0
21	0	0	0	0	0	0	0	0	0	0	0	0	0	0	0
22	0	0	0	0	0	0	0	0	0	0	0	0	0	0	0
23	0	0	0	0	0	0	0	0	0	0	0	0	0	0	0
24	0	0	0	0	0	0	0	0	0	0	0	0	0	0	0
25	0	0	0	0	0	0	0	0	0	0	0	0	0	0	0
26	0	0	0	0	0	0	0	0	0	0	0	0	0	0	0
27+	0	0	0	0	0	0	0	0	1	1	2	0	0	1	5
28	0	0	0	0	0	0	2	5	45	92	103	88	36	11	380
29	0	0	0	0	0	0	1	9	27	54	100	54	32	10	287
30	0	0	0	0	0	0	4	8	11	10	10	5	2	1	51
31	0	0	0	0	0	0	0	0	0	0	0	0	0	0	0
32	0	0	0	0	0	0	0	0	0	0	0	0	0	0	0
33	0	0	0	0	0	0	0	0	0	0	0	0	0	0	0
34	0	0	0	0	0	0	0	0	0	0	0	0	0	0	0
35	0	0	0	0	0	0	0	0	0	0	0	0	0	0	0
36I	0	0	0	0	0	0	7	22	82	157	215	147	70	23	0

FIGURE B-3. continued

APPENDIX C

Windfield Definition

Analysis of the wind data confirmed the tracer test observation of an upward divergence of winds across the site. This upward divergence is true both for low winds in Figures C-1 and C-2 and for moderate winds in Figure C-3 and C-4. These plots are based on 15-min average values.

Figures C-1 and C-3 show the divergence in height between the conductors and the measurement tower. The heights plotted on the differences in the near-surface and conductor height computed trajectories. For reference, the v and u winds at the conductor height are also plotted. Winds perpendicular to the conductors are the v components with positive v toward the profile tower. In both C-1 and C-3 positive v's are associated by net upward trajectories relative to the local slope. Negative values of v refer to trajectories on the other side of the conductors.

Winds relative to the ground have a consistent tendency for a net upward component. This divergence increases with height over the site. The magnitude of this divergence relative to local surfaces in presented in Figures C-1 and C-3. For periods with significant winds perpendicular to the conductors (v), the 26-m downwind divergence is 2 m to 4 m between surface and conductor height winds.

Figures C-2 and C-4 are the computed heights at 26 m downwind of the conductor centerline. The release heights adjusted for the perpendicular elevation difference are plotted as reference horizontal lines for each height. The computed intersection heights show considerable more variation than the computed divergences in Figures C-1 and C-3. These changes are largely the effects of changes in slope at the site with direction. The upward divergence of wind trajectories is evident in these figures by the progressive increase in the height going up the tower.

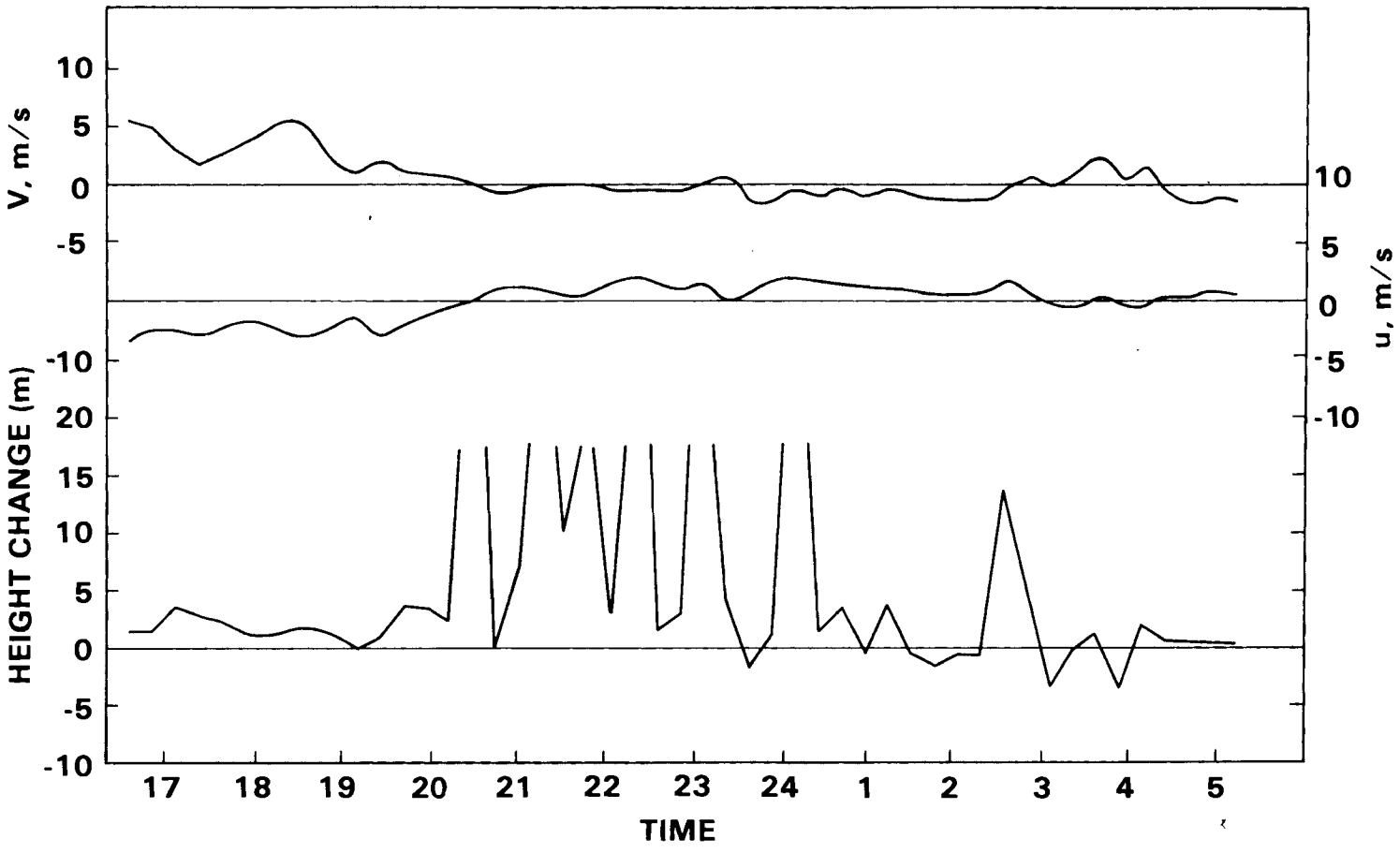

FIGURE C-1. Computed Height Change Between Near Surface and Conductor Height Trajectories at 26 m Downwind: Low Wind Speed Example

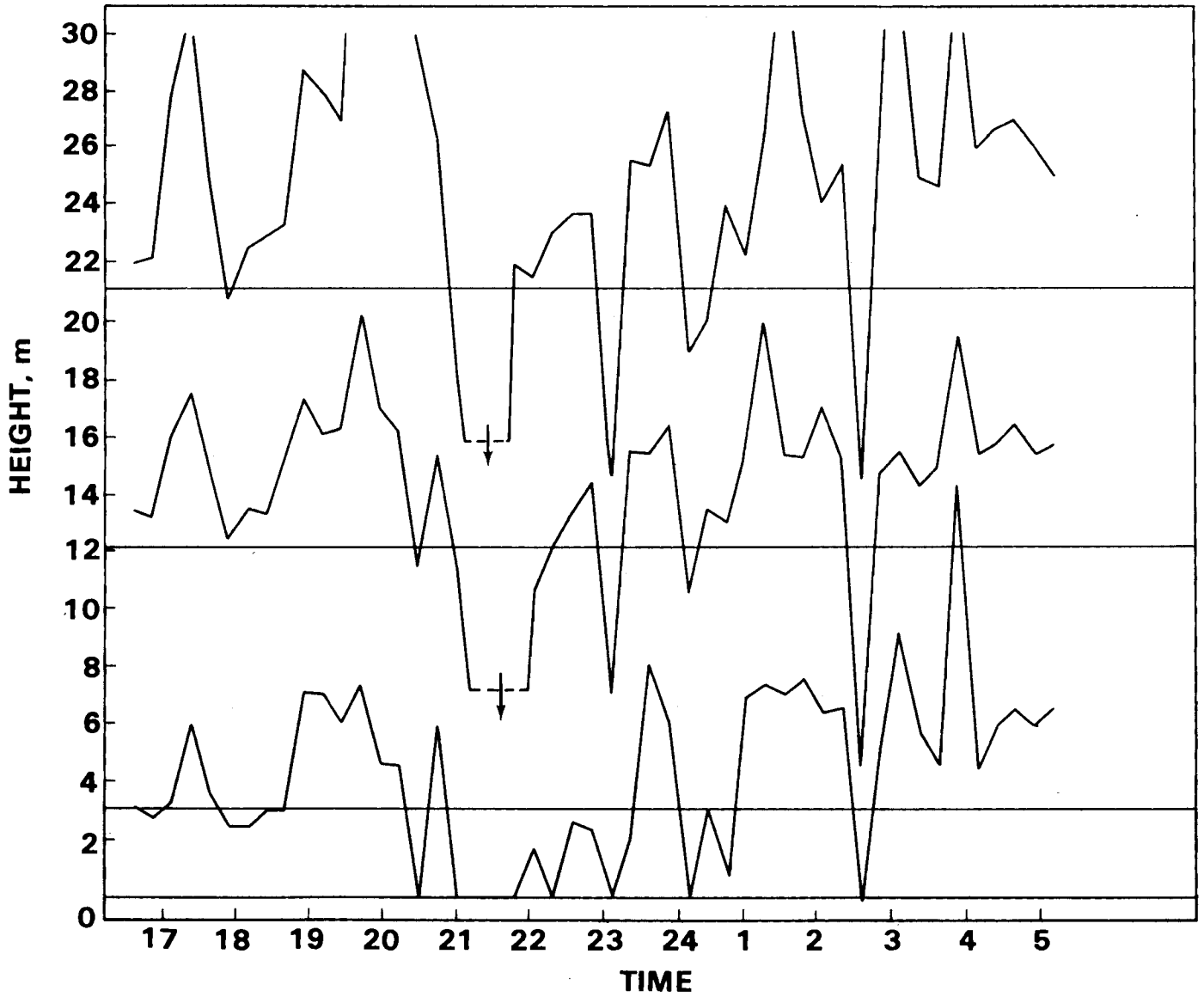

FIGURE C-2. Computed Trajectory Heights 26 m Downwind for the Three Heights of Wind Data: Low Wind Speed Example

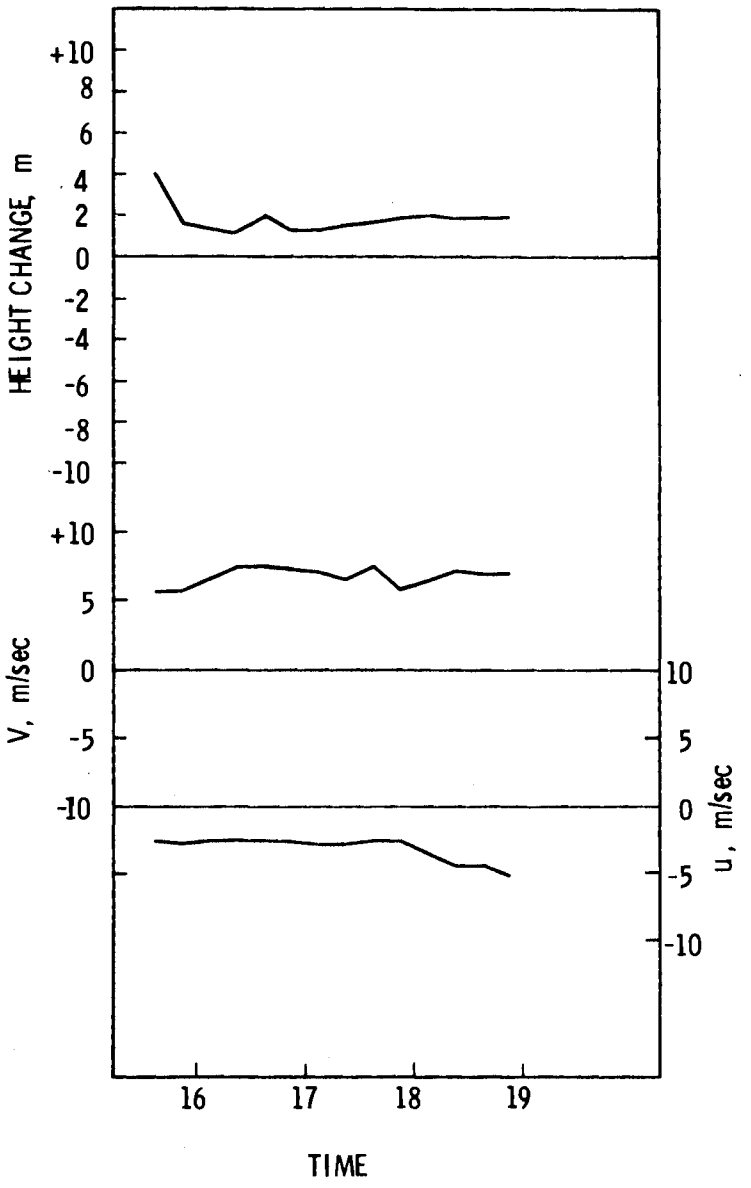

FIGURE C-3. Computed Height Change Between Near Surface and Conductor Height at 26 m Downwind: Moderate Wind Speed Example

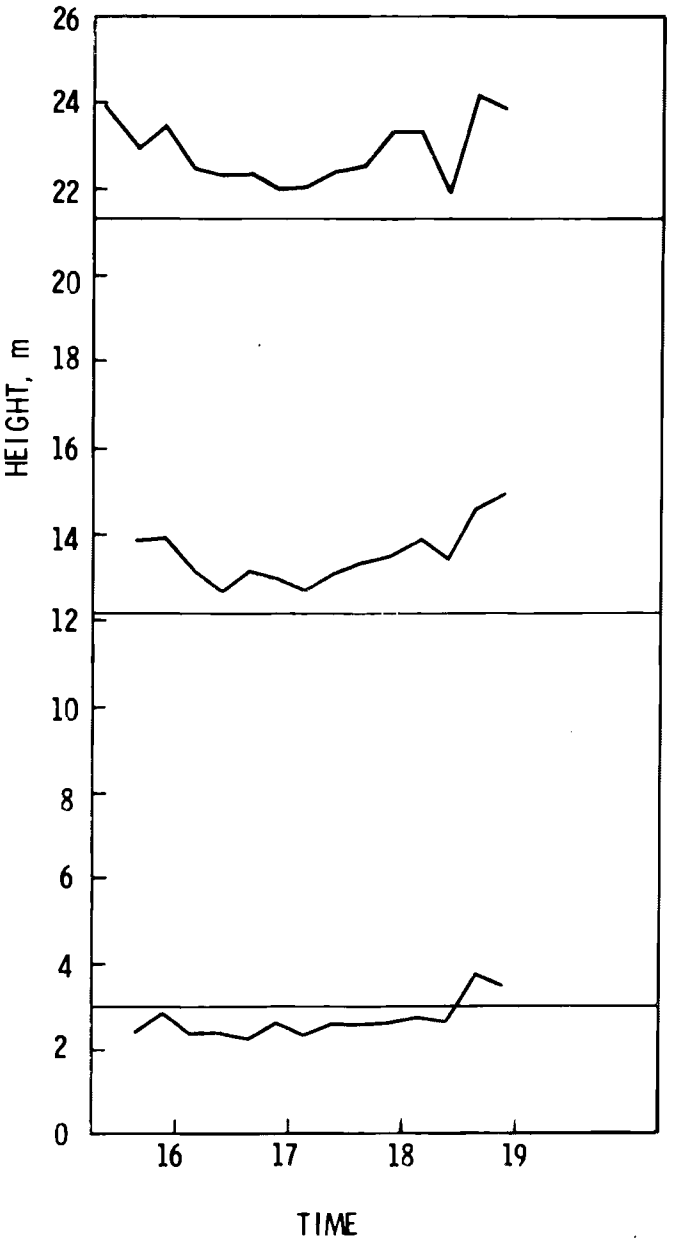

FIGURE C-4. Computed Trajectory Heights 26 m Downwind for the Three Heights of Wind Data: Moderate Wind Speed

APPENDIX D

Aerosol Data Summary

The particle size distributions at The Dalles site were measured using a custom Open Cavity Laser, Model ASAS-300 A manufactured by Particle Measuring Systems Inc., Boulder, CO. The average particle number distribution is given in Figure D-1. The plot in Figure D-1 is based on a series of data taken at two size range settings for periods of 15 to 40 min between 10:00 and 17:00 on September 29, 1977. The size range settings are given in Tables D-1 and D-2. The plot is based on five runs with size range 1 and ten runs with size range 2. These plots show the variability that occurred and are typical plots of ambient particle size distributions for a relatively clean atmosphere.

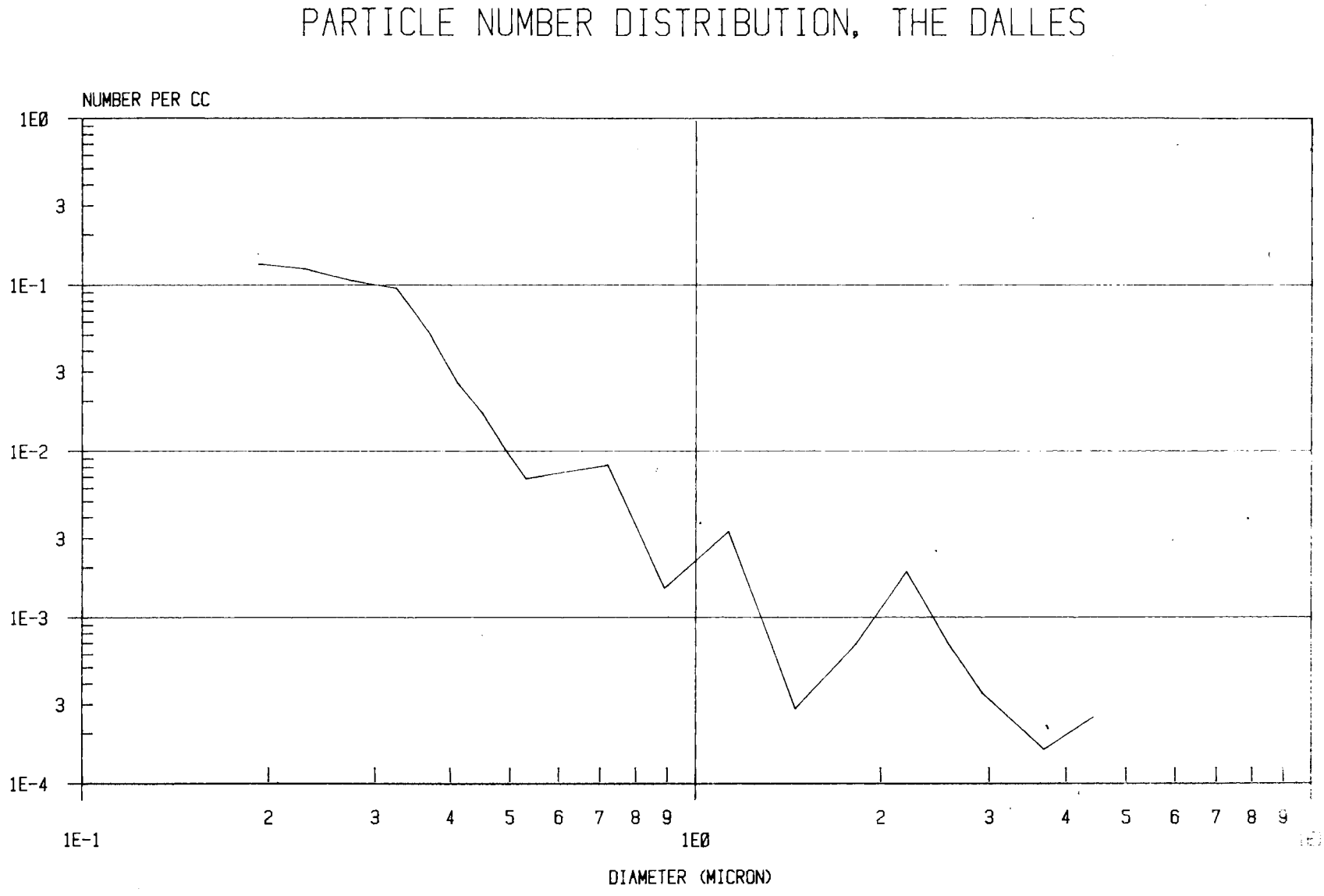

FIGURE D-1. Particle Number Densities at The Dalles, Size Range #1

TABLE D-1. Size Range #1

Channel	Size (micron)	Interval (micron)
1	0.45 - 0.55	0.10
2	0.55 - 0.65	0.10
3	0.65 - 0.79	0.14
4	0.79 - 0.99	0.20
5	0.99 - 1.27	0.28
6	1.27 - 1.64	0.37
7	1.64 - 2.01	0.37
8	2.01 - 2.38	0.37
9	2.38 - 2.75	0.37
10	2.75 - 3.12	0.37
11	3.12 - 3.49	0.37
12	3.49 - 3.86	0.37
13	3.86 - 4.23	0.37
14	4.23 - 4.60	0.37
15	4.60 - 4.97	0.37

TABLE D-2. Size Range #3

Channel	Size (micron)	Interval (micron)
1	0.175 - 0.21	0.035
2	0.21 - 0.25	0.04
3	0.25 - 0.30	0.05
4	0.30 - 0.35	0.05
5	0.35 - 0.39	0.04
6	0.39 - 0.43	
7	0.43 - 0.47	
8	0.47 - 0.51	
9	0.51 - 0.55	
10	0.55 - 0.59	
11	0.59 - 0.63	
12	0.63 - 0.67	
13	0.67 - 0.71	
14	0.71 - 0.75	
15	0.75 - 0.79	0.04

APPENDIX E

Fixed-Height Ozone Studies

Fixed height refers to the fixed position of the ozone intake lines at 12 m on both sides of the test conductors. These tests were conducted to study specific site characteristics.

Dependence of ozone concentrations on ambient wind speed is shown for one case in Figure E-1. These data were during precipitation conditions. Both the upwind and downwind ozone concentrations increased with increasing wind speeds. The difference between the monitors is not significant in view of the relative accuracy of the monitors, although the slope of the curves may be significant.

The shape of the difference curve on the lower part of Figure E-1 shows a minimum value at 2.5 m/sec. Combination of the wind speed dependence corona (Equation 1) and the inverse dependence on wind speed for dispersion (Equation 7) predicts a minimum source term for 2-to-3 m/sec winds and an approximate balancing of the effects at higher wind speeds, both of which appear in Figure E-1. Corresponding background data during precipitation conditions were not available to evaluate the validity of this effect.

Data from other cases for higher winds indicated a slight tendency for higher downwind ozone concentration at winds indicated between 0 and 9 m/sec (about +0.3 ppb per m/sec). The explanation of this increase may be either a real increase ozone production with increase in wind speed, or a change in the maximum plume elevations as a function of wind speed. The latter change refers to the fact that the ozone intakes are at the same height as the conductors. Since the winds at this site tend to flow more parallel to the ground at higher wind speeds, the fixed monitors will be sampling closer to plume centerline at higher wind speeds.

Figure E-2 contains the results of a 4-day background monitoring study of wind speed, wind direction, ozone and nitrogen oxide (NO) concentrations. The conductors were at 500 kV until 14:00 on December 2, 1977, at which time they were de-energized for the remainder of the reported period. The ozone trace is from the upwind monitor and should not be influenced by the energized lines. The downwind ozone monitor data are not available for the

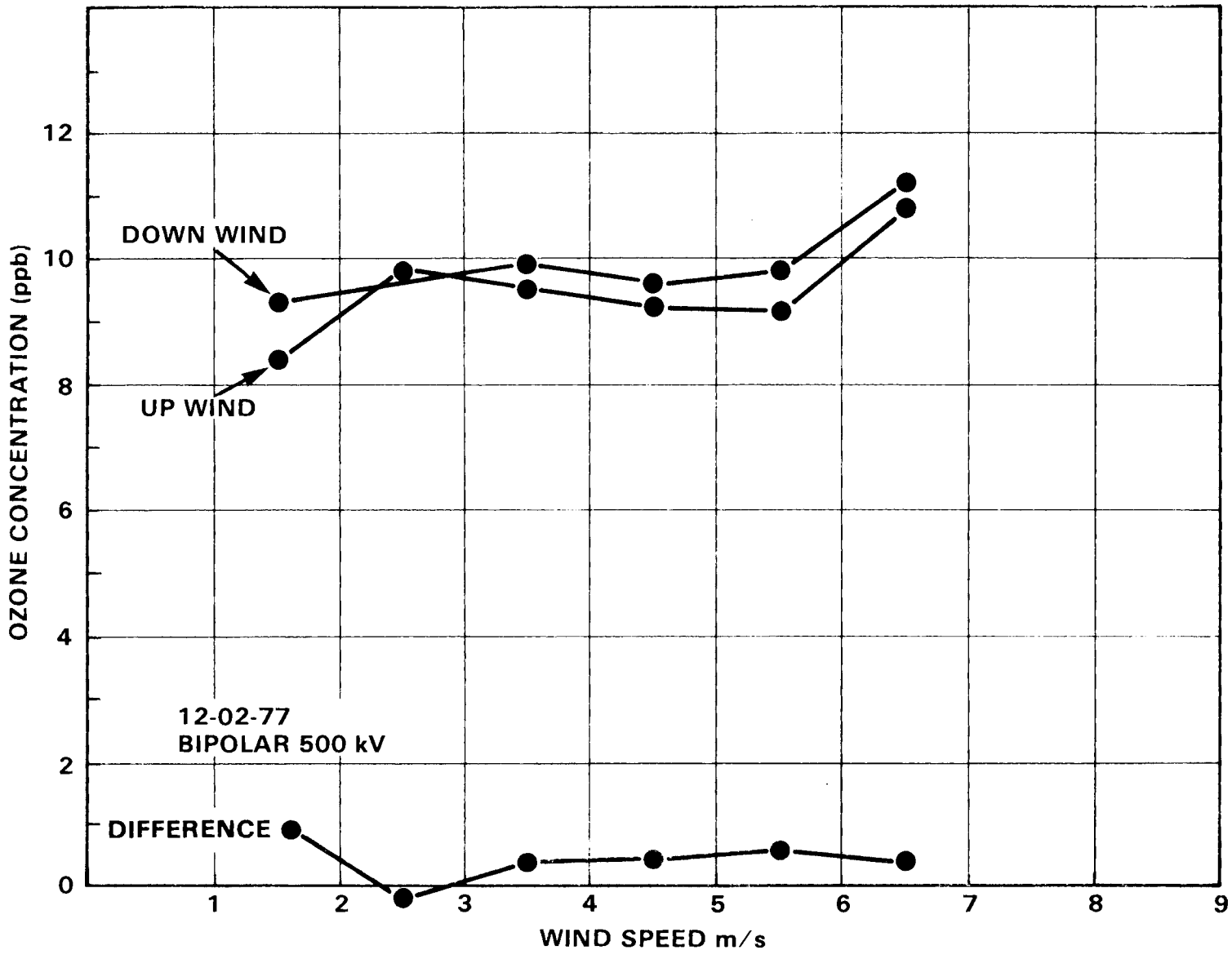

FIGURE E-1. Ozone Concentration Values as a Function of Wind Speed at Upwind and Downwind Locations.

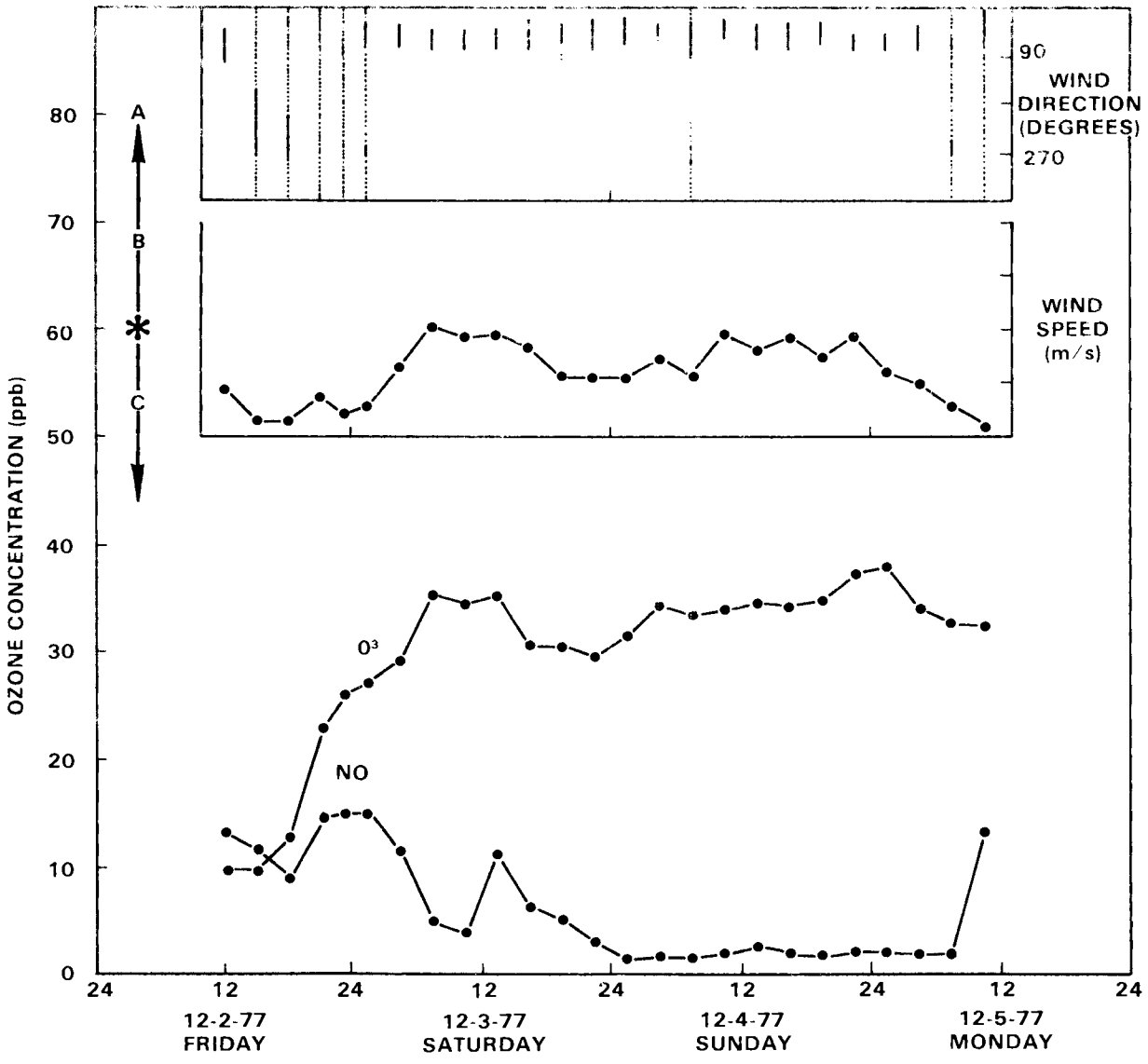

FIGURE E-2. Fixed-Height Monitoring Study of Background Conditions at The Dalles Site

entire period. The scale for the NO concentrations is relative as a result of the lack of an accurate NO calibration for this test.

The initially low ozone concentrations reflect the precipitation conditions, as reported in the main text, for this period. The higher ozone concentrations later in the day reflect the ending of the precipitation conditions for the duration of the monitoring period.

APPENDIX F

Individual Profiles for Case Study #1

This appendix contains detailed individual profiles of ozone, temperature, and humidity variables from case study #1 (November 28, 1974 from 15:27 to 17:56). The profiles are discussed and explained in the main text. This series contain all major changes in concentrations at the monitors; only periods with vertical and low concentration (less than 4 ppb) ozone profiles at both monitors are omitted. However, a number of profiles that fall in this latter category are included for continuity and comparison. Table 4.1 contains the voltage and current data for these tests.

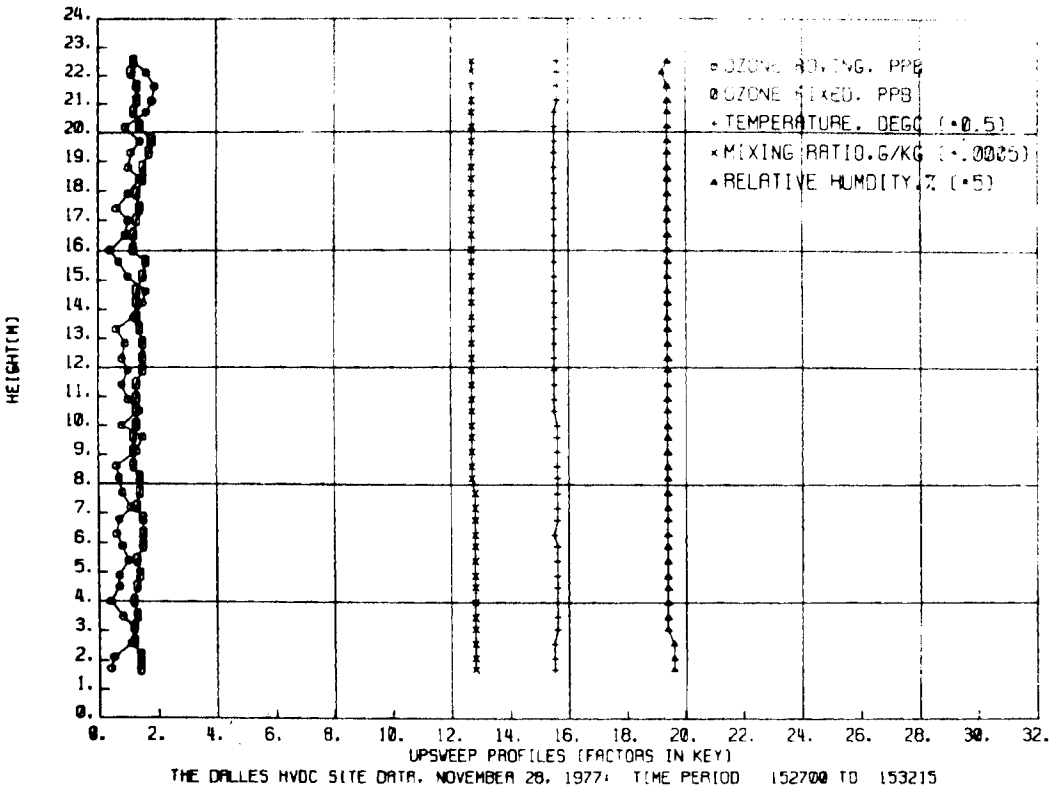

FIGURE F-1. Vertical Profiles for Case Study Number 1, ±550 kV

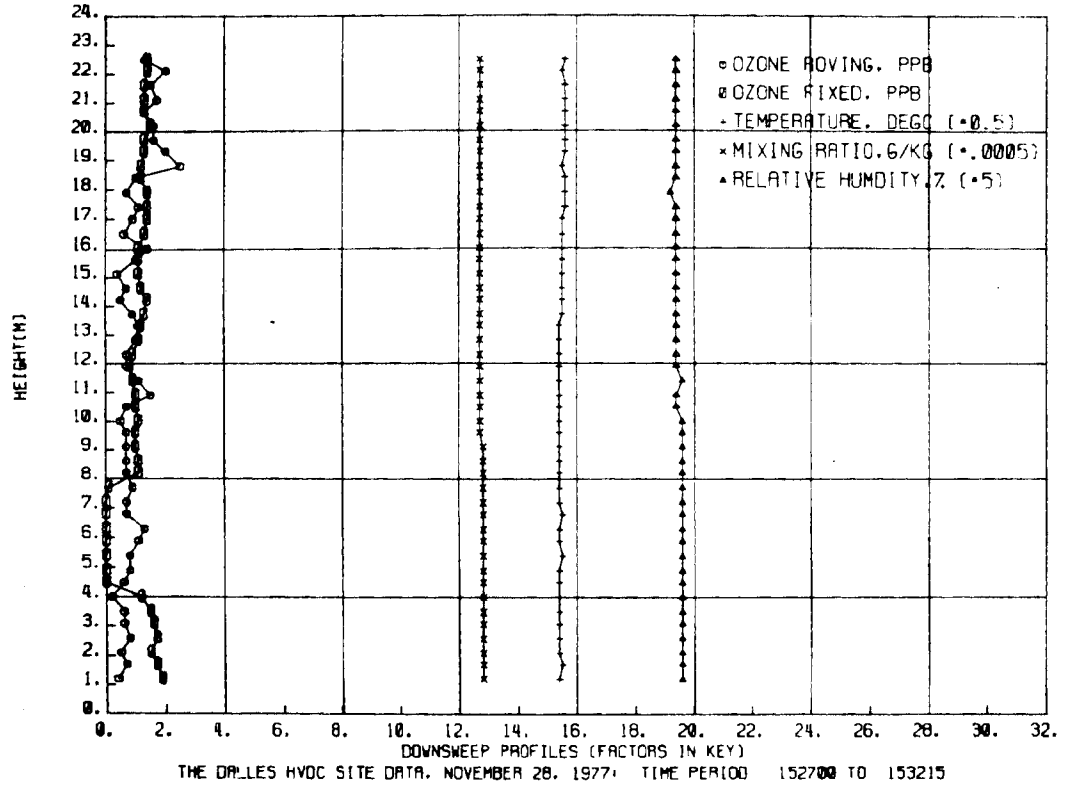

FIGURE F-2. Vertical Profiles for Case Study Number 1, ±550 kV

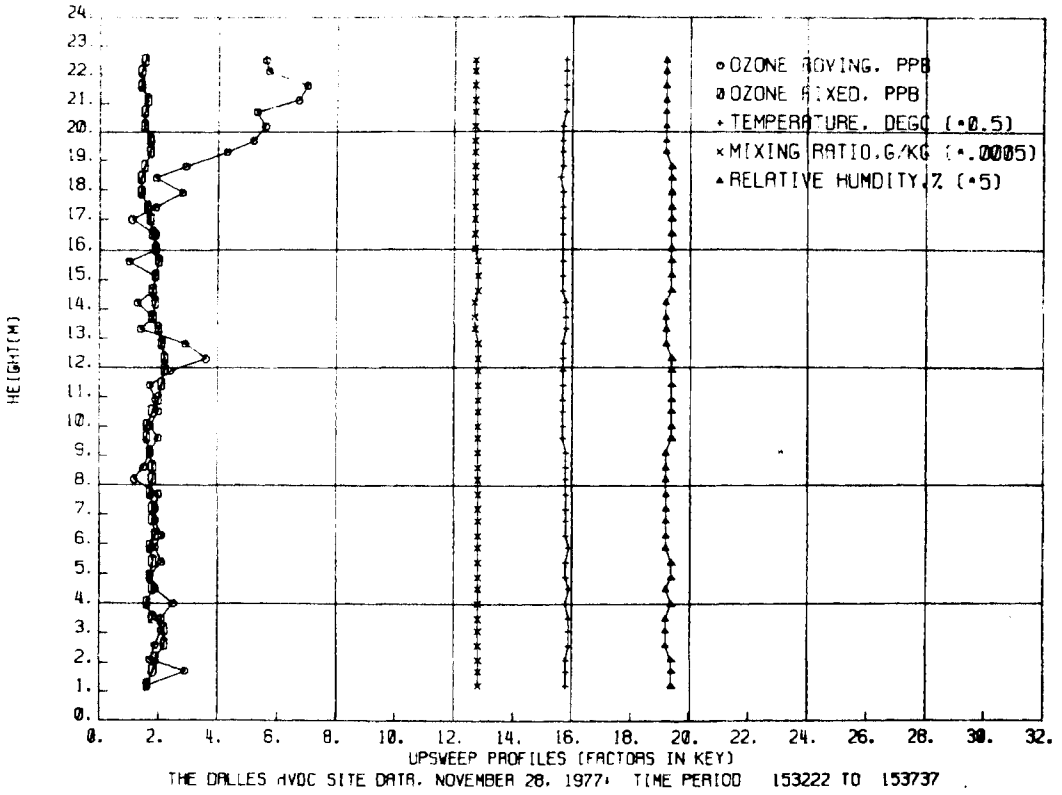

FIGURE F-3. Vertical Profiles for Case Study Number 1, ±550 kV

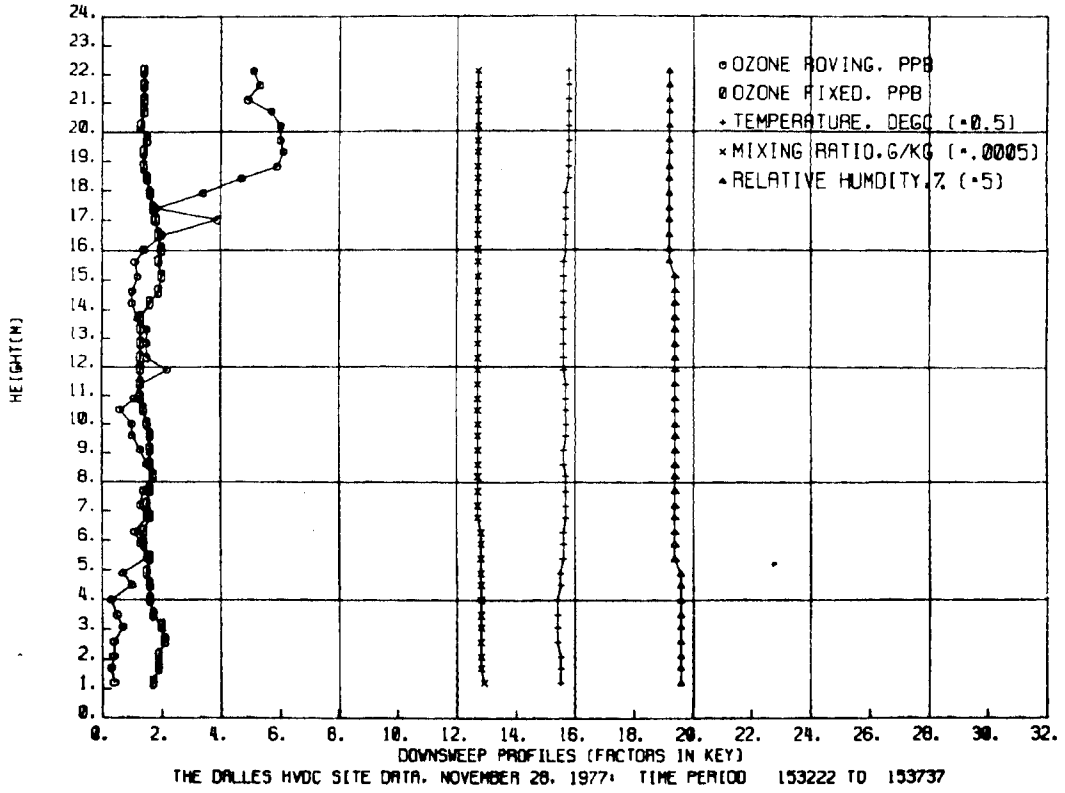

FIGURE F-4. Vertical Profiles for Case Study Number 1, ±550 kV

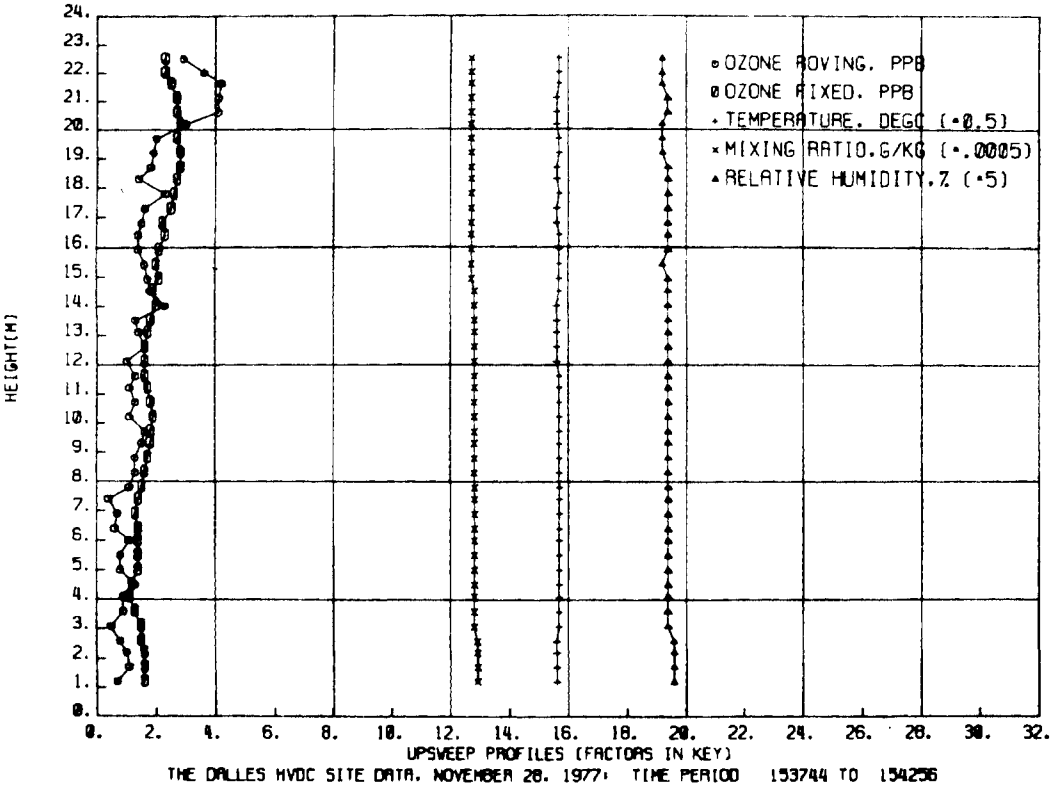

FIGURE F-5. Vertical Profiles for Case Study Number 1, ±550 kV

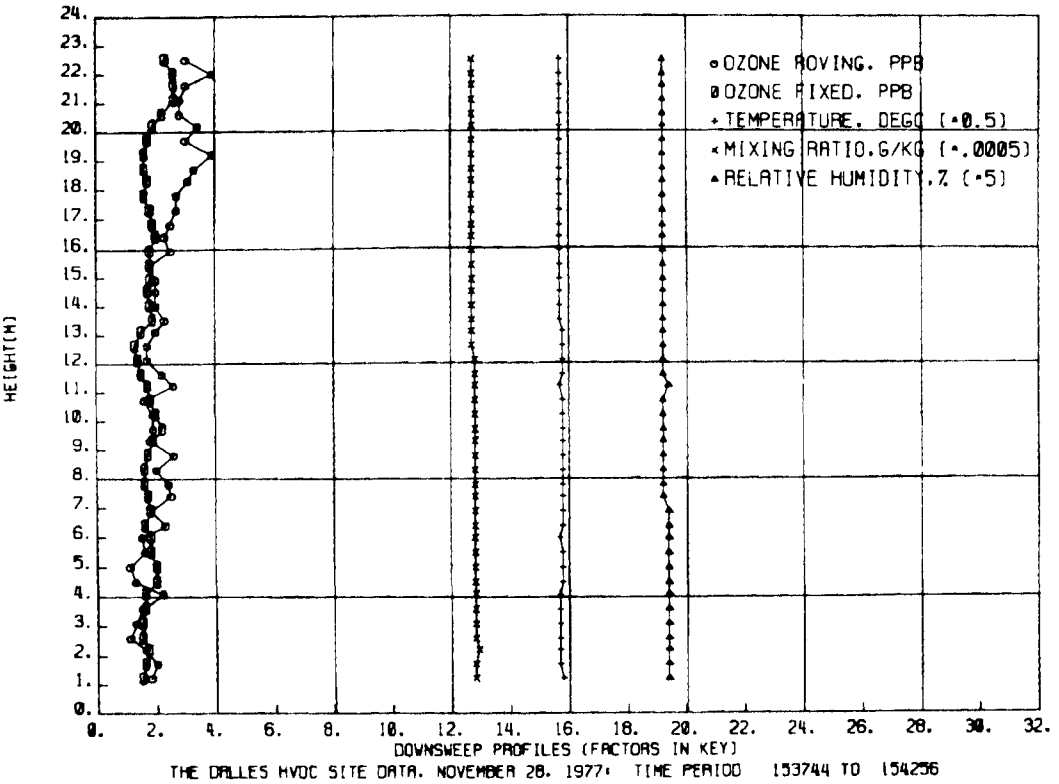

FIGURE F-6. Vertical Profiles for Case Study Number 1, ±550 kV

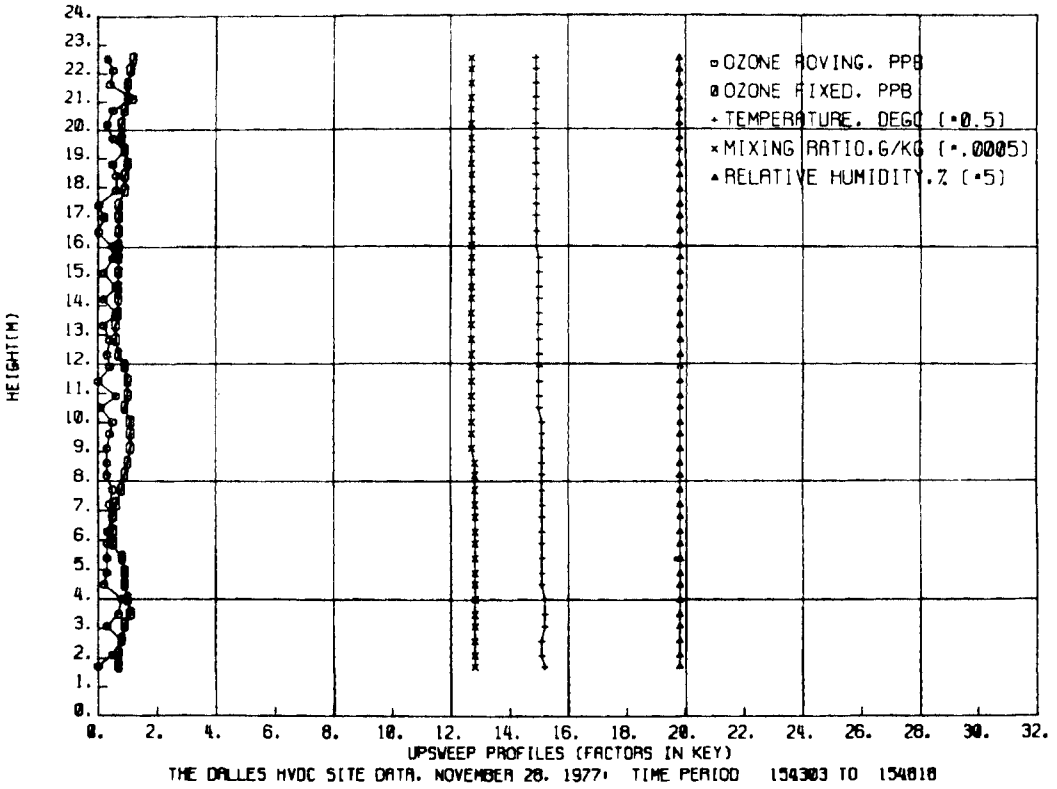

FIGURE F-7. Vertical Profiles for Case Study Number 1, ±550 kV

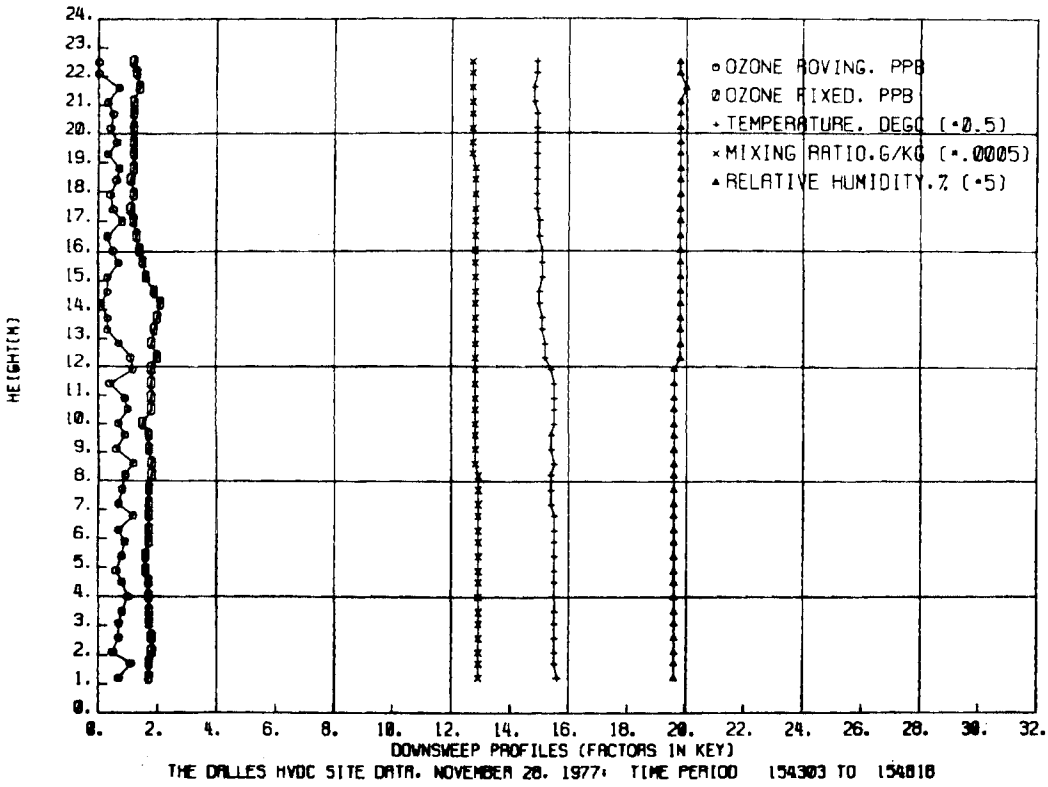

FIGURE F-8. Vertical Profiles for Case Study Number 1, ±550 kV

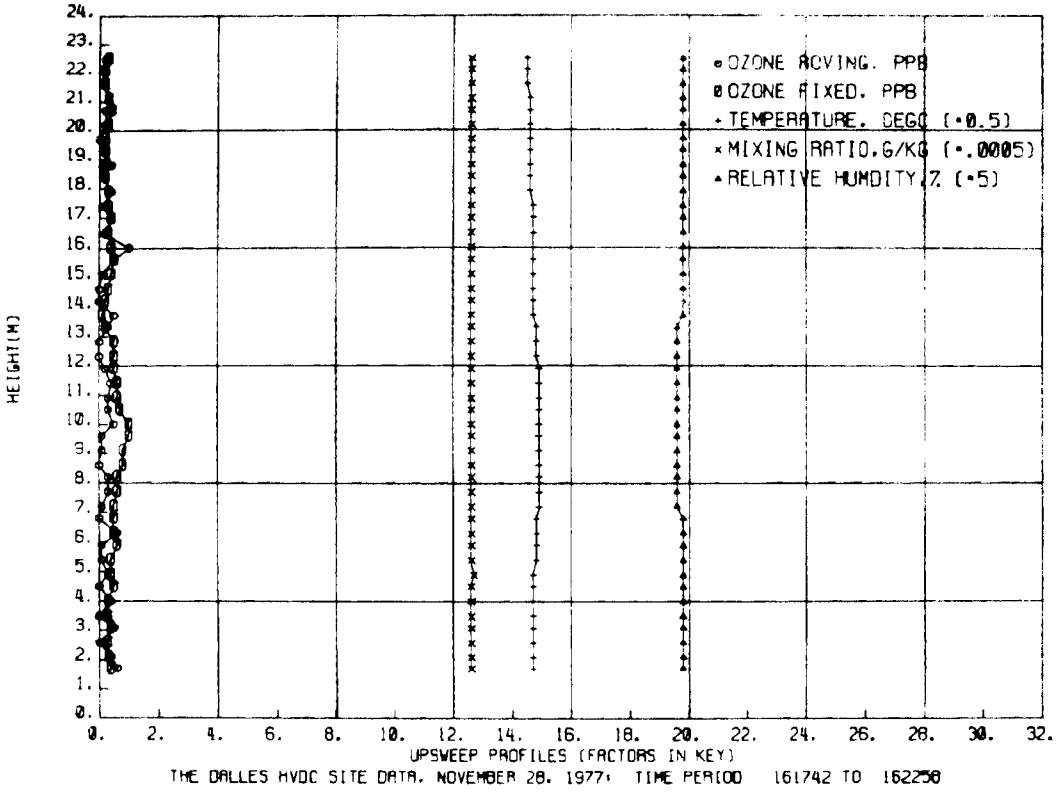

FIGURE F-9. Vertical Profiles for Case Study Number 1, ±550 kV

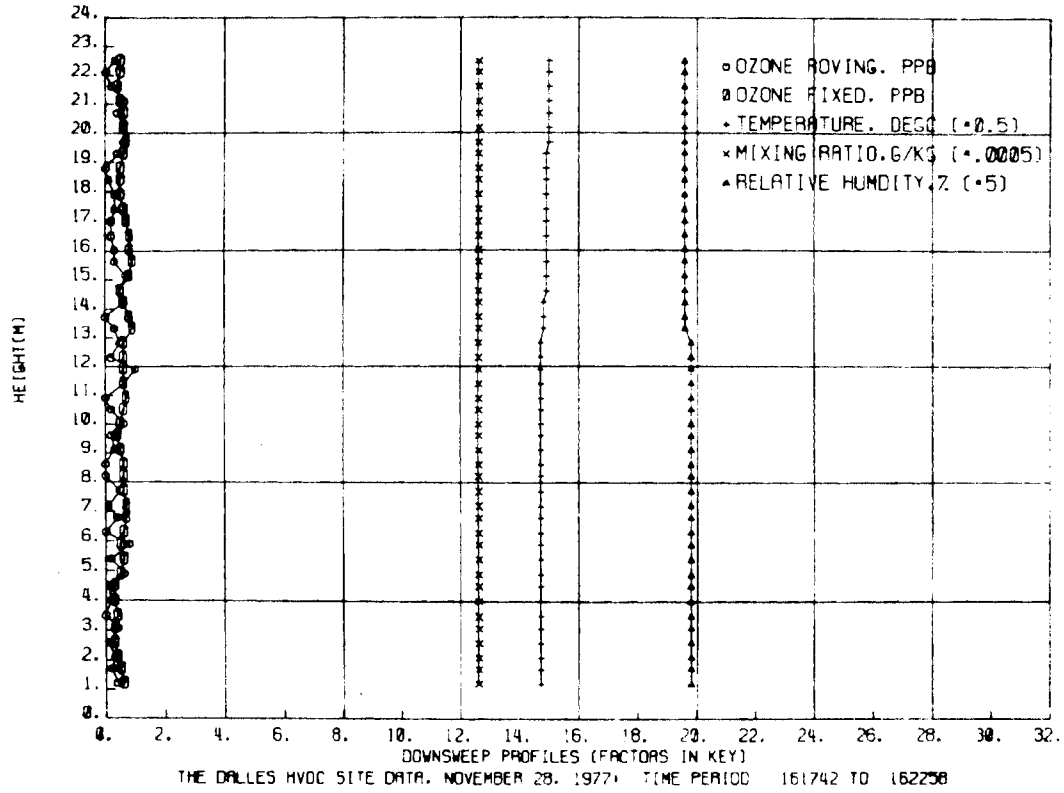

FIGURE F-10. Vertical Profiles for Case Study Number 1, ±550 kV

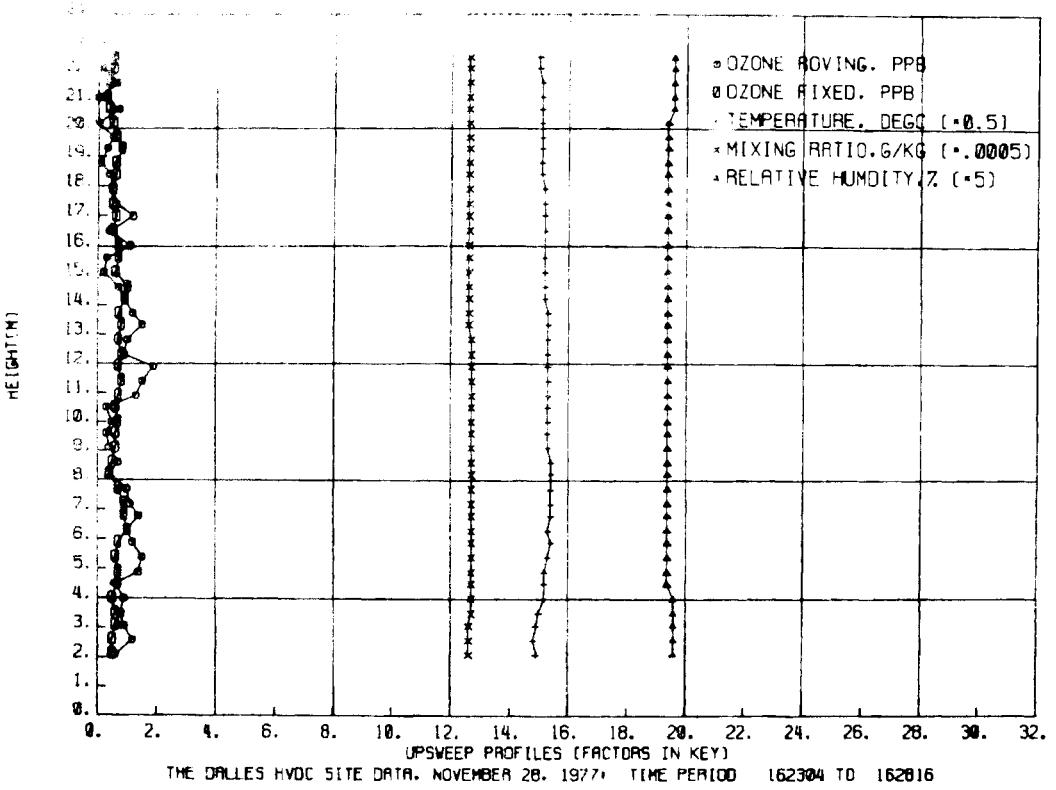

FIGURE F-11. Vertical Profiles for Case Study Number 1, ±550 kV

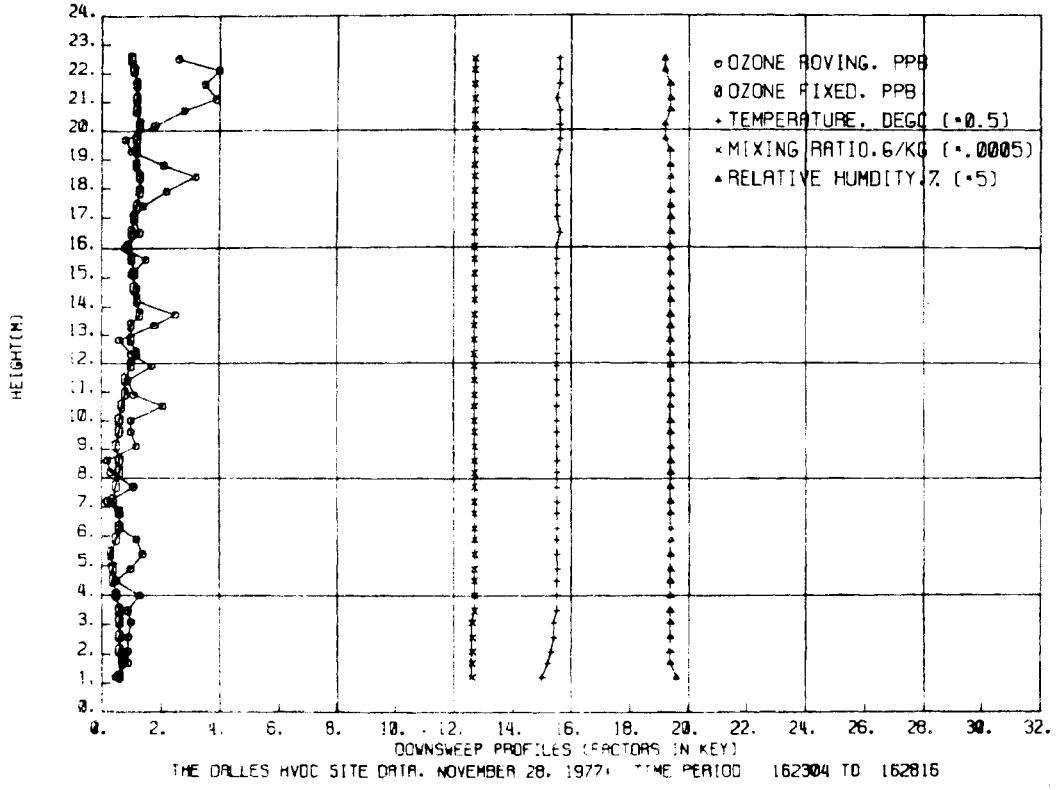

FIGURE F-12. Vertical Profiles for Case Study Number 1, 550 kV

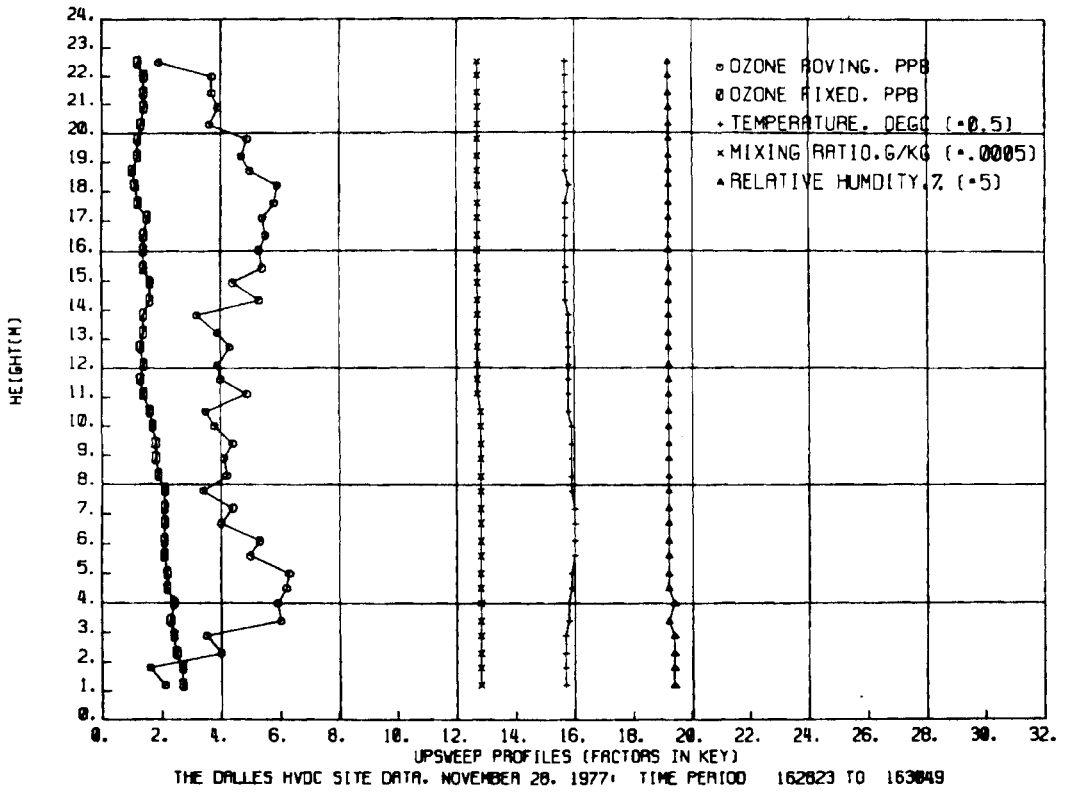

FIGURE F-13. Vertical Profiles for Case Study Number 1, ±550 kV

(Downsweep profile data not available for this period)

FIGURE F-14

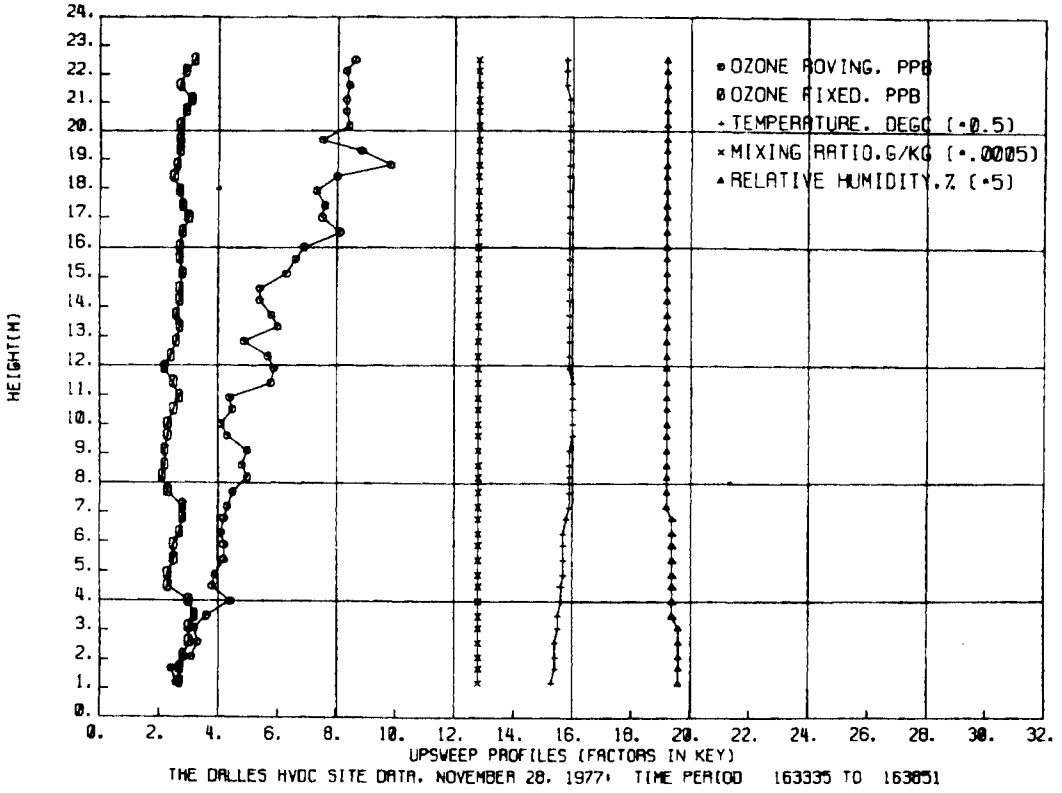

FIGURE F-15. Vertical Profiles for Case Study Number 1, ±550 kV

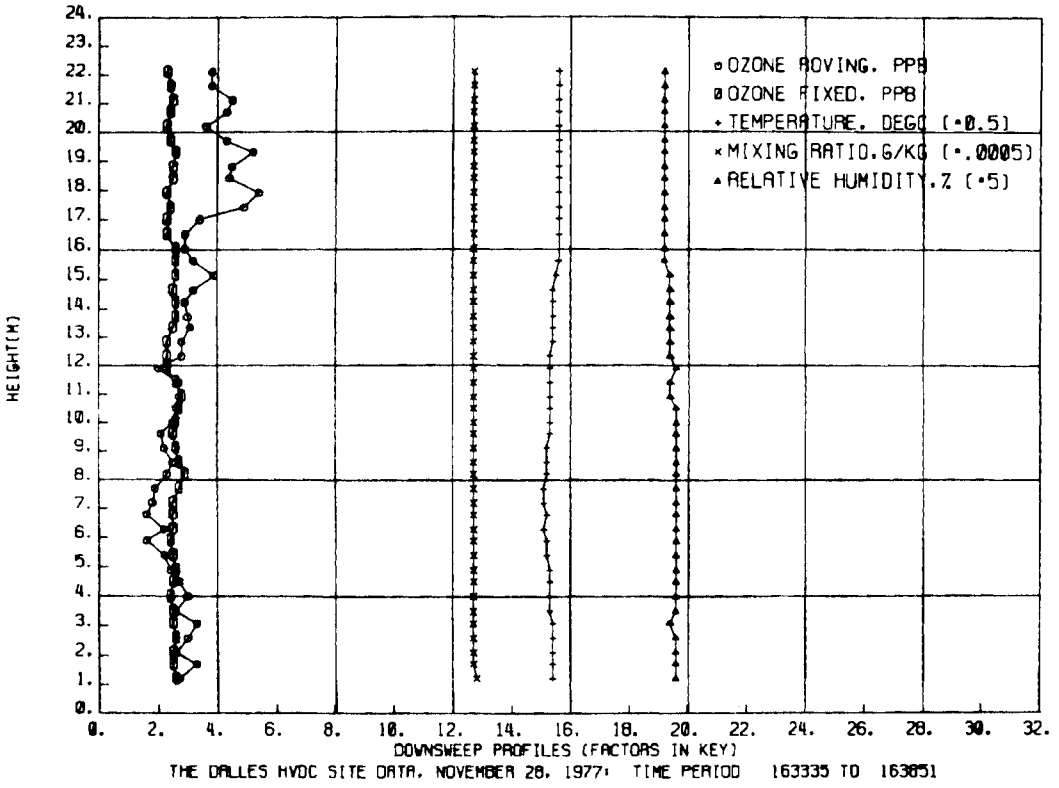

FIGURE F-16. Vertical Profiles for Case Study Number 1, ±500 kV

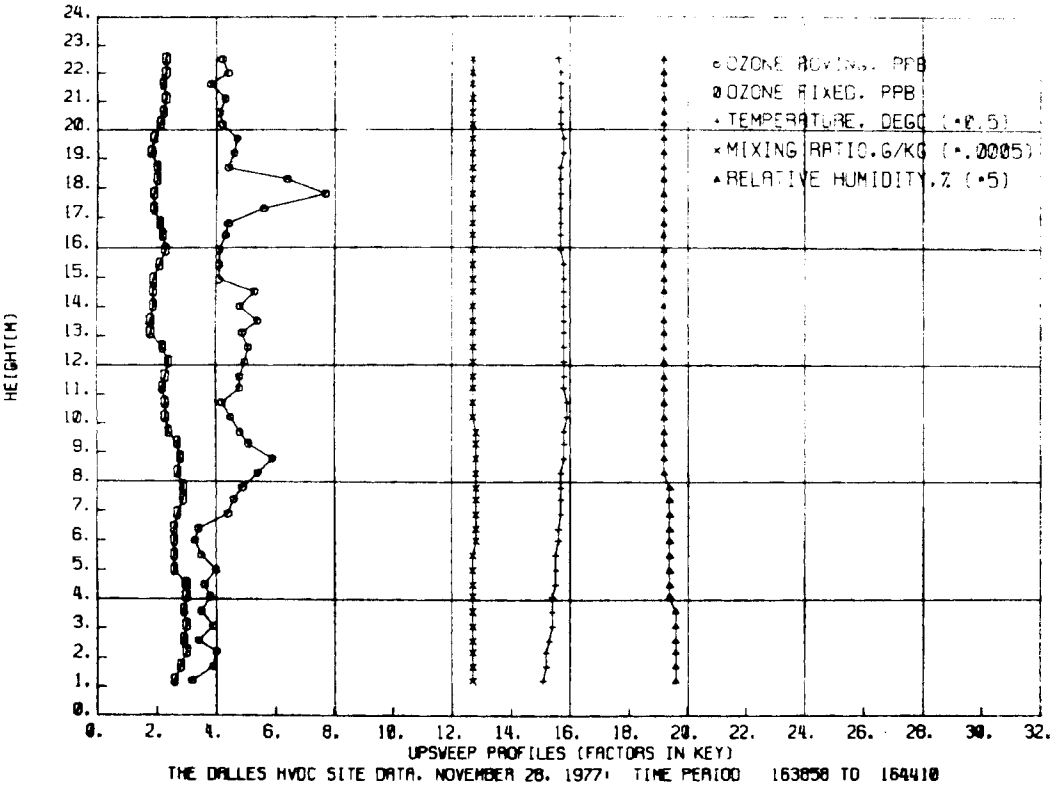

FIGURE F-17. Vertical Profiles for Case Study Number 1, ±500 kV

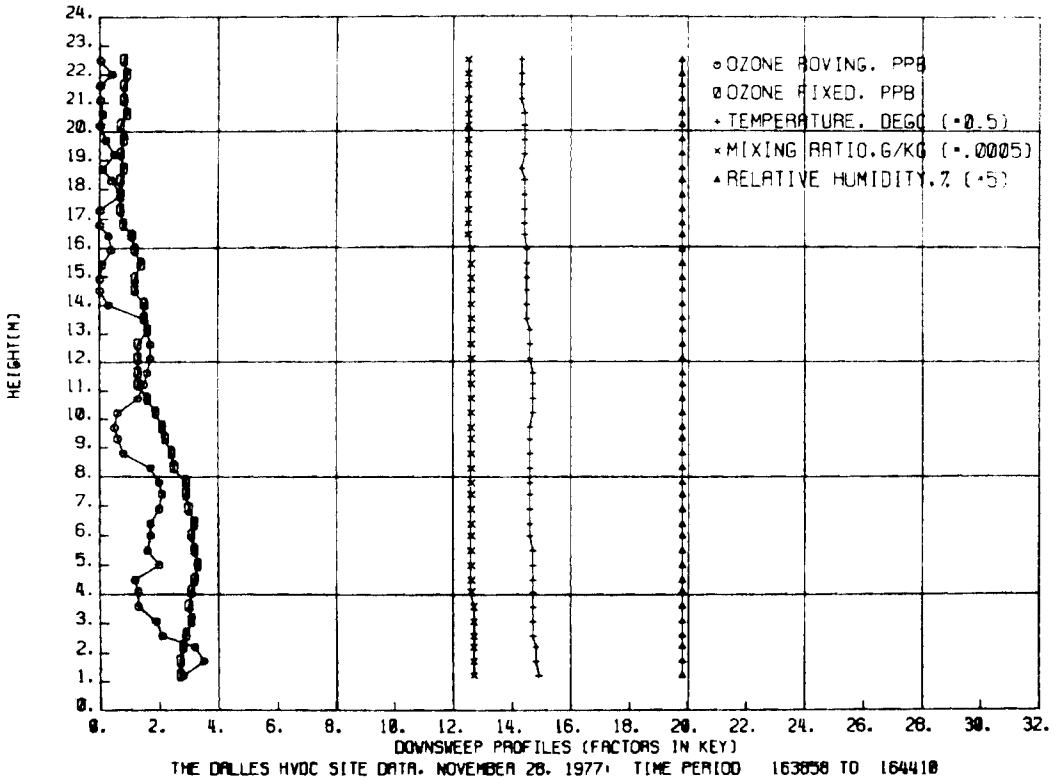

FIGURE F-18. Vertical Profiles for Case Study Number 1, ±500 kV

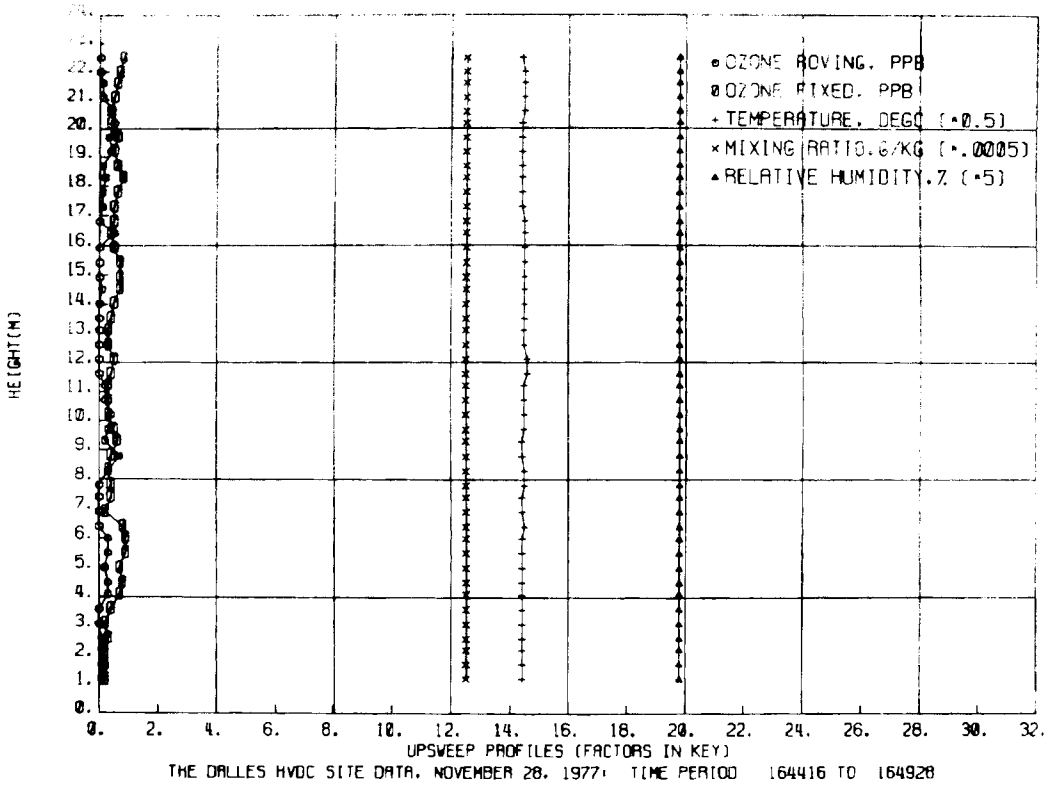

FIGURE F-19. Vertical Profiles for Case Study Number 1, ±500 kV

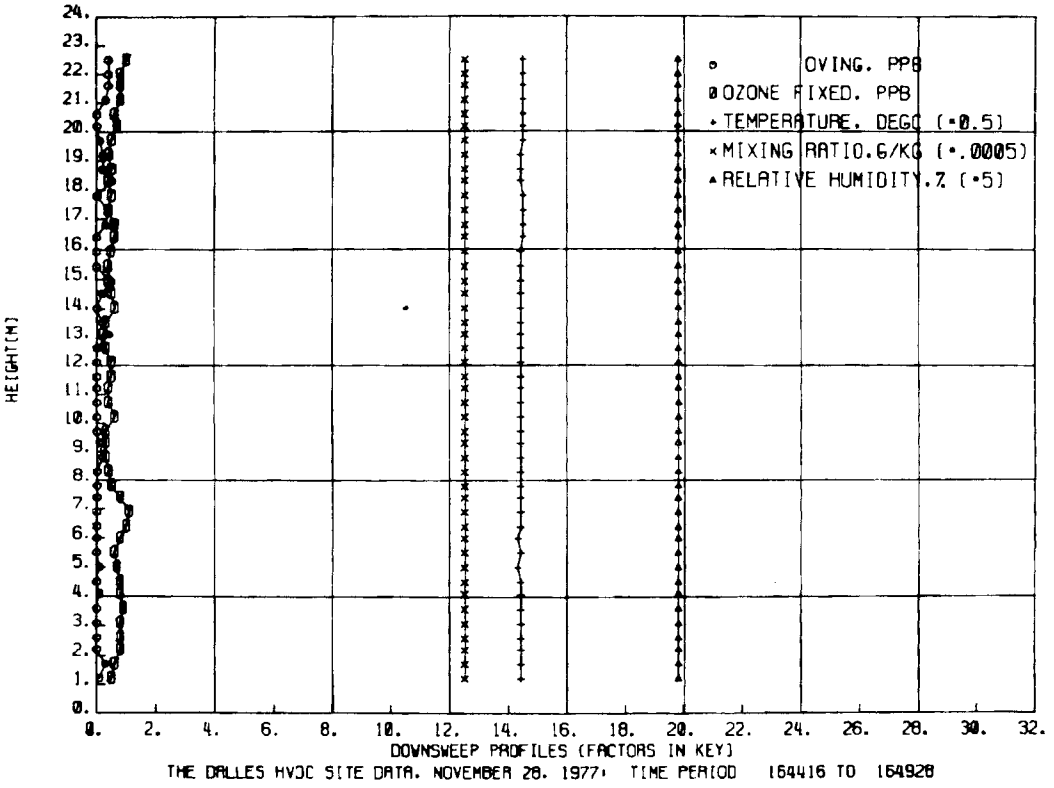

FIGURE F-20. Vertical Profiles for Case Study Number 1, ±500 kV

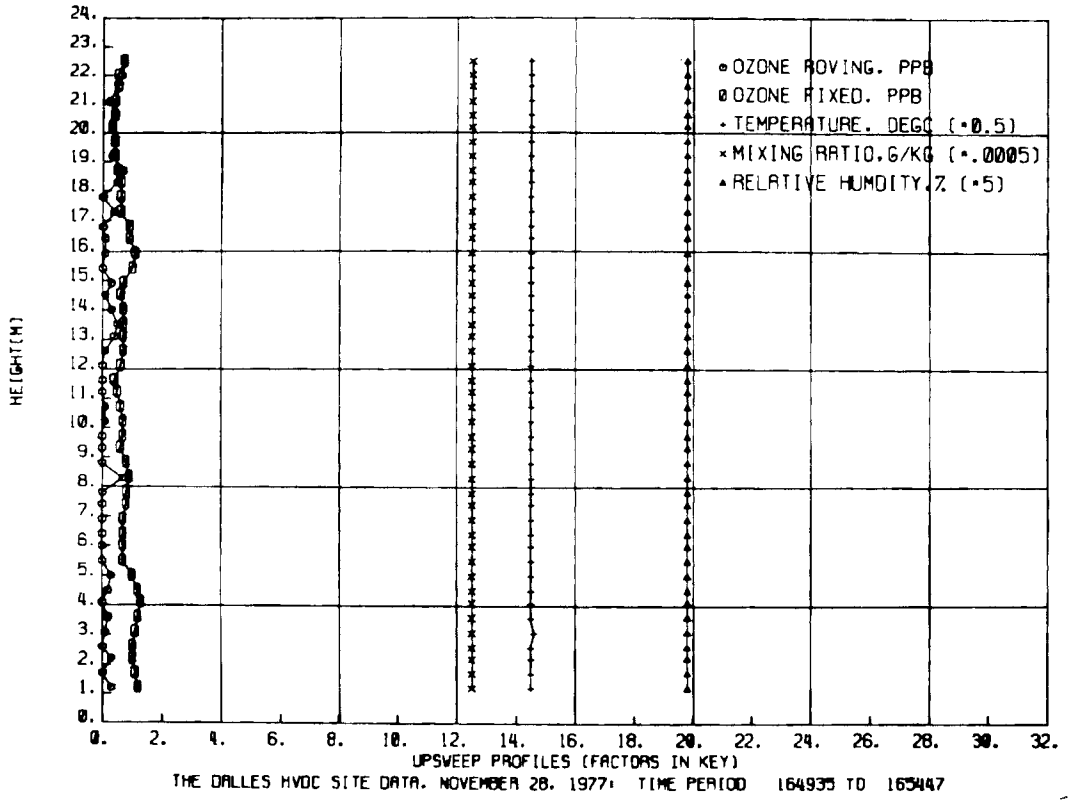

FIGURE F-21. Vertical Profiles for Case Study Number 1, ±500 kV

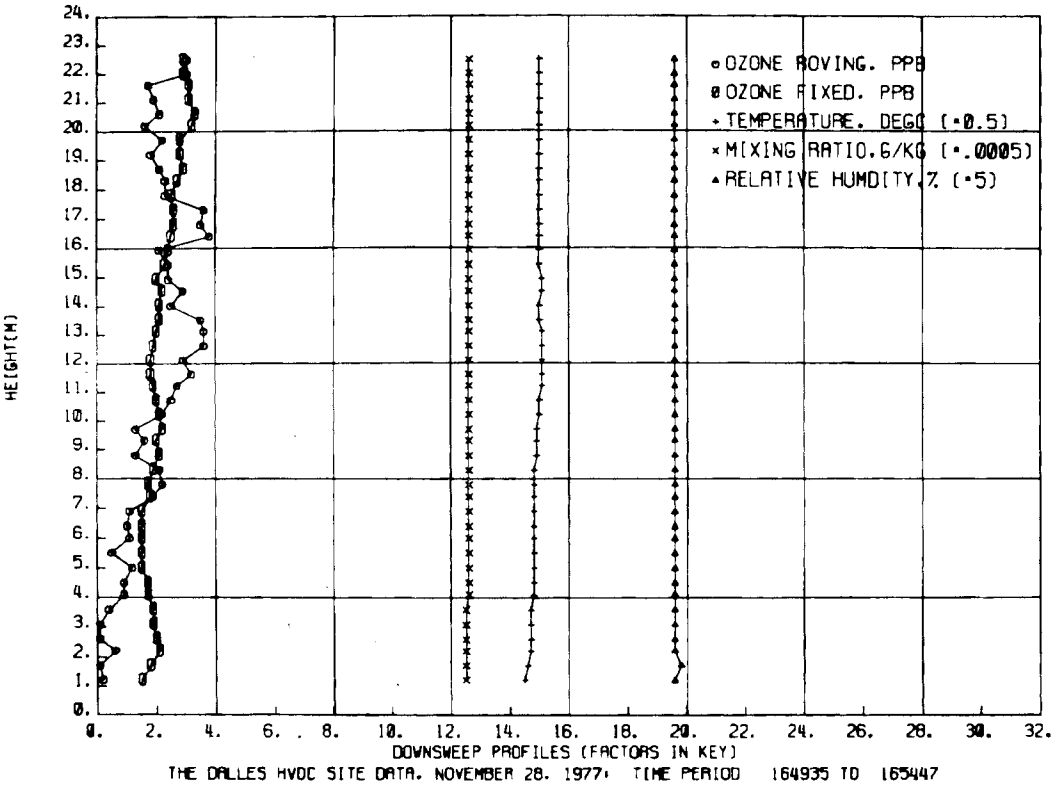

FIGURE F-22. Vertical Profiles for Case Study Number 1, ±500 kV

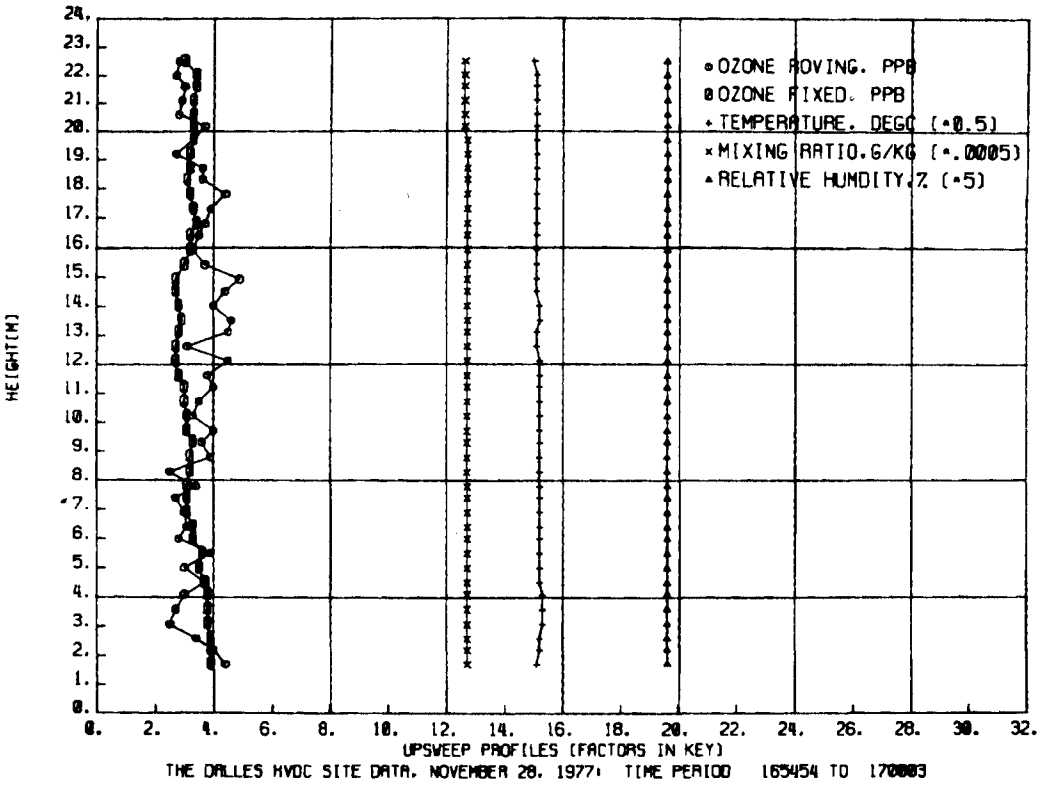

FIGURE F-23. Vertical Profiles for Case Study Number 1, ±500 kV

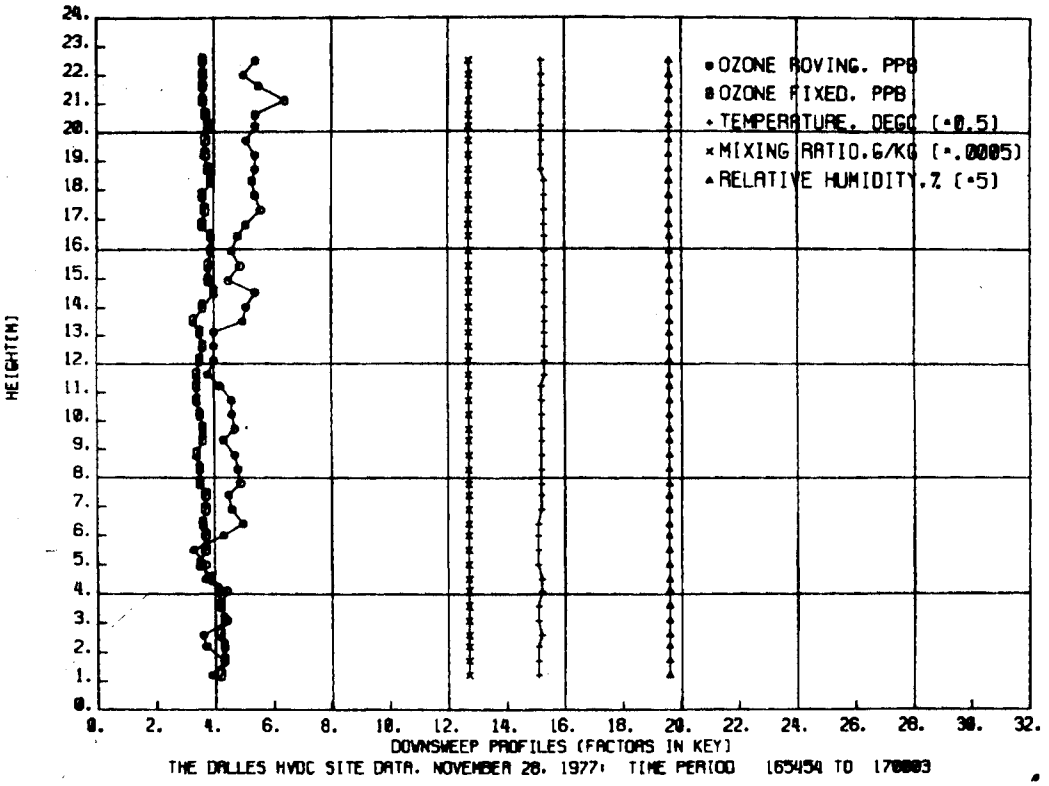

FIGURE F-24. Vertical Profiles for Case Study Number 1, ±500 kV

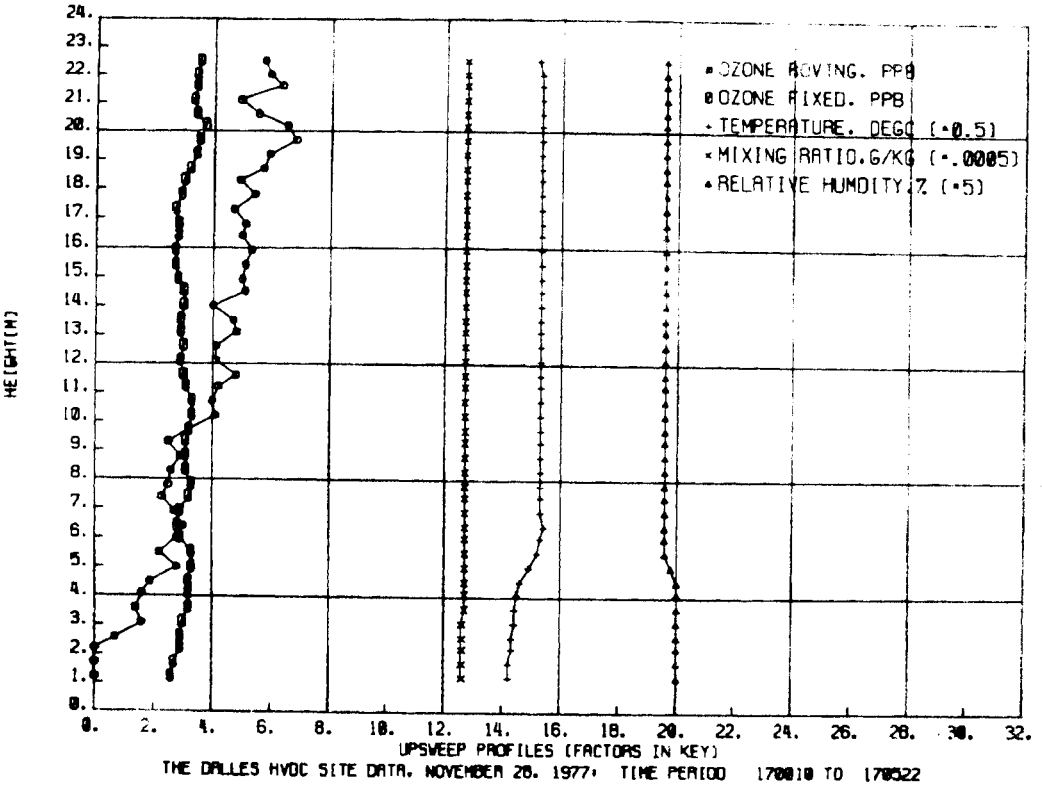

FIGURE F-25. Vertical Profiles for Case Study Number 1, ±500 kV

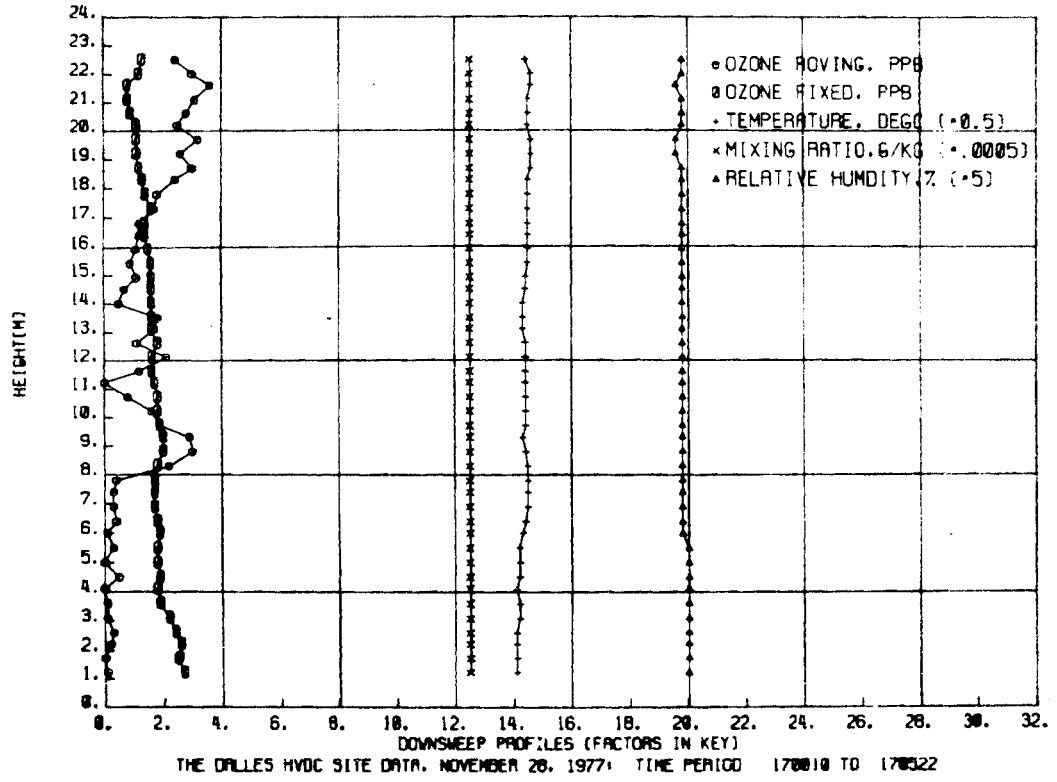

FIGURE F-26. Vertical Profiles for Case Study Number 1, ±500 kV

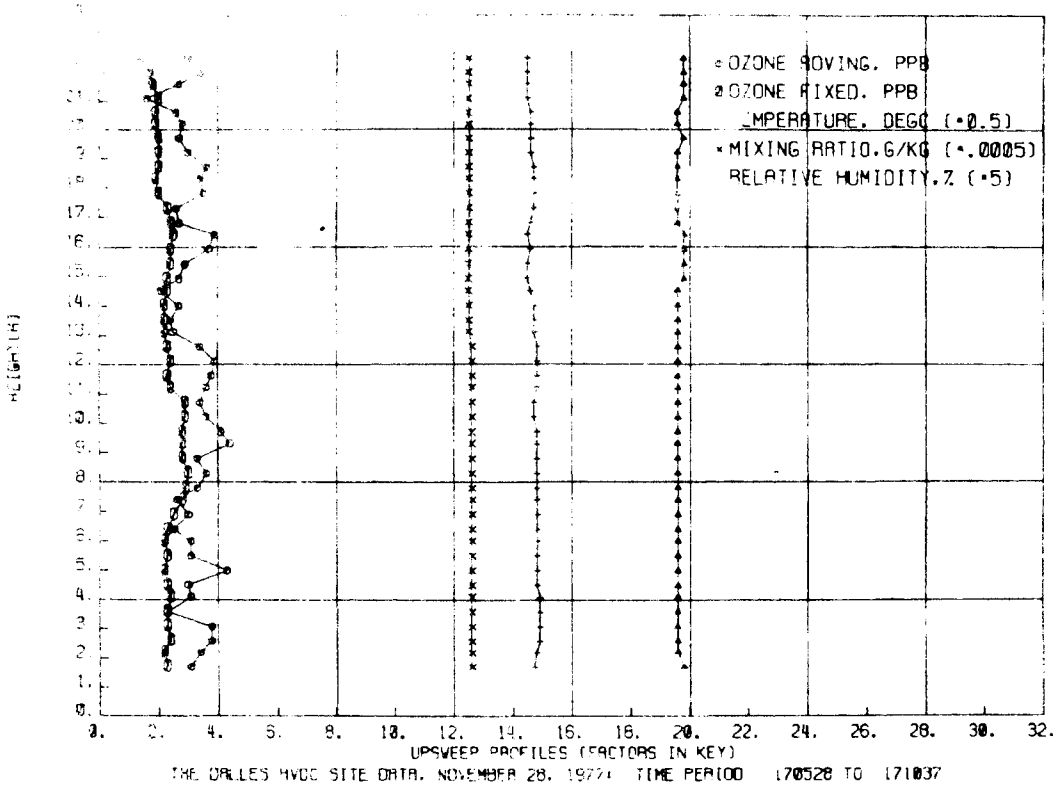

FIGURE F-27. Vertical Profiles for Case Study Number 1, ±500 kV

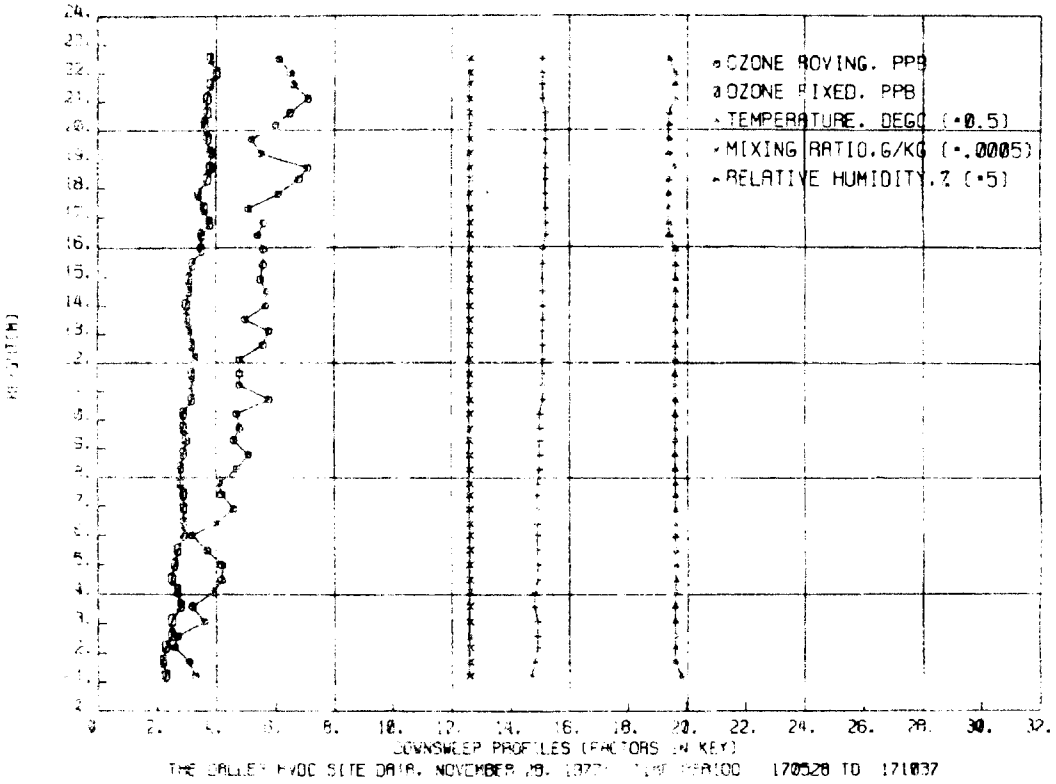

FIGURE F-28. Vertical Profiles for Case Study Number 1, ±500 kV

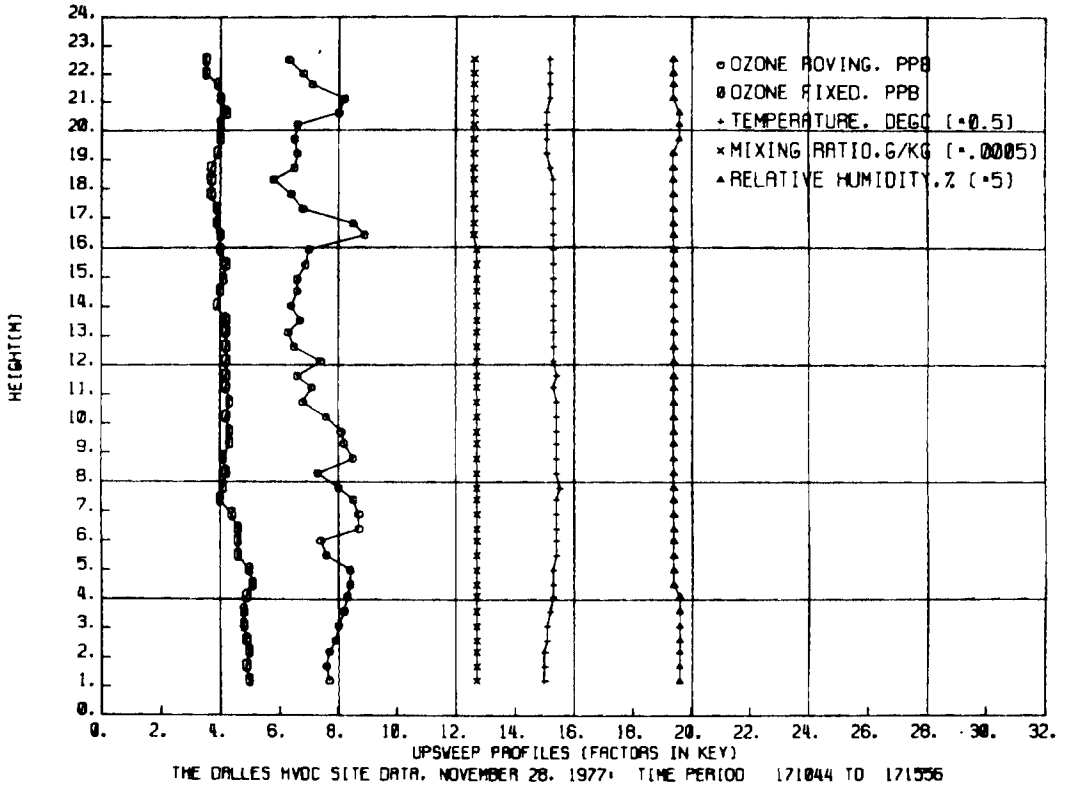

FIGURE F-29. Vertical Profiles for Case Study Number 1, ±500 kV

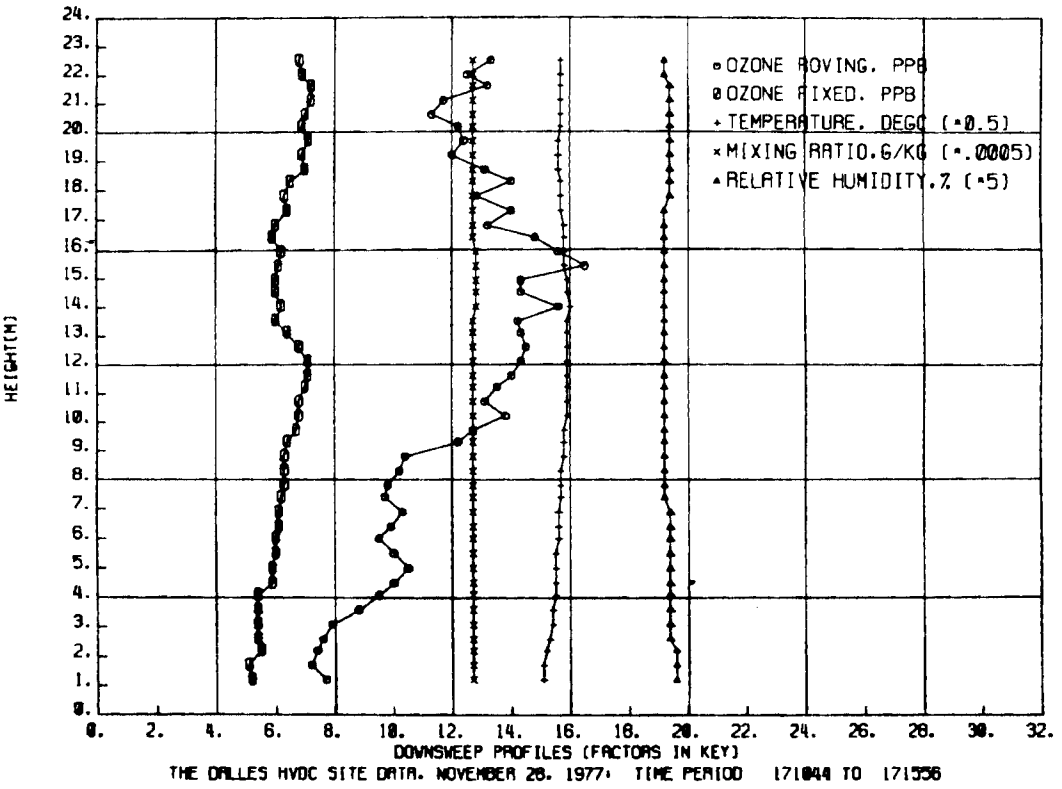

FIGURE F-30. Vertical Profiles for Case Study Number 1, ±500 kV

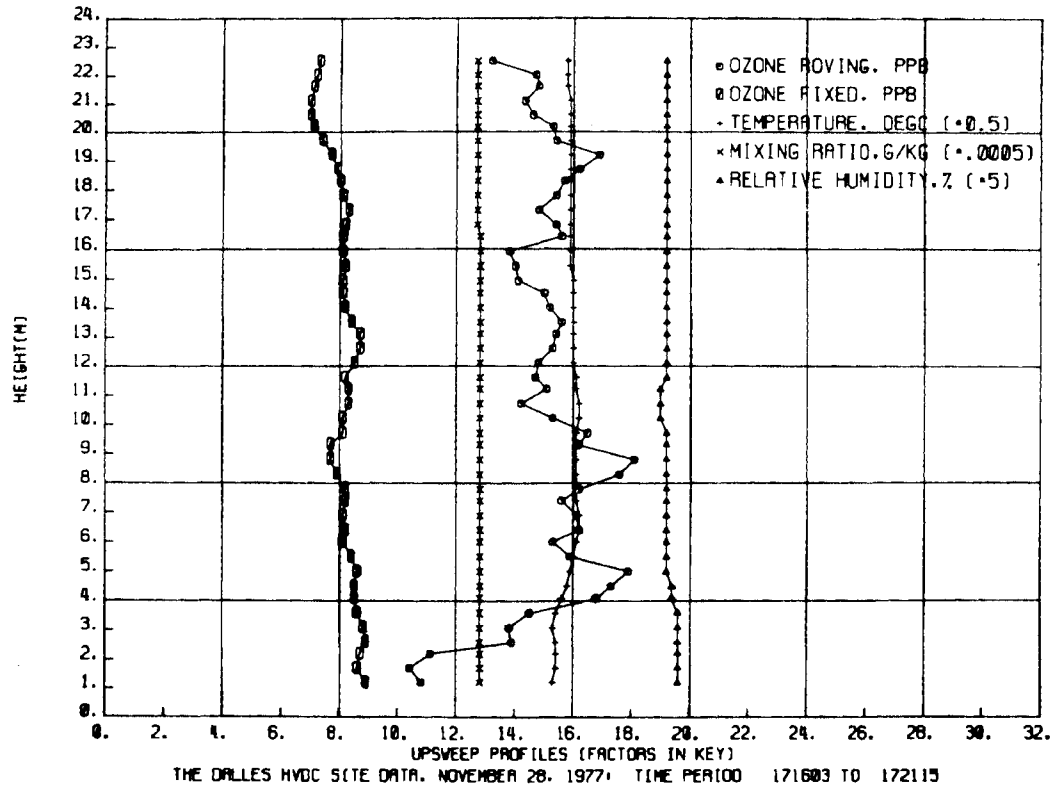

FIGURE F-31. Vertical Profiles for Case Study Number 1, ±500 kV

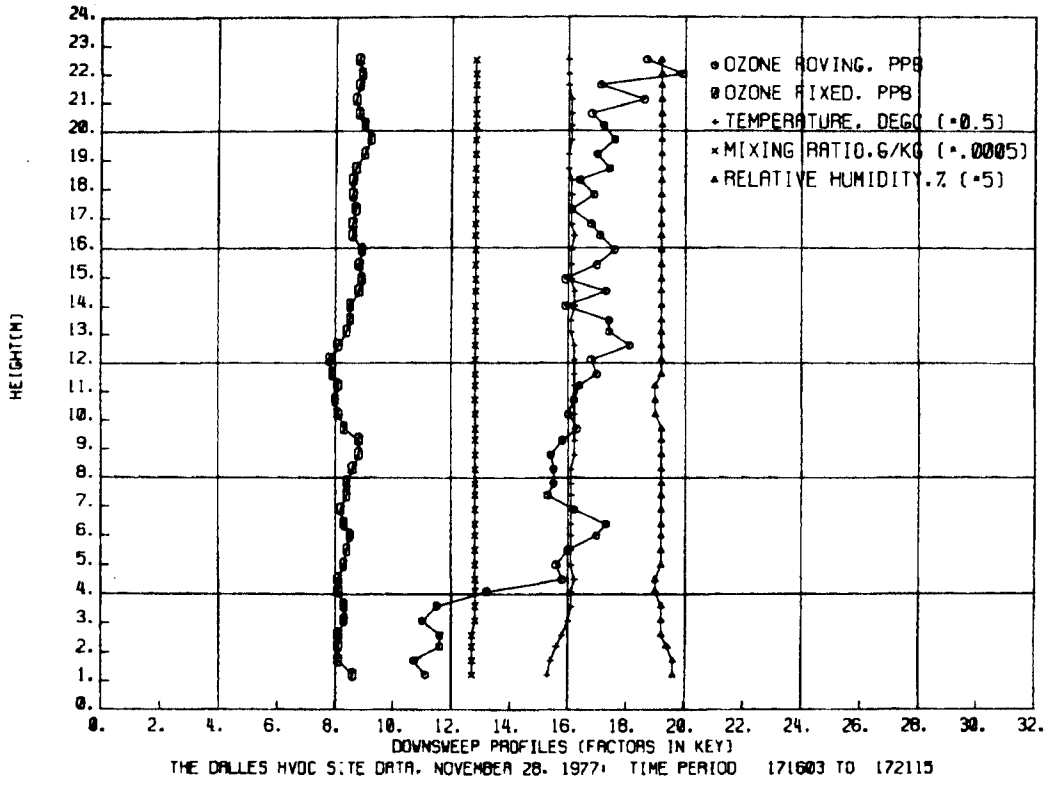

FIGURE F-32. Vertical Profiles for Case Study Number 1, ±500 kV

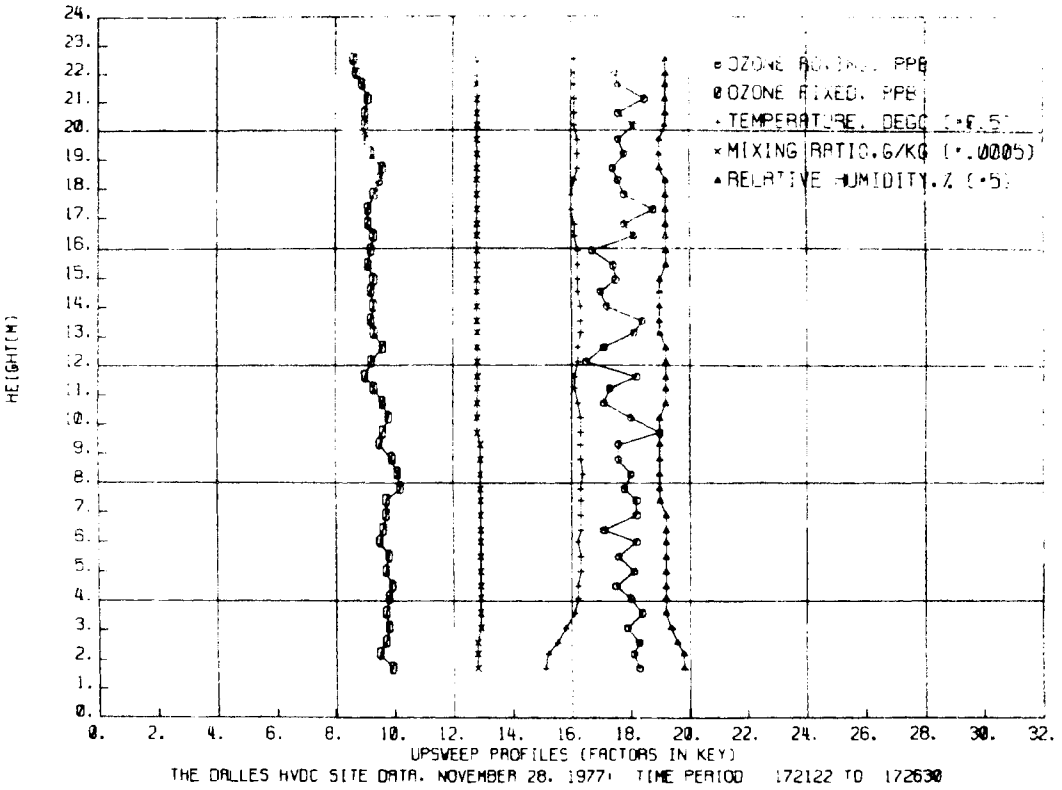

FIGURE F-33. Vertical Profiles for Case Study Number 1, ±500 kV

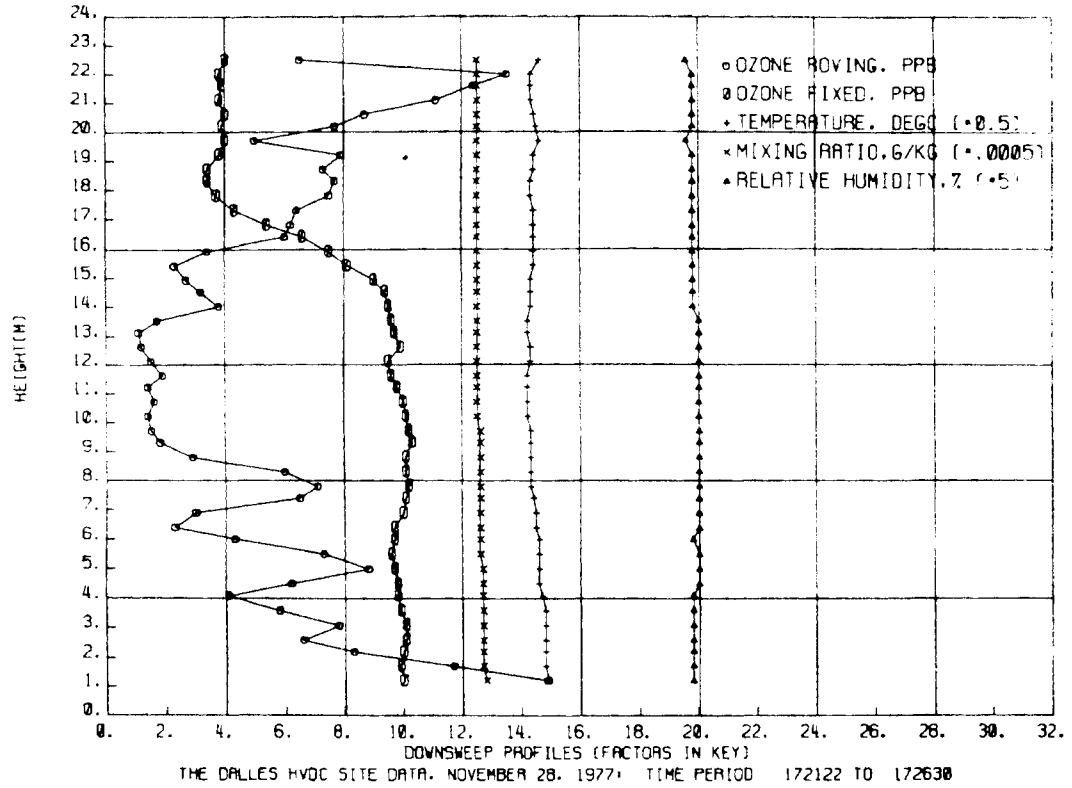

FIGURE F-34. Vertical Profiles for Case Study Number 1, ±500 kV

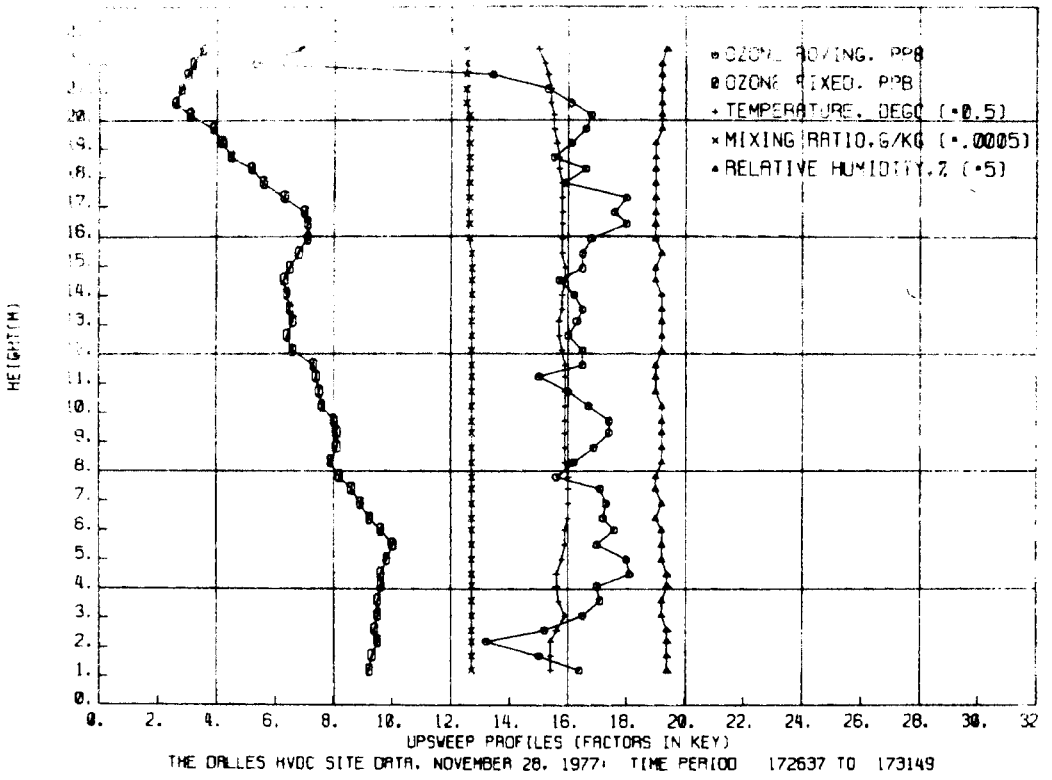

FIGURE F-35. Vertical Profiles for Case Study Number 1, ±500 kV

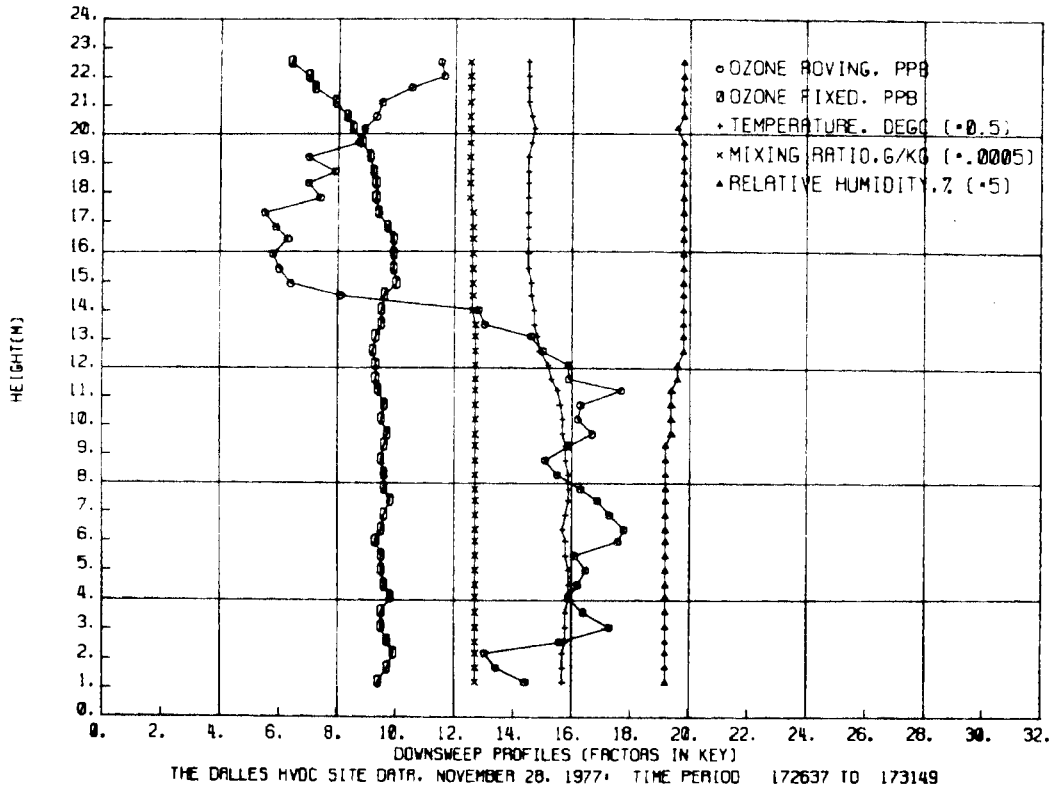

FIGURE F-36. Vertical Profiles for Case Study Number 1, ±500 kV

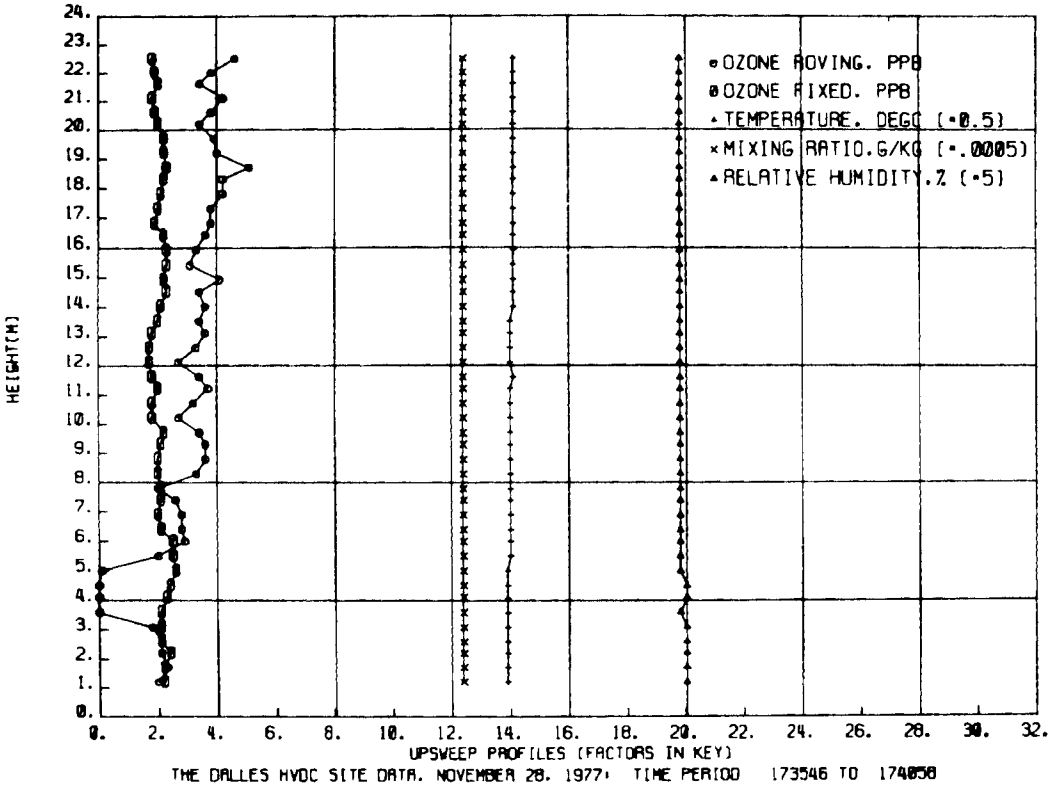

FIGURE F-37. Vertical Profiles for Case Study Number 1, ±500 kV

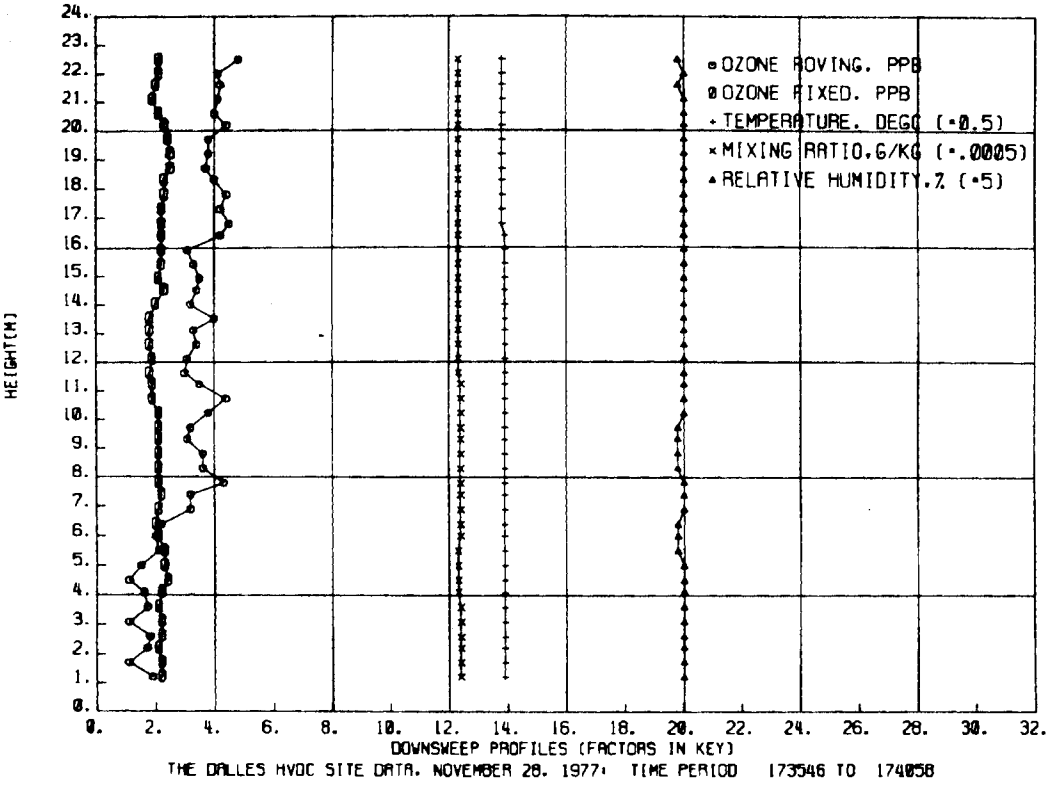

FIGURE F-38. Vertical Profiles for Case Study Number 1, ±500 kV

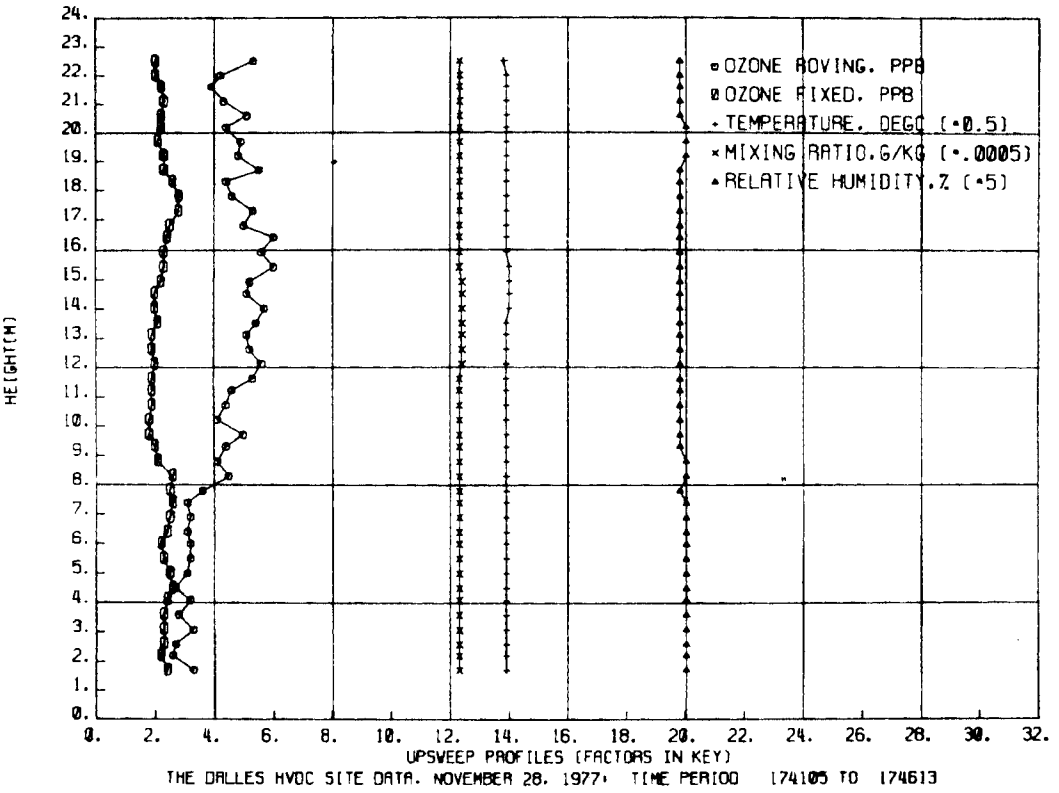

FIGURE F-39. Vertical Profiles for Case Study Number 1, ±500 kV

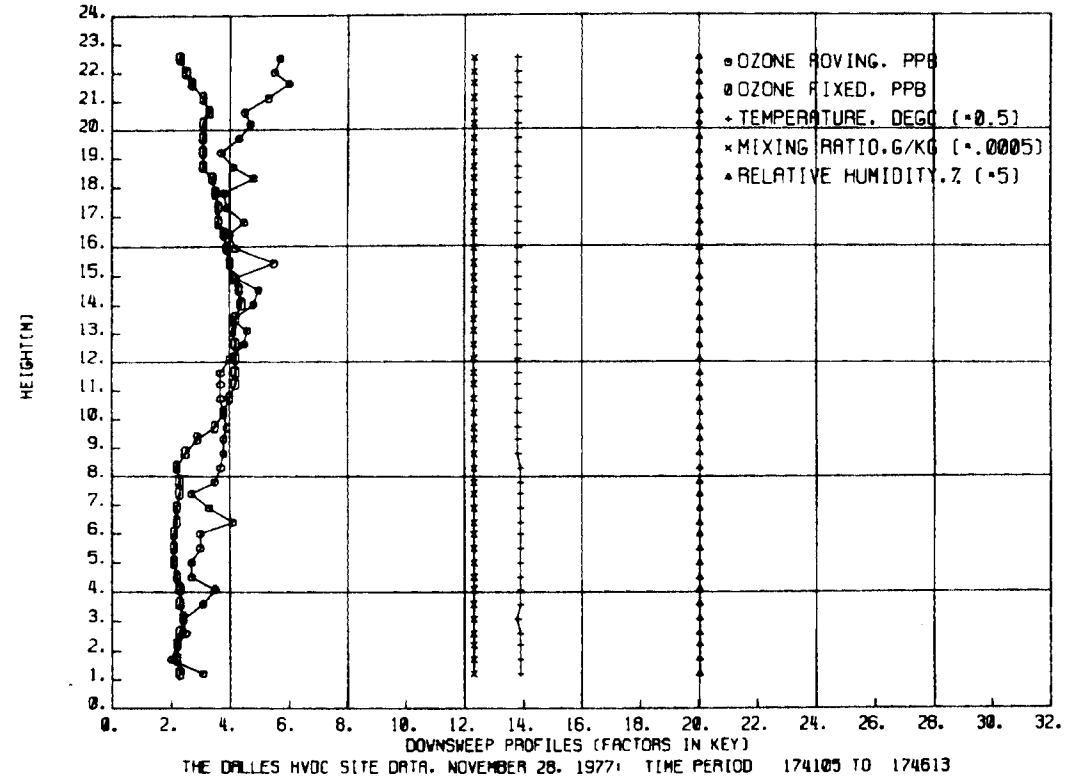

FIGURE F-40. Vertical Profiles for Case Study Number 1, ±500 kV

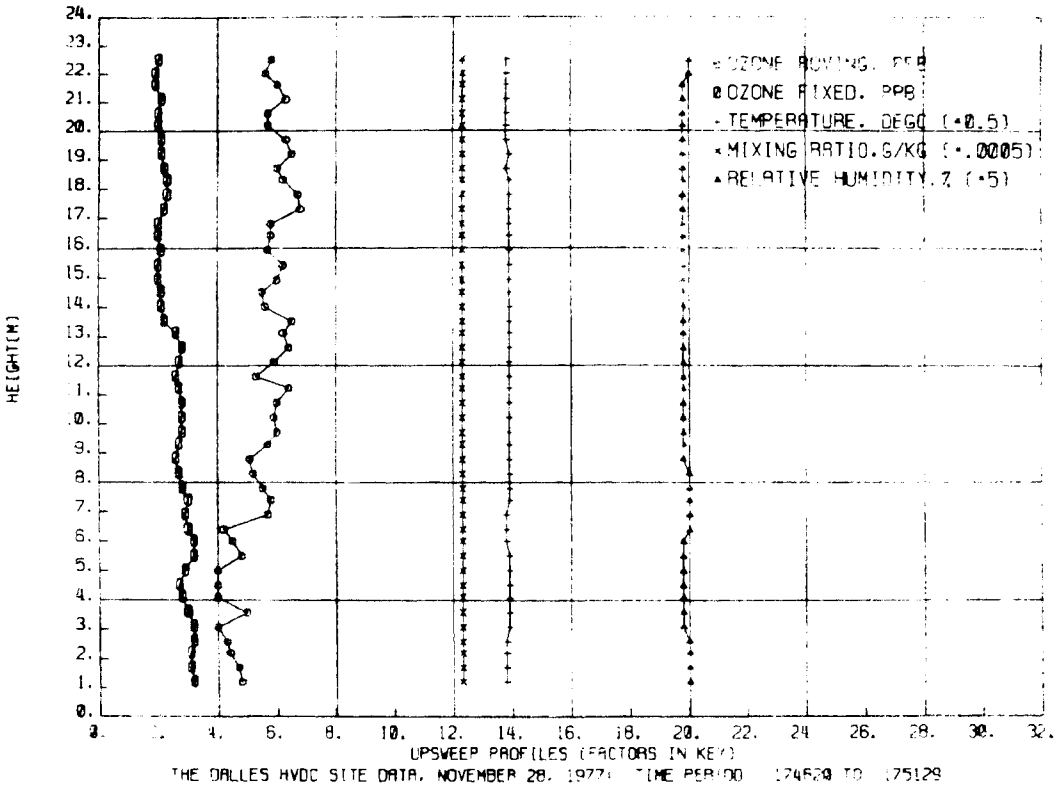

FIGURE F-41. Vertical Profiles for Case Study Number 1, ±500 kV

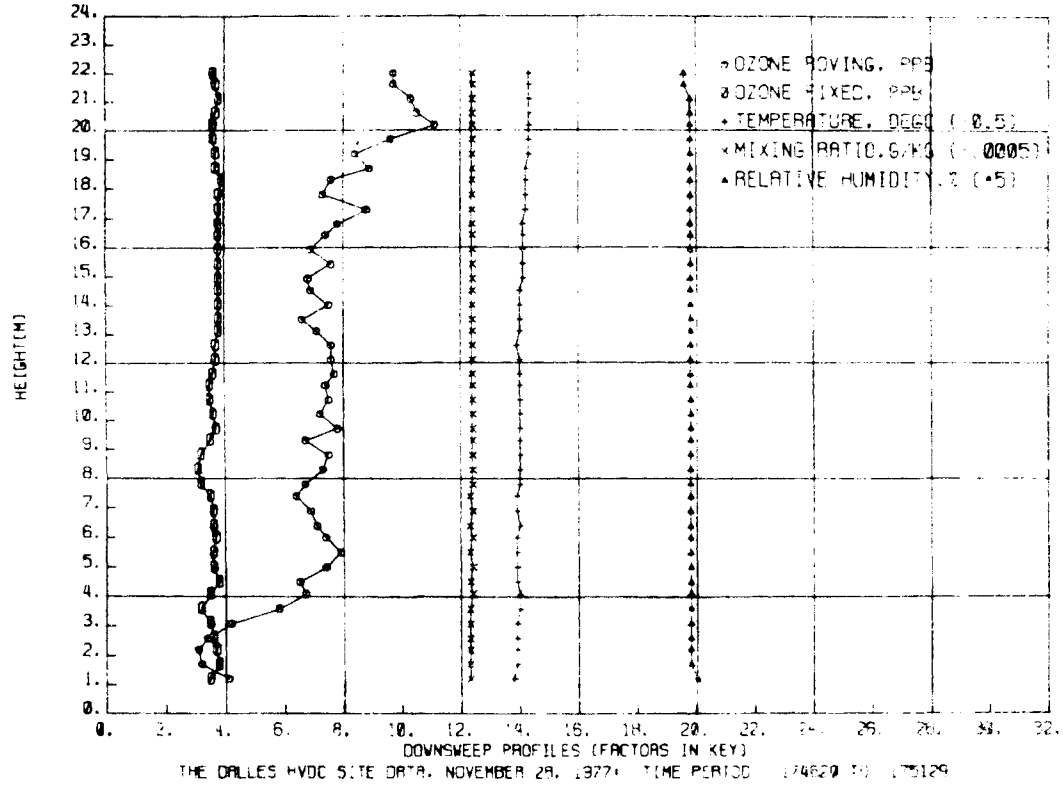

FIGURE F-42. Vertical Profiles for Case Study Number 1, ±500 kV

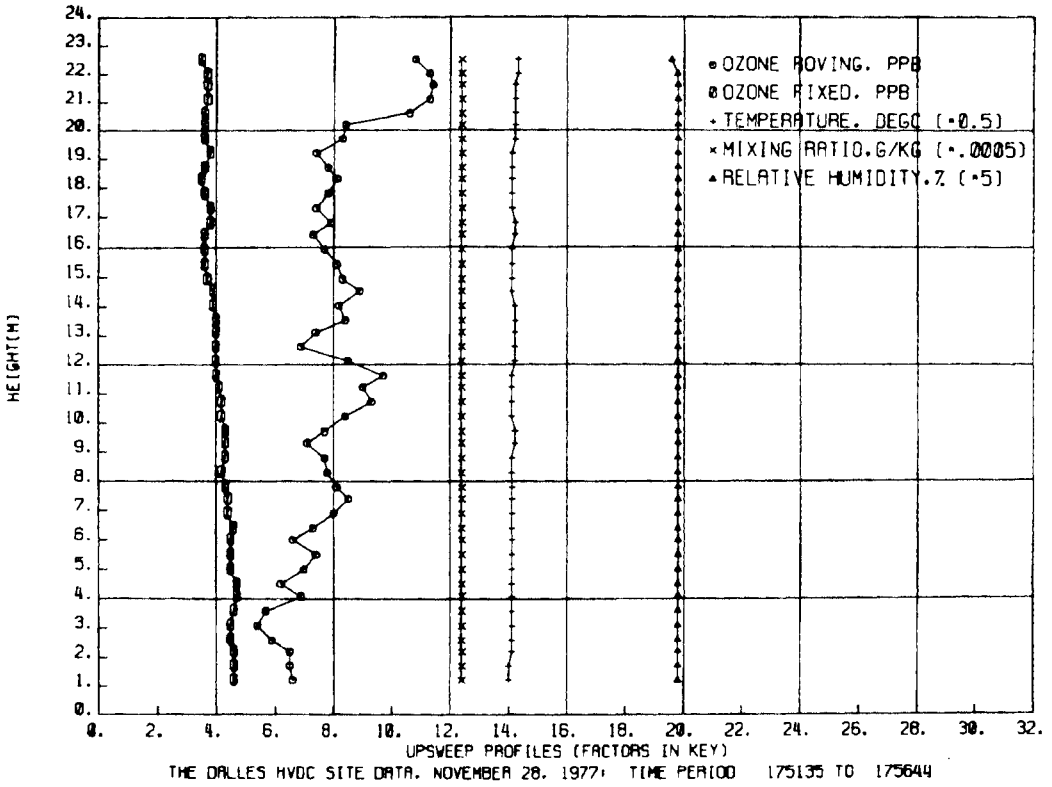

FIGURE F-43. Vertical Profiles for Case Study Number 1, ±500 kV

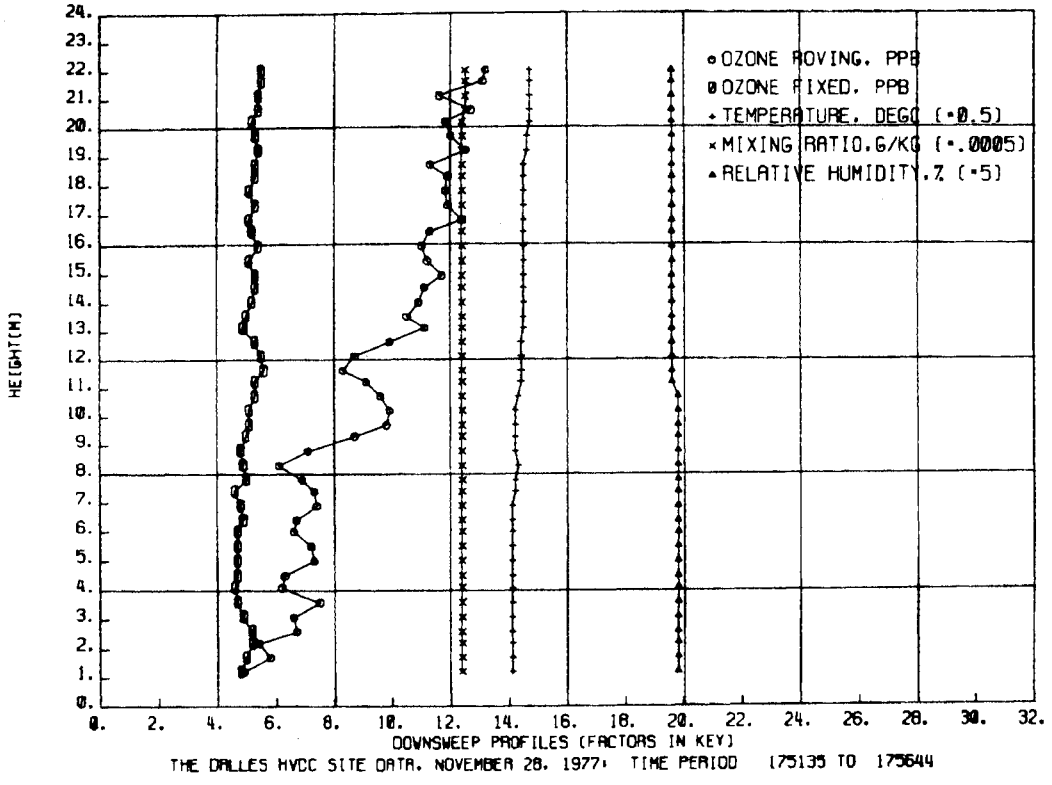

FIGURE F-44. Vertical Profiles for Case Study Number 1, ±500 kV

APPENDIX G

Profiles for Case Study #2

This appendix contains individual detailed profile plots from case study #2 (February 2, 1977 from 7:13 to 9:31). These figures are explained in the text. See Appendix B for the wind field definition for this case study. Table 4.2 contains the voltage and current data for these tests.

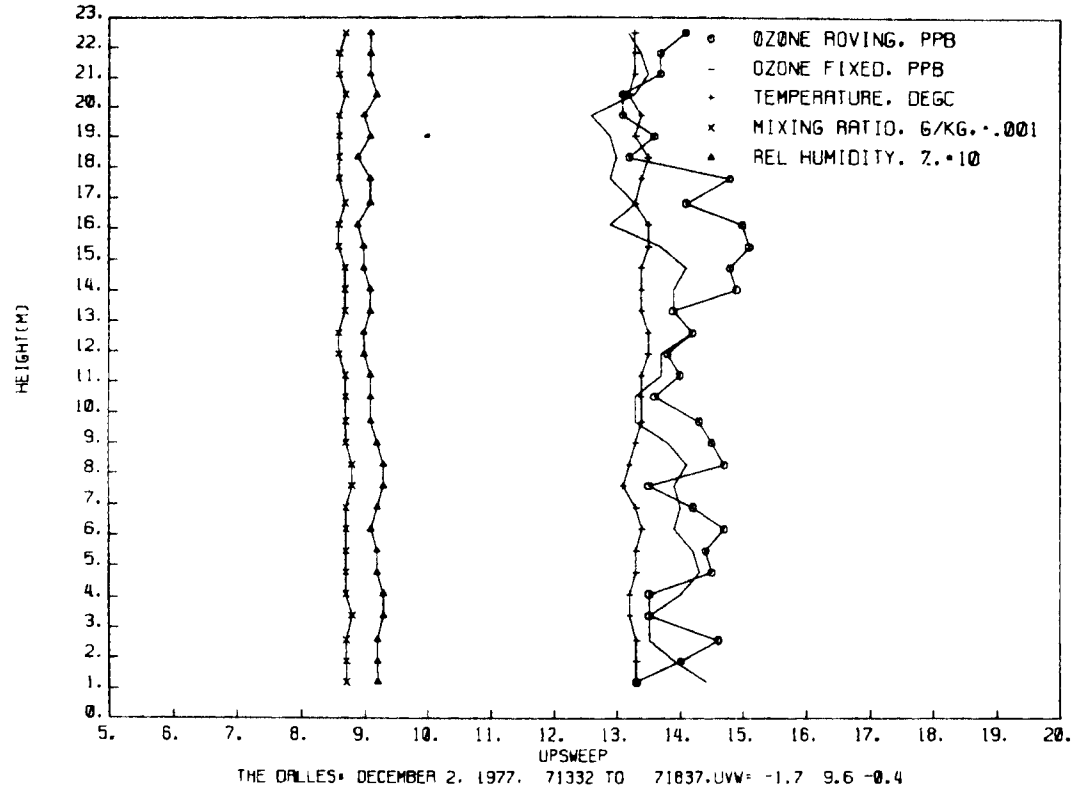

FIGURE G-1. Vertical Profiles for Case Study Number 2, ±500 kV

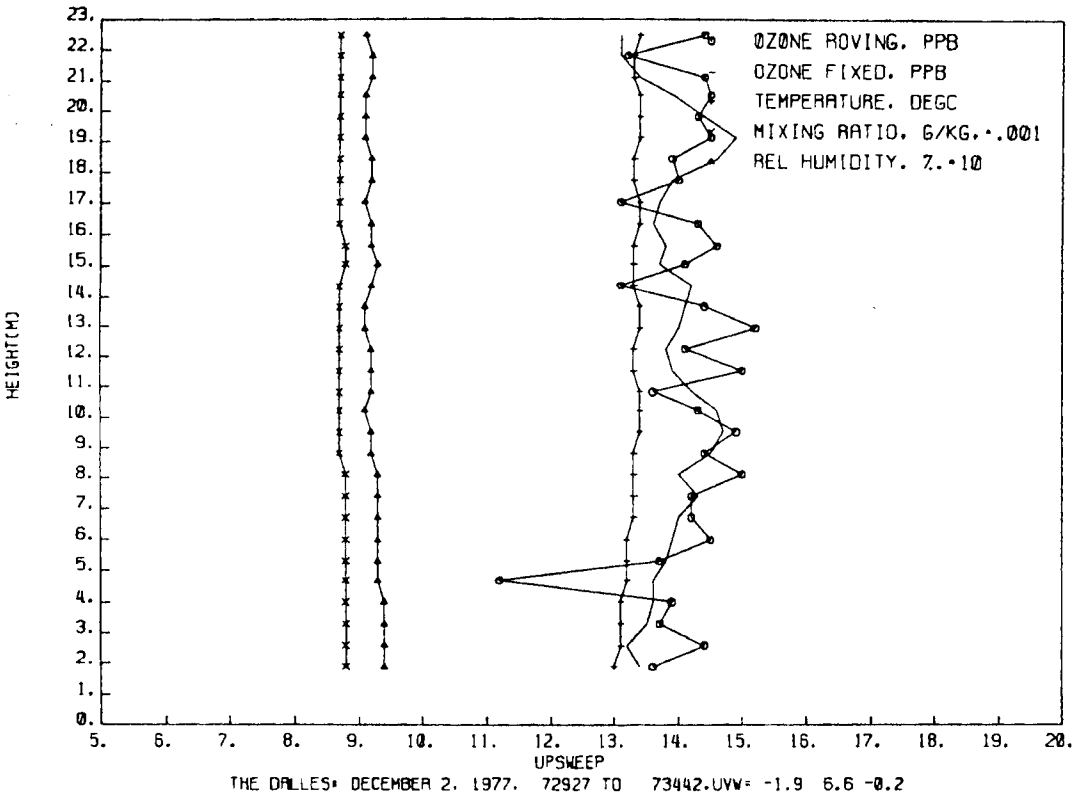

FIGURE G-2. Vertical Profiles for Case Study Number 2, ±500 kV

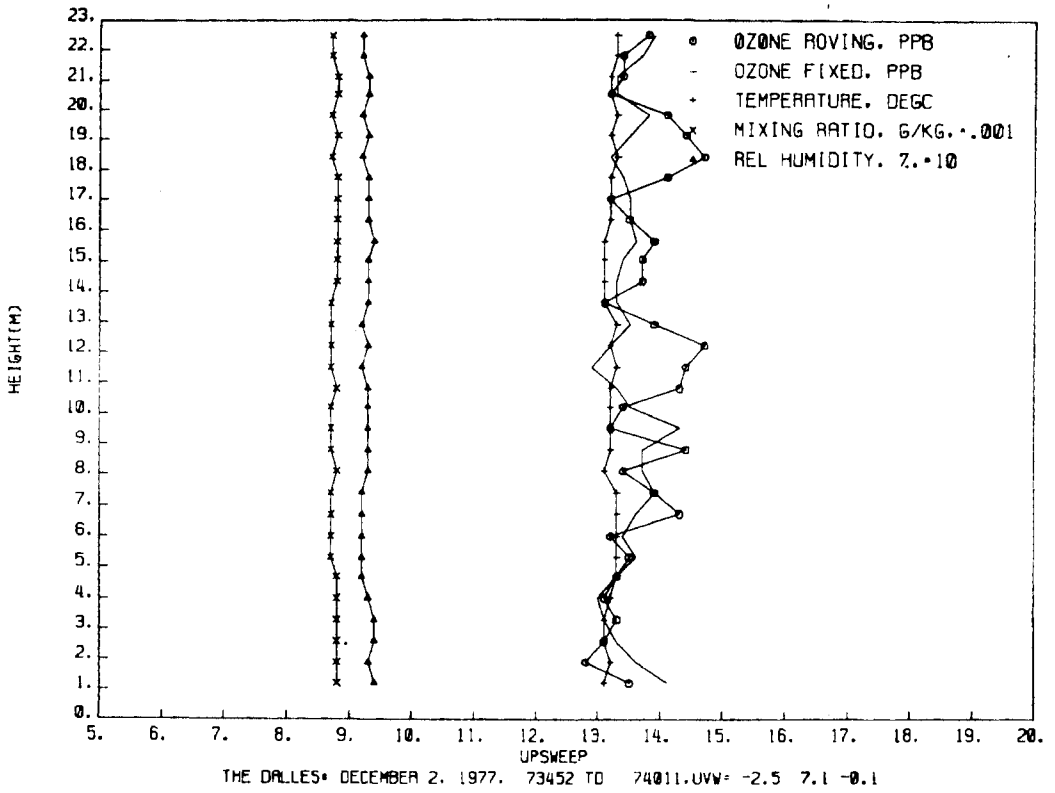

FIGURE G-3. Vertical Profiles for Case Study Number 2, ±500 kV

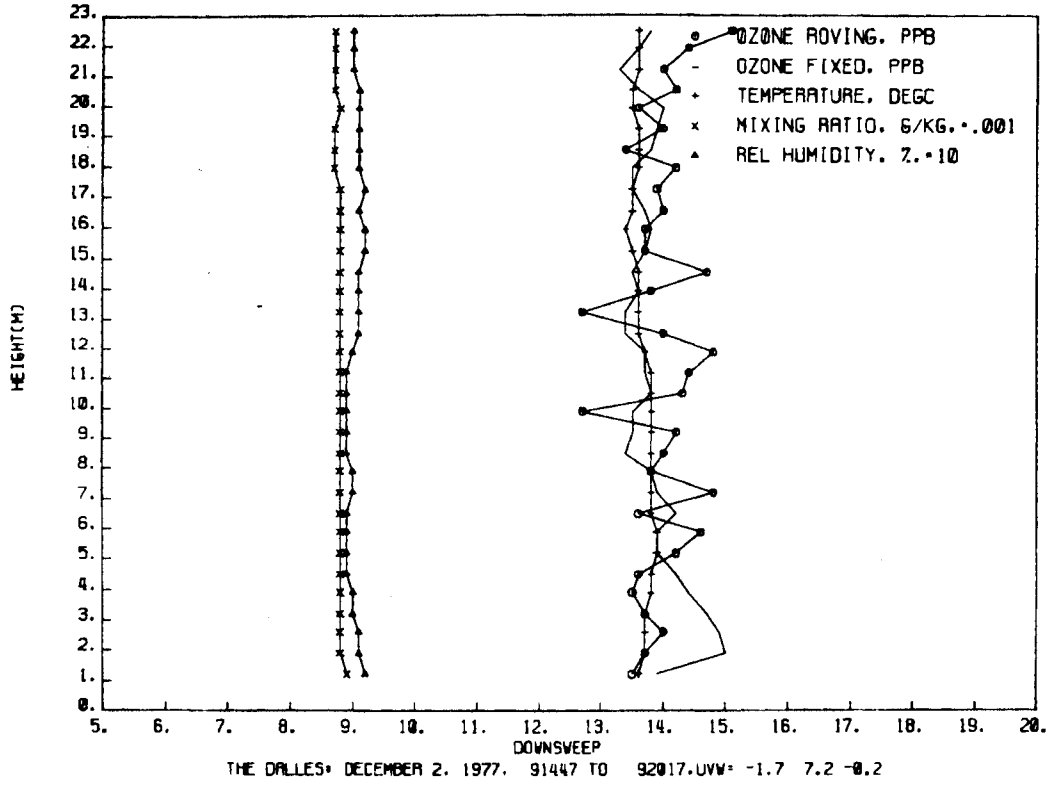

FIGURE G-4. Vertical Profiles for Case Study Number 2, ±500 kV

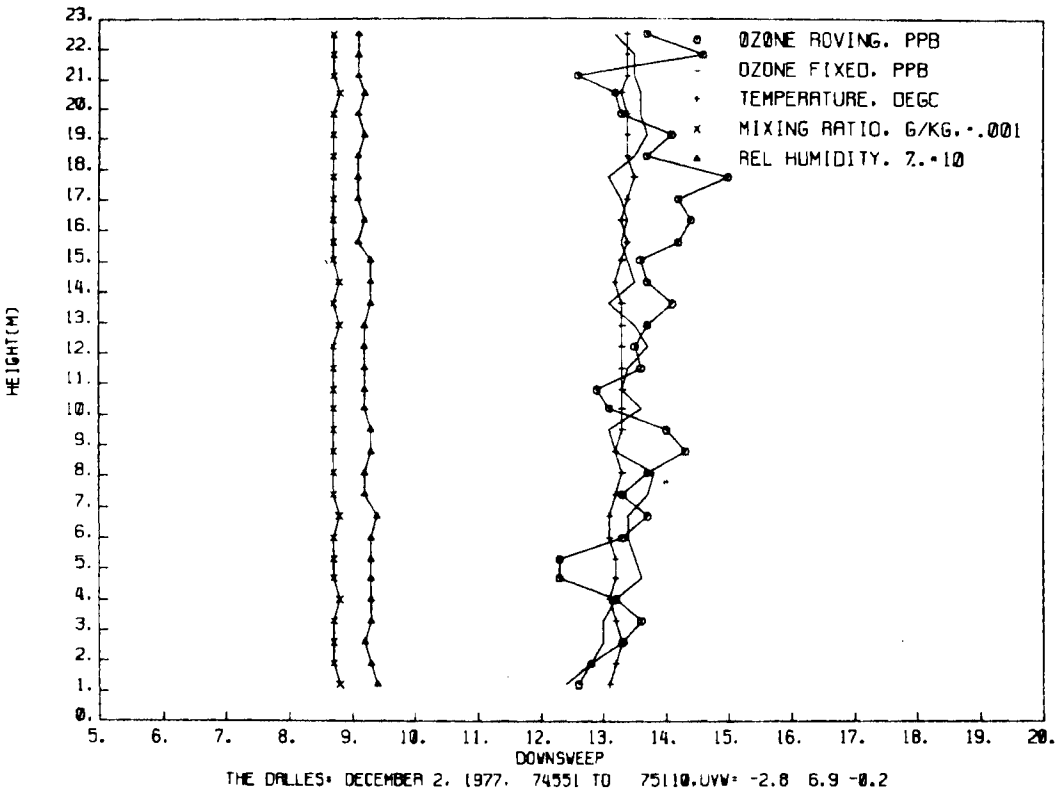

FIGURE G-5. Vertical Profiles for Case Study Number 2, ±500 kV

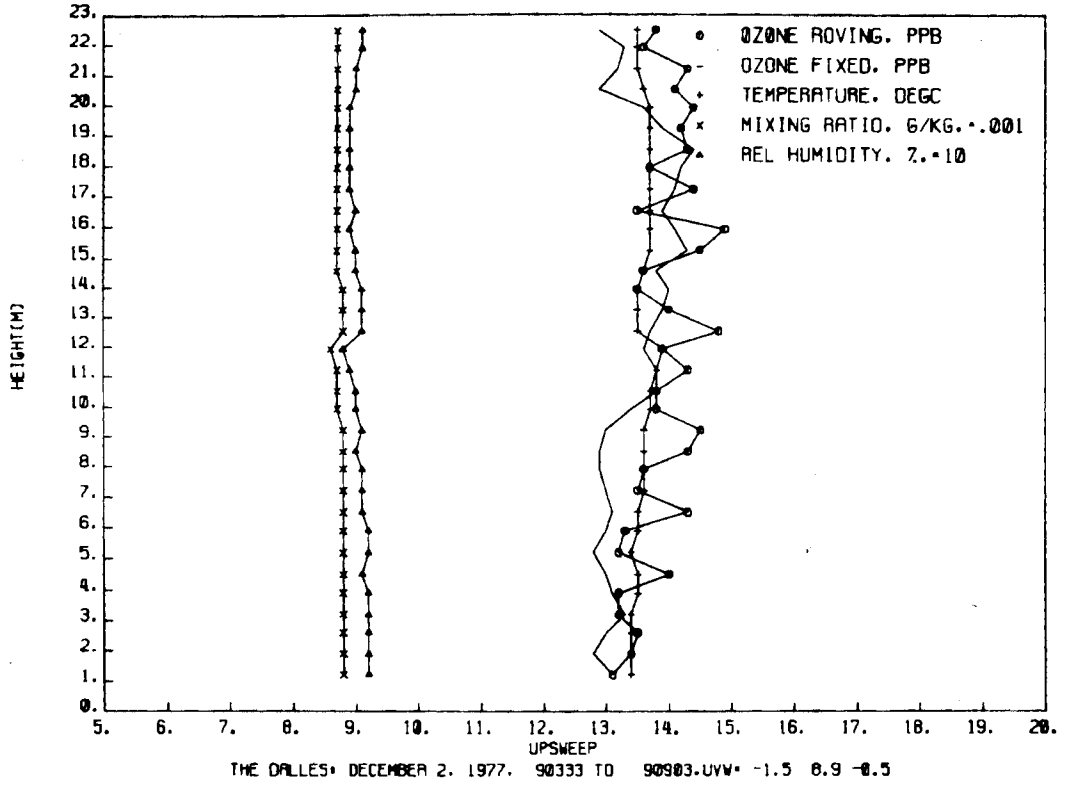

FIGURE G-6. Vertical Profiles for Case Study Number 2, ±500 kV

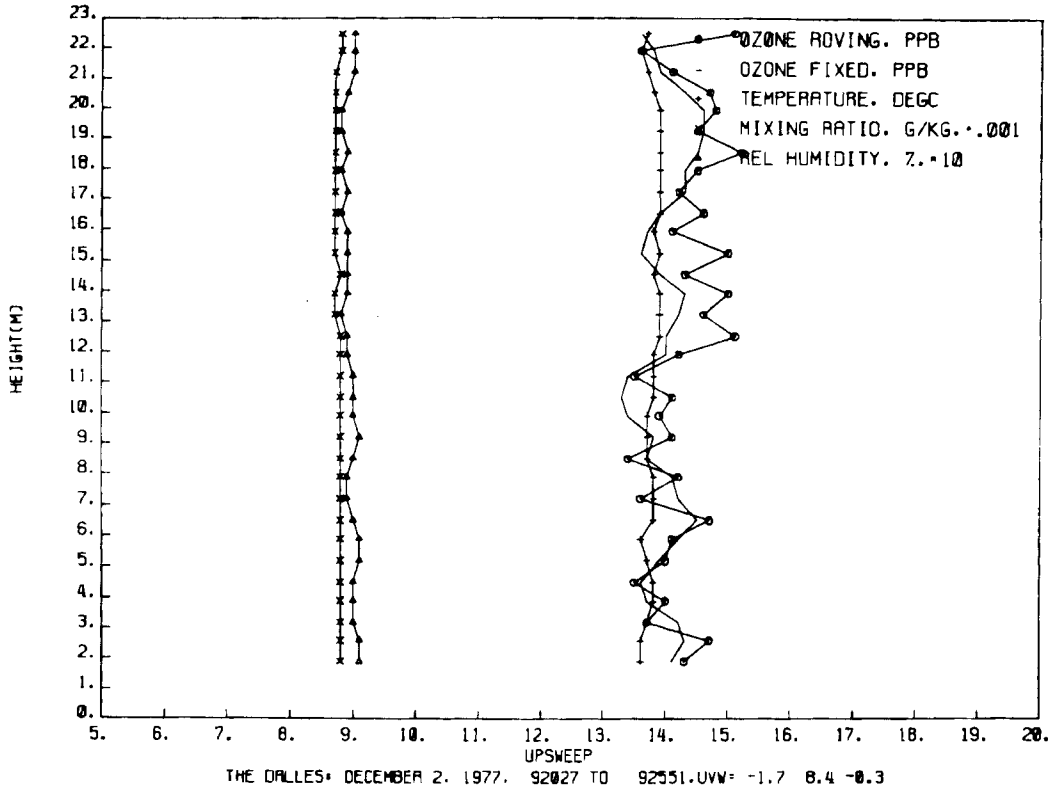

FIGURE G-7. Vertical Profiles for Case Study Number 2, ±500 kV

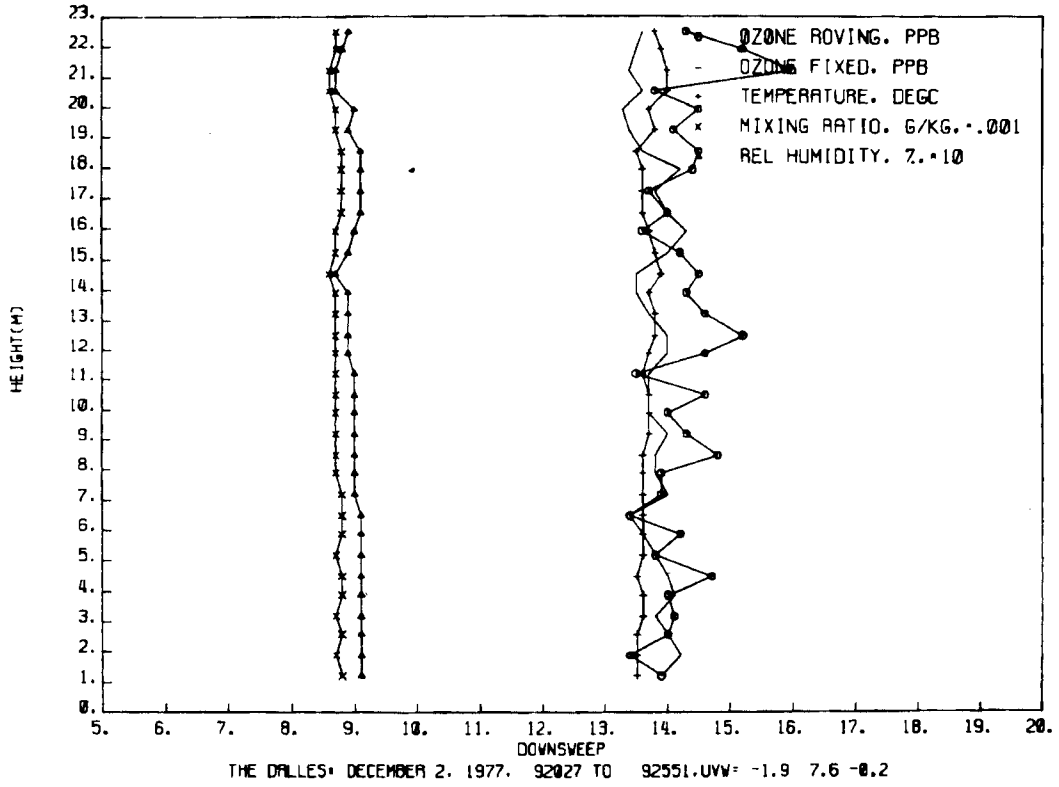

FIGURE G-8. Vertical Profiles for Case Study Number 2, ±500 kV

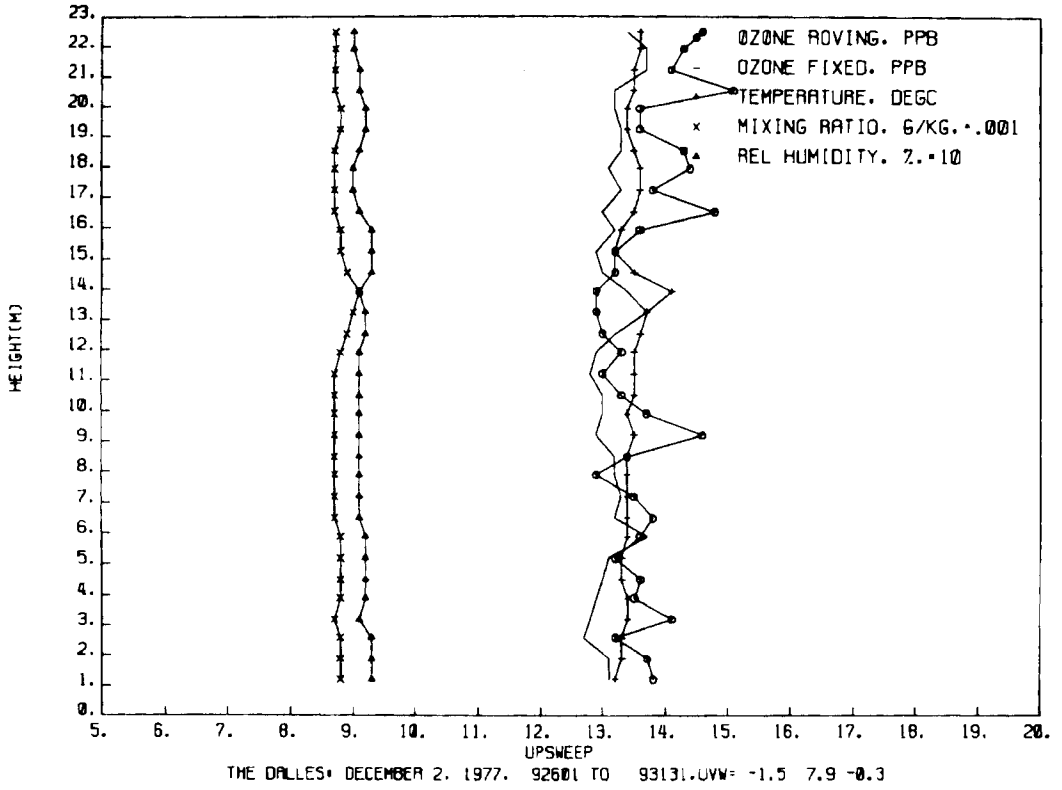

FIGURE G-9. Vertical Profiles for Case Study Number 2, ±500 kV

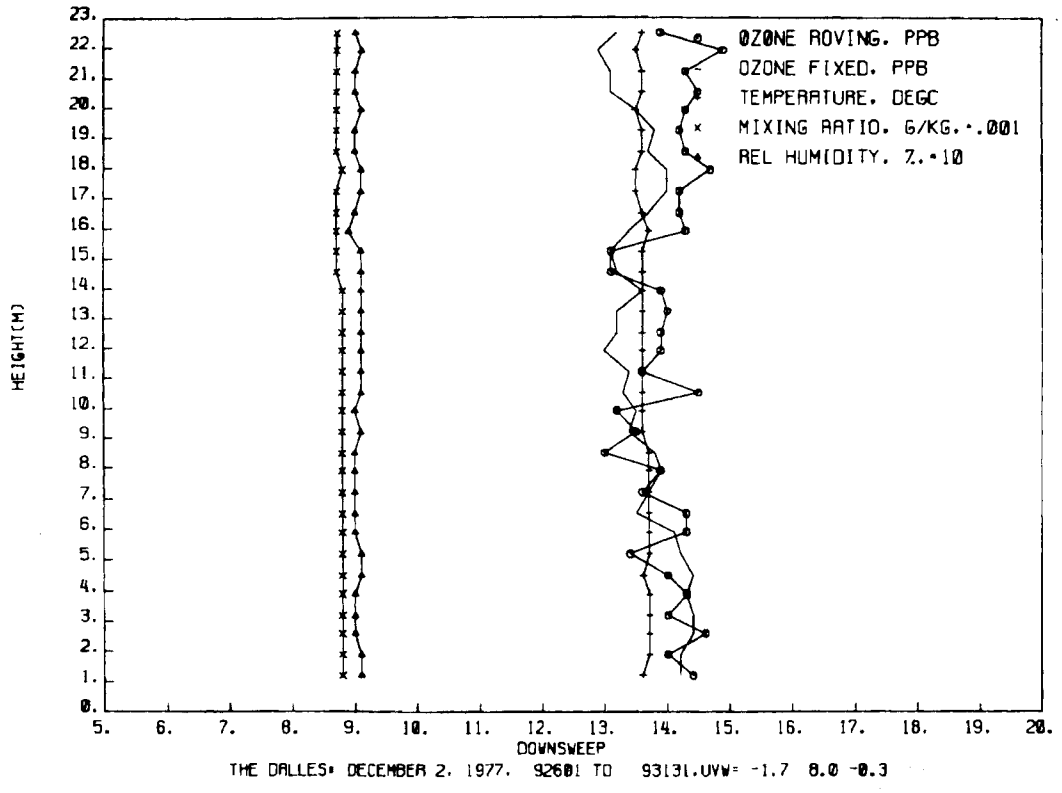

FIGURE G-10. Vertical Profiles for Case Study Number 2, ±500 kV